Analytical strategies for the detection of counterfeit erectile dysfunction drugs

Pierre-Yves Sacré

Pharmacien

Promotors : Dr. J. De Beer
Dr. P. Chiap

Thesis presented to fulfil the requirements for the degree of
Doctor in Biomedical and Pharmaceutical Sciences (PhD)

Academic year 2011-2012

The work presented in this thesis would not have been accomplished without the help of a great number of people.

First of all, I would like to thank my promoters: Dr. Jacques De Beer for providing me the opportunity of doing research in the field of drug analysis and reviewing my papers; Prof. Jacques Crommen and Dr. Patrice Chiap for the academic following and the critical comments on the chromatographic part of the present work.

I also want to thank Prof. Thomas De Beer for introducing me to the NIR and Raman measurements and allowing me to use the resources of its laboratory. Special thanks to Lien Saerens for spending time measuring the Raman microscopic maps and Anneleen Burggraeve for introducing me to the NIR measurements.

I would like to thank Mr Roy Vancauwenberghe and the Federal Agency for Medicines and Health Products for introducing me to the world of counterfeits and providing the samples used throughout this work.

The introduction and initiation to chemometrics was made possible by Dr. Eric Deconinck. Eric followed, guided and helped me all along this work. Without his help, this thesis would never have existed. For all of this, for your great support for the publication of my papers, for evaluating them with great care and our daily discussions, thank you.

I would like to thank my colleagues of the laboratory, namely Patricia, Peggy, Jean-Luc, Michael (especially during the coffee pauses), Thierry, Rosette, Chantal, Nora, Goedele, Veronique, Willy, Jurgen, Bart.
Special thanks to Sebastien for the jokes, the lab experiments and all the funny moments we had.

Thank you Mr Petit.

Of course, I would like to thank my parents, grandparents, sister, parents-in-law and brother-in-law for their permanent support.
Special thanks to my wife since she have always supported me and cheered me up when I was down. Thank you for your patience and support.

Summary of the thesis:

Since the late eighties, when it was first mentioned, the worldwide phenomenon of pharmaceutical counterfeiting has been growing. Belgian customs often find presumed counterfeited medical products in Belgian airports and ports because of their central position in Europe and their importance in the transit of goods. Further and deeper analyses are required to assess the counterfeit character of these goods and to provide a scientific basis for the eventual legal procedure.

As reference laboratory for the Federal Agency for Medicines and Health Products (FAMHP), the Scientific Institute of Public Health (IPH) frequently analyses illegal and counterfeit pharmaceutical preparations. The present research project was started with the objective of evaluating several existing methods and developing new analytical methods to detect counterfeit erectile dysfunction drugs. This thesis is focused on the analysis of illegal samples of phosphodiesterase type 5 inhibitors (PDE5-i) containing drugs because these are the most counterfeited pharmaceutical specialities in Belgium. The research was divided into a spectroscopic and a chromatographic part:

Infrared based spectroscopic techniques have already demonstrated their ability to detect counterfeit drugs. The first part of the study evaluates the capacity of each technique (mid-infrared (mid-IR), near-infrared (NIR) and Raman spectroscopy) separately and their combinations to discriminate genuine from illegal tablets. Then, the Classification And Regression Trees (CART) algorithm has been used to classify the different samples following the classification system of the Dutch National Institute for Public Health and the Environment (RIVM).

The second spectroscopic approach uses Raman microspectroscopy mapping to detect counterfeited Viagra®. This technique allows the detection of different compounds according to their Raman spectrum but also the study of the distribution of a selected ingredient among the core of a tablet.

The chromatographic part consists of the development and validation of a new Ultra High Pressure Liquid Chromatography method coupled with a UV diode array detector (UHPLC-DAD) and compatible with mass spectrometry (MS) to detect and quantify the three authorised phosphodiesterase type 5 inhibitors (sildenafil, tadalafil and vardenafil) and five of their analogues in illegal pharmaceutical preparations. This method was validated between +/- 5% acceptance limits using the total error approach and was compared to the official Viagra® assay method.

The ability of HPLC-UV impurity fingerprints to detect illegal samples and to predict whether a new unknown sample is genuine has also been evaluated.

The developed analytical methods may be included in a general approach to detect counterfeit drugs containing PDE5-i. This generic approach may also be used to detect other types of counterfeited drugs but should then be adapted for each class of medicines.

Résumé de la thèse:

Depuis qu'elle a été mentionnée pour la première fois, à la fin des années quatre-vingt, la contrefaçon médicamenteuse ne cesse de croître. Les douanes belges découvrent fréquemment des produits de santé suspects de contrefaçon aux aéroports et ports belges en raison de la situation centrale au niveau européen de ces derniers et de leur importance dans le transit de marchandises. Des analyses approfondies sont généralement nécessaires pour confirmer le caractère contrefait de ces produits et pour donner une base scientifique à une éventuelle procédure judiciaire.

En tant que laboratoire de référence pour l'Agence Fédérale des Médicaments et Produits de Santé (AFMPS), l'Institut Scientifique de Santé Publique (ISP) analyse fréquemment des préparations pharmaceutiques contrefaites et illégales. Le présent projet de recherche a démarré avec l'objectif d'évaluer différentes méthodes existantes et de développer de nouvelles méthodes analytiques pour détecter les contrefaçons médicamenteuses. Cette thèse est consacrée à l'étude d'échantillons illégaux de médicaments contenant des inhibiteurs de la phosphodiestérase de type 5 (PDE5-i). En effet, les médicaments des troubles de l'érection constituent la principale classe de médicaments contrefaits en Belgique. Les travaux de recherche ont été divisés en deux parties : l'une spectroscopique et l'autre chromatographique :

Les techniques spectroscopiques basées sur l'étude du rayonnement infrarouge ont déjà démontré leur intérêt dans la détection des médicaments contrefaits. La première partie du travail évalue la capacité de chaque technique (infrarouge moyen (mid-IR), infrarouge proche (NIR) et spectroscopie Raman) séparément et leurs combinaisons à discriminer les comprimés originaux des comprimés illégaux de Viagra® et Cialis®. Ensuite, l'algorithme « Classification And Regression Trees » (CART) a été utilisé pour construire un modèle permettant de prédire la classe des différents échantillons suivant la classification proposée par le RIVM (Institut National Néerlandais pour la Santé Publique et l'Environnement).

La deuxième approche spectroscopique utilise la cartographie microspectroscopique Raman pour détecter les contrefaçons de Viagra®. Cette technique permet la détection de différents composés grâce à leur spectre Raman mais également l'étude de la distribution d'un ingrédient spécifique dans le cœur du comprimé.

La partie chromatographique comprend le développement et la validation d'une nouvelle méthode UHPLC (Ultra High Pressure Liquid Chromatography) couplée à un

détecteur UV à barrette de diodes (DAD) pour détecter et quantifier les trois PDE-i autorisés (sildénafil, tadalafil et vardénafil) ainsi que cinq de leurs analogues dans des préparations pharmaceutiques illégales. La méthode a été validée par l'approche de l'erreur totale avec des limites d'acceptation de +/-5% et a été comparée à la méthode officielle de dosage du Viagra®. Elle utilise une phase mobile compatible avec la spectrométrie de masse.

La capacité des empreintes digitales chromatographiques d'impuretés obtenues par HPLC-UV pour détecter les échantillons illégaux a également été testée de même que sa capacité à prédire si un nouvel échantillon suspect est original ou non.

Les méthodes analytiques développées peuvent être incluses dans une approche générique d'analyse de médicaments des troubles de l'érection suspects. Cette approche générale peut également être appliquée à d'autres classes médicamenteuses à condition d'être adaptée à chaque classe étudiée.

AFMPS-FAGG	Belgian Federal Agency for Medicines and health Products
AIDS	Acquired Immuno Deficiency Syndrome
API	Active Pharmaceutical Ingredient
cAMP	Cyclic Adenosine MonoPhosphate
CART	Classification And Regression Trees
CCD	Charge-Coupled Detector (Raman spectroscopy)
CCR	Correct Classification Rate
cGMP	Cyclic Guanosine MonoPhosphate
ESI	ElectroSpray Ionisation (mass spectrometry)
FAMHP	Belgian Federal Agency for Medicines and Health Products
FDA	Food and Drug Agency (USA)
FN	False Negative
FP	False Positive
FT-IR	Fourier Transformed InfraRed Spectroscopy
GMP	Good Manufacturing Practice
GTP	Guanosine TriPhosphate
HorRat	Horwitz Ratio
HPLC	High Performance Liquid Chromatography
IMPACT	International Medical Products Anti-Counterfeiting Taskforce
k-NN	k-Nearest Neighbour
LC-DAD-CD	Liquid Chromatography coupled to Diode Array Detector and Circular Dichroism detector
LC-MS	Liquid Chromatography coupled to Mass Spectrometry detector
LDA	Linear Discriminant Analysis
LLQ	Lowest Limit of Quantification
LOOCV	Leave-One-Out Cross-Validation
NIR	Near InfraRed Spectroscopy
NIR-CI	Near InfraRed Spectroscopy Chemical Imaging
NMR	Nuclear Magnetic Resonance
NO	Nitrogen monoxide
NOS	Nitrogen monoxide Synthase
OOS	Out Of Specifications
PC	Principal Component
PCA	Principal Component Analysis
PDE5-i	PhosphoDiEsterase type 5 Inhibitors (erectile dysfunction drugs)
PLS; D-PLS	Partial Least Square; Discriminant Partial Least Square analysis
PPT	Pharmaceutical Parallel Trade
PSI	Pharmaceutical Security Institute
RIVM	Dutch National Institute for Public Health and the Environment
RSD	Relative Standard Deviation
SD	Standard Deviation
SIMCA	Soft Independent Modelling by Class Analogy
TLC	Thin Layer Chromatography
TN	True Negatives
TP	True Positives

UHPLC   Ultra High Pressure Liquid Chromatography

I. Introduction

1. **General context:**

The counterfeiting of medicines exists for millennia. At the first century of our era, Pedanius Dioscorides, a Greek physician, already warned about the dangers of adulterated drugs [1]. Since then, many crises of falsification of medicines have been documented [2]. Most of those crises implicated falsified herbal medicines and resulted in many deaths due to the lack of efficacy and/or toxicity of adulterated drugs.

At the Conference of Experts on the Rational Use of Drugs in Nairobi (Kenya) in 1985, the World Health Organization (WHO) first cited the counterfeiting of medicines. In 1988, a World Health Assembly Resolution (41.16) recommended to "initiate programmes for the prevention and detection of export, import and smuggling of falsely labelled, spurious, counterfeited or substandard pharmaceutical preparations" [3]. This leads to the launch of many international initiatives among which the International Medical Products Anti-counterfeiting Taskforce (IMPACT) started by the WHO in 2006. In parallel, the major pharmaceutical companies established the Pharmaceutical Security Institute (PSI) in 2002. Its role is to collect data to identify the extent of the counterfeiting problem and to provide assistance in the coordination of international inquiries.

According to PSI data, the international trade of counterfeit medicines is in permanent growth (see Figure I.1).
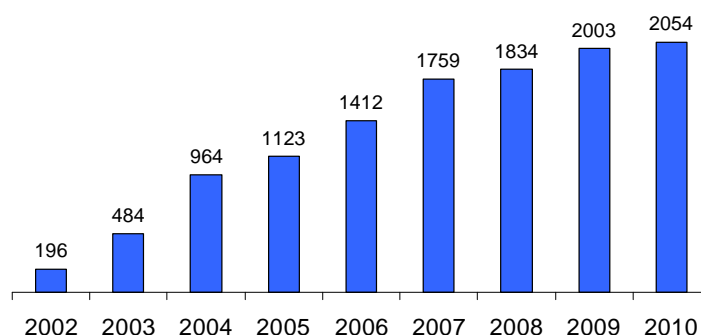
Figure I.1.: Total number of reports of counterfeiting, illegal diversion and theft incidents for eight consecutive years
(adapted from [4])

Many reasons may explain this growth: the lack of effective enforcement agencies in developing countries; the high price of the genuine drugs for poor people in developing countries; the fact that China and India do not recognise European and American patent laws and finally the lack of harmonised legal framework to define the pharmaceutical crime and

3

the penalties to apply. There are more and more evidences that the trade in counterfeit drugs is linked to international organised crime. Indeed, the trade of counterfeit drugs is more lucrative than the trade of narcotics and the criminal penalties for pharmaceutical counterfeiting are often less severe than for the trafficking of narcotics [5,6].

2. <u>Estimation of the counterfeiting of drugs in the world:</u>

It is estimated that counterfeit drugs represent 7% of the worldwide pharmaceutical market (should represent more than € 700 billions in 2012) [7,8]. Africa, Asia and many countries in Latin America are the most affected areas with more than 30% of the medicines on sale that are counterfeited [9]. The industrialized countries (e.g. USA, EU, Australia, Canada, Japan, and New Zealand) have approximately 1% of their pharmaceutical market affected despite the effective regulatory systems and market controls. Figure I.2 shows how counterfeit medicines may enter the legitimate supply chain. Counterfeit medicines may enter at all stage of the legal distribution chain and the possible reasons are: insufficient controls, multiple ownership, unregulated repackaging, poor traceability requirements by the European Union and the ease of switching of legitimate to counterfeit active pharmaceutical ingredient (API) [10]. The European Pharmaceutical Parallel Trade (PPT) is probably the major weakness in the pharmaceutical supply chain. Indeed, PPT wholesalers not only distribute but also change the packaging, the size and the labelling of original products (which are considered as manufacturing operations). However, they have only distribution licenses and have lighter controls than manufacturing facilities. Another weakness is the recent possibility for a pharmacy to sell medicines on the internet. In general, the more complex the legal chain of supply is, the weaker it becomes and the easier counterfeit medicines can penetrate it [10].

A recent study funded by Pfizer estimates the West-European illicit trade of medicines at € 10.5 billions. This study states that one out of five Europeans has bought a prescription only medicine from an illegal source. Most of these bought their drugs on the Internet. According to a WHO estimation, more than 50% of the medicines bought from websites that conceal their identity are counterfeited [9,11]. These drugs come in most cases from Asian countries (China, India and the Philippines) and from Russia. Figure I.3 shows the Eurasian counterfeit drugs market and connections.
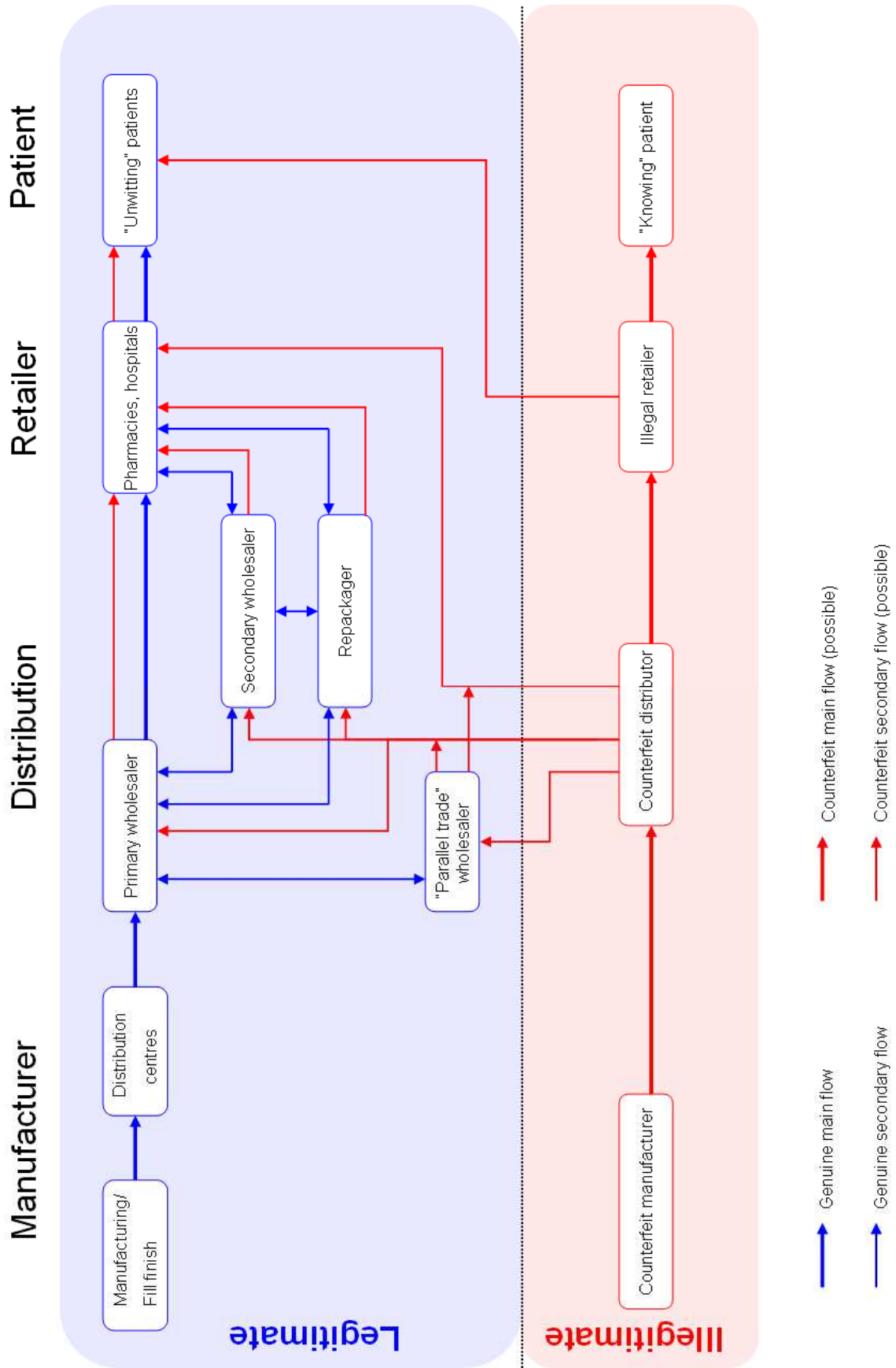
Figure I.2: How counterfeit medicines can enter the legitimate supply chain (adapted from [14])
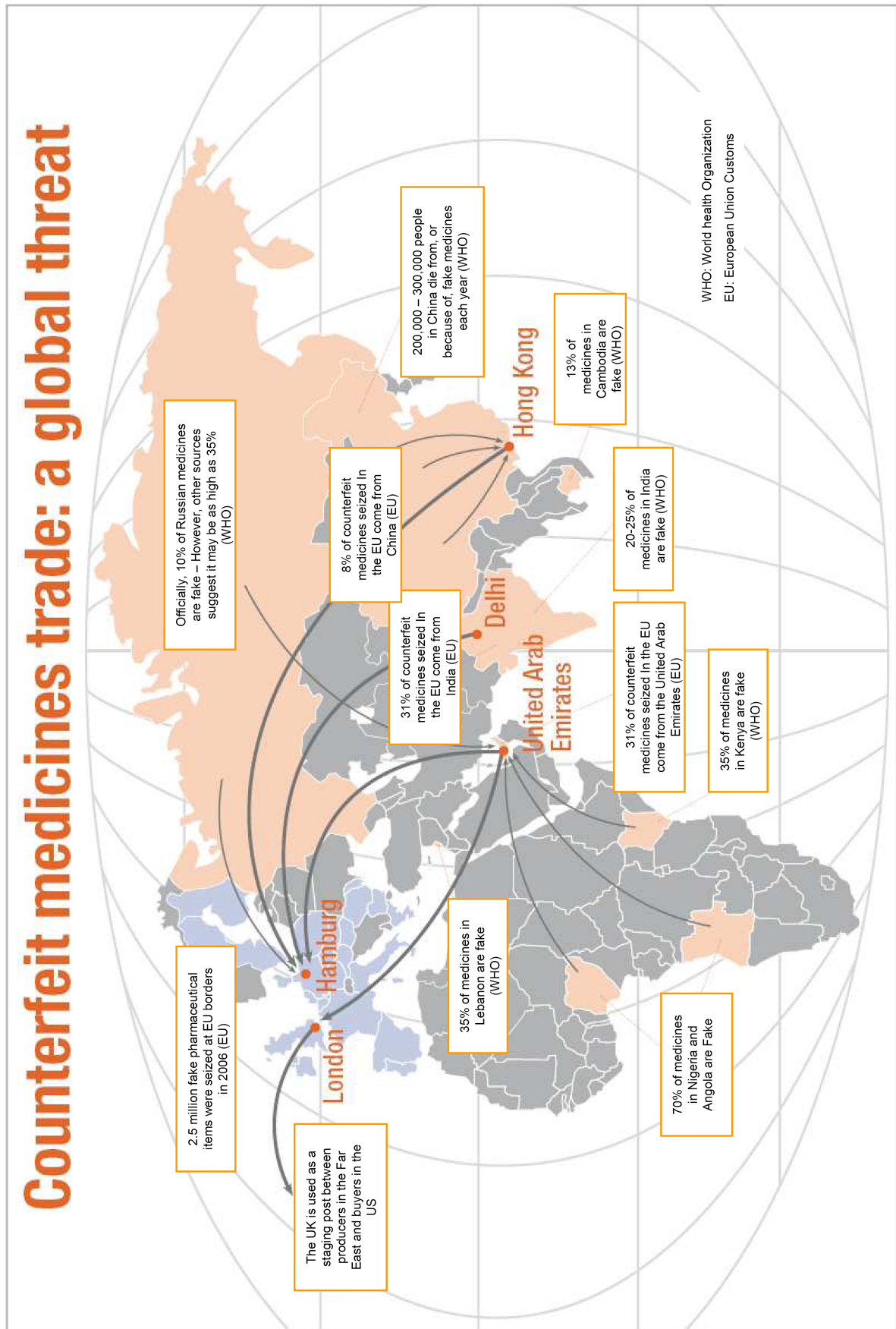
Figure I.3: Representation of the major importation and fabrication area in Europe, Africa and Asia (reproduced from [15])

3. <u>Risks to public health associated with counterfeit drugs:</u>

The pharmaceutical counterfeiting is a global problem. The categories of adulterated drugs and the risks associated vary according to the region considered.

In developing countries, most of the counterfeit drugs are "anti-infective" drugs [12]. This represents a serious public health problem. Indeed, most of the population buy their drugs in the street at low prices. These drugs are often counterfeited or substandard drugs with less or no therapeutic activity. When treating diseases associated with a high untreated mortality such as malaria, pneumonia, meningitis, AIDS, typhoid and tuberculosis with inefficient drugs, mortality and morbidity increase. Moreover, the use of subtherapeutic amounts of active ingredients increases the risk of developing microbial resistance. In this case, even genuine drugs could become inefficient [3].

In industrialized countries, the main therapeutic categories counterfeited are "lifestyle" drugs (weight loss drugs and potency drugs). The risks associated with these drugs are mostly due to the presence of toxic compounds or impurities, too high amounts of active ingredients, presence of unexpected active ingredient or new unknown designer drugs and wrong, missing or inadequate information concerning the use of the drug [13]. Other categories such as antineoplastic drugs or cardiovascular counterfeited drugs have also been found [16]. The fact that counterfeit drugs may be found in the legal market represents a major public health risk. Indeed, besides the potential adverse effects encountered by the users, the patients may not trust medicines anymore even if they are sold in pharmacy. A report of the WHO states that: "*As a consequence of such damaging effects, counterfeit drugs may erode public confidence in health care systems, health care professionals, the suppliers and sellers of genuine drugs, the pharmaceutical industry and national Drug Regulatory Authorities (DRAs). Incorrect labelling as to the source can also be detrimental to the reputation and financial standing of the original and/or current manufacturer whose name has been fraudulently used* [17]."

References :

[1] WHO, Counterfeit drugs – guidelines for the development of measures to combat counterfeit drugs. WHO/EDM/QSM/99.1. Geneva: WHO, 1999

[2] Newton P., Green M., Fernández F., Day N., White N., Counterfeit anti-infective drugs, The Lancet Infectious Diseases (2006) 6, 602-613

[3] Clift C., Combating Counterfeit, Falsified and Substandard Medicines Defining the Way Forward?, Chatham House Briefing Papers, November 2010

[4] http://www.psi-inc.org (last accessed 14-09-2011)

[5] http://www.who.int/mediacentre/factsheets/fs275/en/index.html (last accessed 14-04-2011)

[6] http://www.pfizer.com/files/products/CounterfeitBrochure.pdf (last accessed 14-04-2011)

[7] http://www.prlog.org/10124036-global-pharmaceutical-market-forecast-to-2012.html (last accessed 14-04-2011)

[8] Deisingh A., Pharmaceutical counterfeiting, Analyst (2005) 130, 271-279

[9] http://www.who.int/impact/FinalBrochureWHA2008a.pdf (last accessed 14-04-2011)

[10] EAASM report, European Patient Safety and Parallel Pharmaceutical Trade – a potential public health disaster ?, Surrey, 2007

[11] http://www.securingpharma.com/40/articles/378.php (last accessed 14-04-2011)

[12] http://www.who.int/bulletin/volumes/88/4/10-020410.pdf (last accessed 14-04-2011)

[13] Blok-Tip L., Vogelpoel H., Vredenbregt M.J., Barends D.M., de Kaste D., Counterfeit and imitations of Viagra® and Cialis® tablets: trends and risks to public health, RIVM Report 267041001/2005, Bilthoven, 2005

[14] EAASM report, Packaging Patient Protection recommendations for new legislation to combat counterfeit medicines, Surrey, 2009

[15] EAASM report, The counterfeiting superhighway, Surrey, 2008

[16] http://www.fagg-afmps.be/fr/news/news_pangea_III.jsp (last accessed 14-04-2011)

[17] http://www.who.int/medicines/services/counterfeit/overview/en/index1.html (last accessed 14-04-2011)

II. Aims of the work

Aims of the work:

The main objective of this thesis is the development and evaluation of new analytical methods or approaches for the detection of counterfeit and illegal medicines.

We have focused our work on the analysis of PDE5-i drugs, because it is the most counterfeited class of medicines in Belgium. Therefore, it was possible to obtain a large amount of illegal samples.

After screening the literature, we saw that nearly all methods to detect counterfeit drugs could be divided in two main groups: spectroscopic techniques and chromatographic techniques. Spectroscopic techniques are used as fingerprinting methods and undergo multivariate statistical analysis while chromatographic techniques are essentially used to detect and quantify API in pharmaceutical preparations.

Among spectroscopic techniques, NIR and Raman spectroscopies had already been used to detect counterfeit Viagra®. However, no study evaluated which technique or combination of these techniques provided the best results. Therefore, we have started our work by this evaluation and we have also evaluated FT-IR because it is probably the most common IR spectroscopic technique in analytical laboratories.

The results have been initially evaluated by visual inspection and, secondly, their RIVM class has been predicted by the application of the CART algorithm. (Chapter IV, section 3.2.)

We have also investigated the interest of Raman microspectroscopy mapping. The major interest of this technique is the possibility to analyse the spatial distribution of a selected compound in the studied area. We have investigated whether it is possible to differentiate genuine and illegal samples based on the spatial distribution of sildenafil among the core of the tablets. We have also used Raman microspectroscopy as a sampling method and discriminated illegal from genuine samples based on one hand on the whole spectrum and on the other hand on the Raman peak of lactose. (Chapter IV, section 3.3.)

We have investigated a new approach for the detection of counterfeit medicines: the use of impurity chromatograms as fingerprints. Impurity HPLC-UV chromatograms of the Viagra®-like and Cialis®-like samples have been recorded applying the Pharmeuropa published method. (Chapter V, section 3.2.)

We have also developed a UHPLC-UV method for the analysis of suspect erectile dysfunction samples. This method has been validated for the qualitative and quantitative analysis of the three authorised API (sildenafil, tadalafil and vardenafil) and five of their

analogues. Other API frequently found in such suspect samples (caffeine, yohimbine, trans-tadalafil) have also been separated but not validated. This method has been implemented in the laboratory for routine analysis of suspect PDE5-i samples. (Chapter V, section 3.1.)

Predictive models have been built for each fingerprinting method developed. The relevance of these models was confirmed by internal and external validation.

Finally, based on the developed methods, we propose a general strategy for the analysis of new suspect PDE5-i samples. (Chapter VI)

III. Theoretical background

1. Definitions:

The WHO defines a counterfeit medicine as:

> *"One that is deliberately and fraudulently mislabelled with respect to identity and/or source. Counterfeiting can apply to both branded and generic products. Counterfeit products may include products with the correct ingredients or with the wrong ingredients, without active ingredients, with insufficient (inadequate quantities of) active ingredient(s) or with fake packaging [1]."*

The substandard medicines definition is the non-deliberate and genuine side of the counterfeit medicines definition:

> *"Substandard medicines (also called out of specification (OOS) products) are genuine medicines produced by manufacturers authorized by the NMRA (National Medical Regulatory Authority) which do not meet quality specifications set for them by national standards [1]."*

If these poor-quality drugs do not meet the NMRA specifications, they should not be present on the market. This implicates that either there has been a problem in the controls of the legitimate supply chain or there have been unscrupulous activities and reselling of medicines to be destroyed [2].

The European parliament recently adopted a definition of "falsified medicines" that is a compromise between the counterfeit and substandard medicines definition of the WHO:

> *A falsified medicinal product is "any medicinal product with a false representation of:*
> - o *its identity, including its packaging and labelling, name, composition in respect of any of its components including excipients and strength; and/or*
> - o *its source, including the manufacturer, country of manufacturing, country of origin, marketing authorisation holder; and/or*
> - o *its history, including the records and documents relating to the distribution channels used [3]."*

Practically, the illegal samples seized at the customs may be divided in two main groups (counterfeit or imitations) according to their physical appearance. These two main groups are themselves subdivided in function of the chemical composition of the tablets. This classification, proposed by the RIVM [4], is shown in section 3.1.

2. <u>Phosphodiesterase type 5 inhibitors:</u>

In 1998, Pfizer (NY, USA) obtained the marketing authorisation for its new drug Viagra®. This product contains sildenafil citrate as active ingredient. A few years later, Lilly (Indianapolis, USA) launched Cialis® (containing tadalafil) in 2002 followed by Bayer (Leverkusen, Germany) with Levitra® (containing vardenafil hydrochloride) in 2003. These three drugs are the only authorised PDE5-i for the treatment of erectile dysfunction.

2.1.   Pharmacodynamics:

The physiological mechanism responsible for erection of the penis involves the release of nitric monoxide (NO) in the corpus cavernosum during sexual stimulation (see Figure III.1). Nitric monoxide then activates the enzyme guanylate cyclase, which results in increased levels of cyclic guanosine monophosphate (cGMP), producing smooth muscle relaxation in the corpus cavernosum and allowing inflow of blood resulting in erection.

Phosphodiesterase type 5 (PDE5) is responsible for the degradation of cGMP. When the NO/cGMP pathway is activated during a sexual stimulation, inhibition of PDE5 by the PDE5-i results in increased corpus cavernosum levels of cGMP. These high levels of cGMP induce a sustained erection. Therefore sexual stimulation is required since sildenafil has no direct relaxant effect on isolated human corpus cavernosum but potently enhances the relaxant effect of NO on this tissue [5,6,7].

Actually, eleven families of phosphodiesterase have been identified. Each of these families exerts its role in specific locations (see table III.1). Sildenafil, tadalafil and vardenafil have a relative selectivity towards PDE 5 and they may inhibit other PDE families in function of their local concentrations. These inhibitions explain some of their undesirable effects such as the visual disturbances (inhibition of PDE6), inhibition of platelet aggregation and increased heart rate (inhibition of PDE3) or dyspepsia (inhibition of oesophageal PDE5) [8].
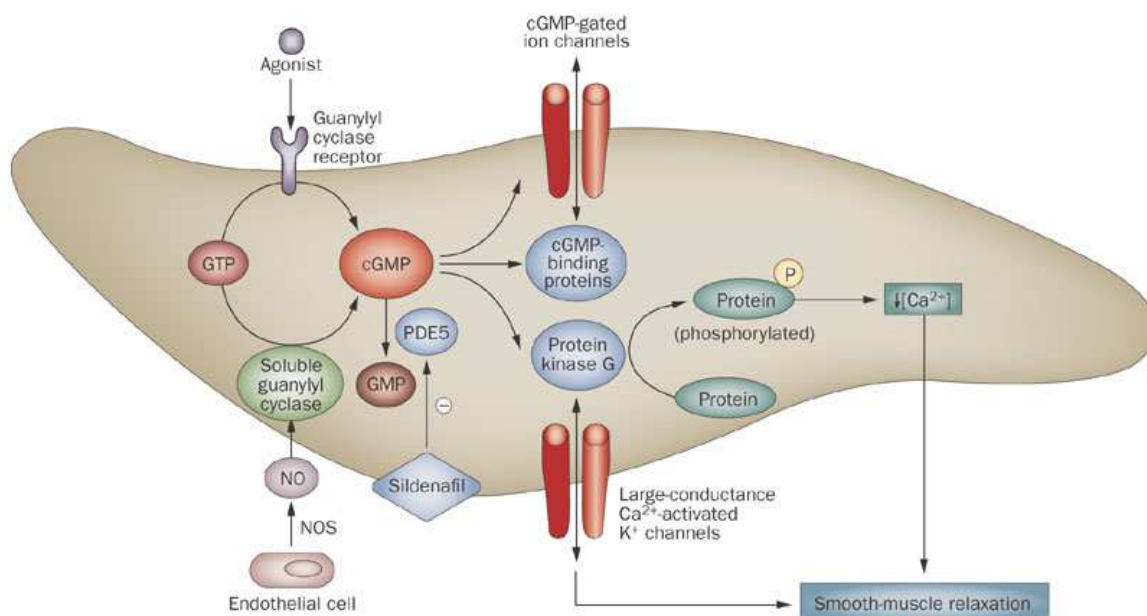
Figure III.1: Physiological mechanism of erection and pharmacological action of sildenafil in promoting smooth-muscle relaxation. Abbreviations: cGMP, cyclic guanosine monophosphate; GMP, guanosine monophosphate; GTP, guanosine triphosphate; NO, nitric oxide; NOS nitric oxide synthase; PDE phosphodiesterase. (reproduced from [5]).

Table III.1 Substrate specificities and distributions of PDE families (reproduced from [8])

PDE	Substrate specificity	Main tissue localization
1	cGMP>cAMP	Brain, heart, vascular smooth muscle
2	cGMP=cAMP	Adrenal cortex, brain, heart, corpus cavernosum
3	cAMP/cGMP	Heart, corpus cavernosum, liver pancreas, vascular smooth muscle, platelets
4	cAMP	Lung, mast cells, vascular smooth muscle
5	cGMP	Corpus cavernosum, lung, vascular smooth muscle, platelets, brain, esophagus
6	cGMP>cAMP	Retina
7	cAMP>>cGMP	Skeletal muscle, T cells
8	cAMP	Testis, thyroid
9	cGMP	Broadly expressed, not well characterized
10	cGMP>cAMP	Brain, testis
11	cGMP=cAMP	Skeletal muscle, prostate, liver, kidney, pituitary, testis

2.2.   History of PDE5-i counterfeiting

Viagra® is one of the most counterfeited drugs in industrialized countries. This is explained by the high prices and by the embarrassment caused by the medical consultation for an erectile dysfunction problem. The Internet is an easy, fast and anonymous way to obtain these kinds of drugs.

Only eighteen months after the approval of the genuine Viagra®, counterfeit tablets containing sildenafil appeared. Tadalafil appeared in Viagra® counterfeits one month before the approval of Cialis® and one year after appeared the first counterfeits of Cialis®. In the Netherlands, in 2004, Viagra® counterfeits represented 98% of the PDE5-i illegal market and Cialis® the last two percent. In 2006, Viagra® represented only 69% of the illegal PDE5-i market while Cialis® (25%) and Levitra® (6%) had become more prevalent [4].

Besides these three approved molecules, numerous analogues exist. Most of them have been found as adulterants of herbal dietary supplement [9-29]. These analogues also show a relative selectivity towards the PDE5 (see table III.2). However, their inhibition potency might be very different of the one of sildenafil and is rarely taken into account for their dosage in illegal preparations. Furthermore, the differences in their chemical structures lead to differences in their pharmacokinetic parameters such as their onset of action, blood levels, half-lives, brain penetration and metabolism. All these parameters are unknown for the analogues. This represents a huge toxicological risk linked to their intake especially when associated with wrong precautions of use [4, 30].

Table III.2   PDE5 *in-vitro* pharmacological potencies of the three approved PDE5-i and some of their analogues (data from [4,30])

Compound	Potency relative to the inhibition of PDE 5 by sildenafil
sildenafil	1
tadalafil	1,4
vardenafil	10,1
piperidino-sildenafil	0,62
acetildenafil	0,9
homosildenafil	1,9
hydroxyhomosildenafil	2,1
morpholinosildenafil	3,9
benzamidenafil	3,9
thiosildenafil	11,63

2.3. Detection of counterfeit PDE5-i

Several analytical techniques have already been used for the detection of counterfeit PDE5-inhibitors. These techniques are separated in two main groups: chromatographic and spectroscopic techniques.

The chromatographic techniques are used for the separation, identification and quantification of the active substances. They may also contribute to the elucidation of the structure of new analogues. Commonly used chromatographic techniques contain cheap and easy ones such as thin layer chromatography (TLC) [31,32] but also more sophisticated and expensive ones such as HPLC-UV [9,12,15,19,20,24,26,28,29,33], LC-MS [9-30] and LC-DAD-circular dichroism [22].

The spectroscopic techniques are often preferred to chromatography for the identification of counterfeit drugs because of the fact that they are fast, need less (or no) sample preparation and some of them are non destructive. Fourier-transformed Infrared spectroscopy (FT-IR) [18,21,34], NIR [31,34], Raman spectroscopy [34,35,36], X-ray diffraction (XRD) [37], colorimetry [38,39] and Nuclear Magnetic Resonance (NMR) [36,40] have demonstrated their utility to detect counterfeit or adulterated drugs.

3. <u>Chemometric tools:</u>

The modern measurement techniques produce an enormous amount of data for which mathematical tools are necessary to be able to extract information and to interpret the data. This application of mathematical and statistical tools is called chemometrics.

3.1. Principal Component Analysis [41]

Principal component analysis is a feature reduction technique. When analysing several samples with a spectroscopic technique, absorbance values at several hundreds of wavelengths are obtained for each sample. The studied samples are called the "objects" and the absorbance values are called the "variables". The number of dimensions of an analysis is equal to the number of variables. In this example, the analysis has several hundreds of dimensions and the graphical visualization of the data is therefore not possible since human beings cannot visualize plots of more than three dimensions. The number of variables must be reduced to three or less. PCA provides the means to achieve this goal.

Let us consider the following example: thirty tablets have been analysed and the absorbance at three wavelengths were measured. The data are organised in a table where the 30 objects constitute the rows and the three variables ($x1$, $x2$ and $x3$) constitute the columns (10 x 3 matrix). As this problem is a three-dimensional problem, the data may be plotted as shown in Figure III.2.
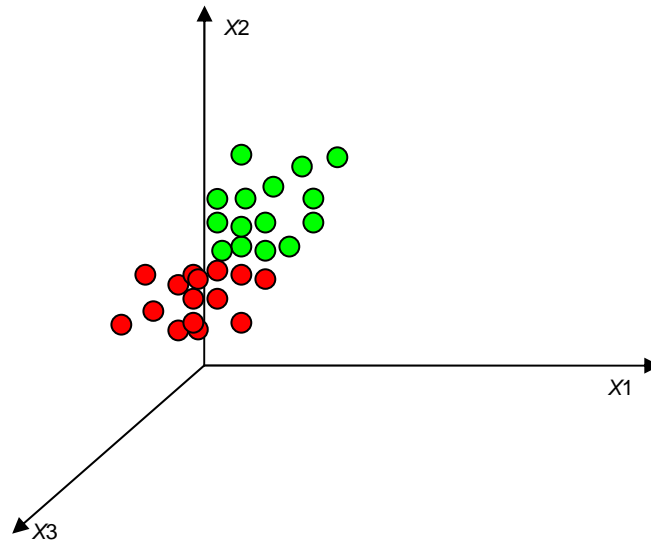
Figure III.2: Three dimensional plot of the dataset described in the text. The green and the red dots represent the projection of two groups of objects in the space described by the three variables

As one can see, no discrimination of the samples may be realised based on the three dimensional plot. A reduction of the variables, leading to a bi-dimensional representation may provide a clearer insight in the data.

To achieve this goal, a first principal component (PC1) is defined to explain the largest possible variation of the data. PC1 accounts therefore for most of the information. A second principal component (PC2) is then defined to explain the remaining variation around PC1. By definition, PC2 is orthogonal to PC1. The principal components (PC1 and PC2) are called *latent variables* while the original variables ($x1$, $x2$ and $x3$) are called *manifest variables*. The projection of an object i along a principal component PCp is called its score s_{ip}. The score is a weighted sum of the manifest variables and is defined as:

$$s_{ip} = \sum_j v_{jp} \times x_{ij} \qquad\qquad\qquad\qquad \text{(eq III.1)}$$

where v_{jp} is the weight (or *loading*) of manifest variable j on PCp and x_{ij} is the value of the ith object for manifest variable j.

The weight of the variables represents the importance of the variable to explain the variation of the data. As can be seen in Figure III.3 and III.4, the reduction of dimensions allows now an easy interpretation of the data showing two clear groups of samples.
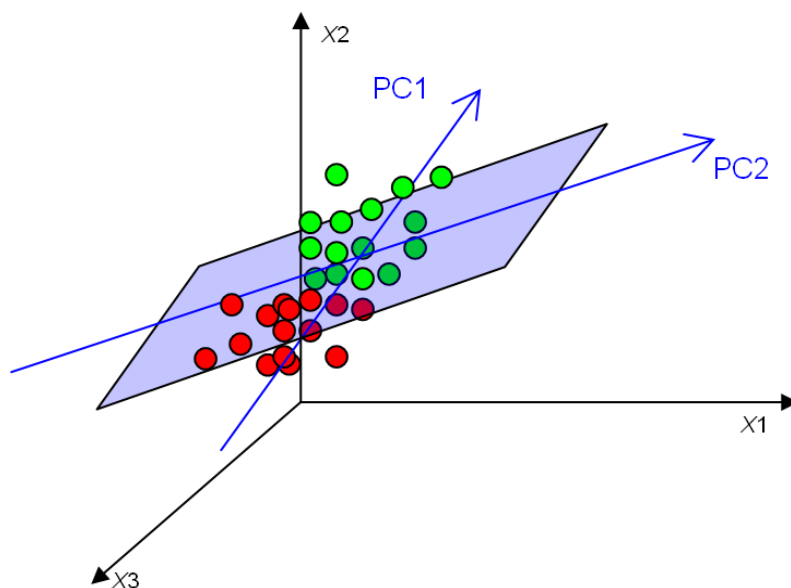
Figure III.3: Three dimensional plot of Figure 2 with the plane described by the two first principal components (PC1 and PC2).
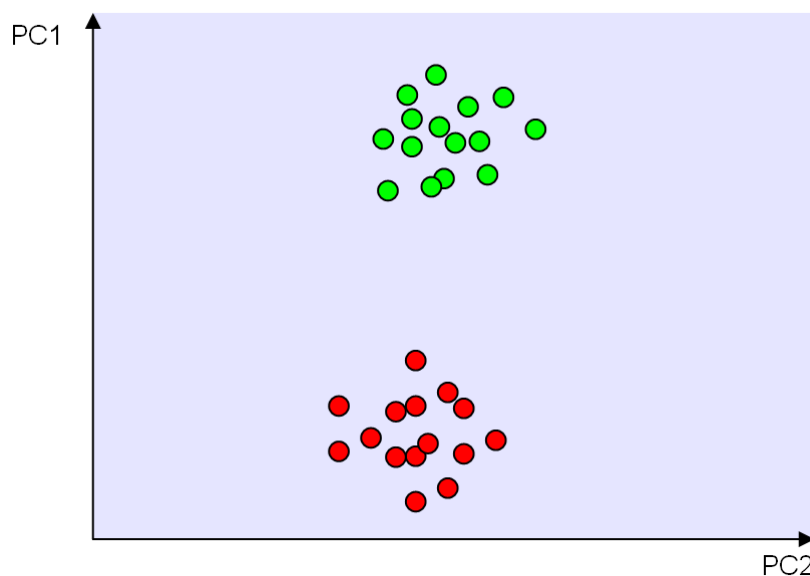
Figure III.4: Score plot of the dataset described in the text in the PC1-PC2 plane.

This example can be generalized to higher dimension analysis. For *n* objects described by *m* manifest variables, *m* principal components can be defined. As the explained variation of the data by the principal components (PCs) is decreasing when the number of the PC increases, the first PCs represent the information and the other PCs represent the noise.

3.2. Partial Least Square Analysis (PLS) [41]

The partial least square analysis is a supervised method for multivariate calibration. The PLS latent variables, called PLS-factors, are also constructed by making linear combinations of the manifest variables. The difference with PCA is that the weights of the original variables are chosen to maximise the covariance (measure of the association between two variables) between the describing variables (e.g. absorbance values) and the response variable (e.g. counterfeit or genuine tablet). This will lead to latent variables more related with the response than those obtained with PCA.

3.3. Kennard and Stone algorithm [42, 43]

The Kennard and Stone algorithm is a uniform mapping algorithm. It has been used to construct the training and the test sets starting from a dataset. The test set must be distributed as uniformly as possible among the training set to ensure that the main sources of data variability will be incorporated during the construction of a model. This leads to a more robust classification model.

The Kennard and Stone algorithm chooses the objects of the training set maximising the minimal Euclidian distance between each selected point and all the others.

The Euclidian distance is given by:

$$d_{ij} = \sqrt{\sum_{l=1}^{k}\left(x_{il} - x_{jl}\right)^2} \qquad\qquad \text{(eq III.2)}$$

where l (ranging from 1 to k) represents the variables and i and j represent the two points.

In our case, the selection of the objects started with the furthest object from the mean point. The second chosen object i_0 is the furthest point from the previous one, i, etc:

$$d_{selected} = \max_{i_0}(\min_{i}(d_{i,i_0})) \qquad\qquad \text{(eq III.3)}$$

Then, all the other objects are selected in the same way until the selected number of objects of the training set is reached. The remaining objects are included in the test set.

3.4.   Linear Discriminant Analysis (LDA) [41]

The linear discriminant analysis (LDA) is a feature reduction method (like PCA) that defines optimal boundaries between the classes.

Let us take, for example, a dataset with two classes (A and B) defined by two variables (x_1 and x_2). Figure III.5 shows the objects in the bi-dimensional space. Probability ellipses are drawn for each class, with the same probability level, until they touch each other (Figure III.6.). Line *a* is the tangent to the two ellipses at the point O where the two ellipses meet. Line *a* can be considered as the boundary separating A from B. Mathematically, the boundary is defined by the line *d* (perpendicular to *a*).

One can project a new, unknown, object (e.g. E in Figure III.6) on line d. Its score gives its location on d:

$$D = w_0 + w_1 x_1 + w_2 x_2 \qquad\qquad\qquad \text{(eq III.4)}$$

where w_1 is its weight associated to its value of the variable x_1 and w_2 is its weight associated to its value of the variable x_2.
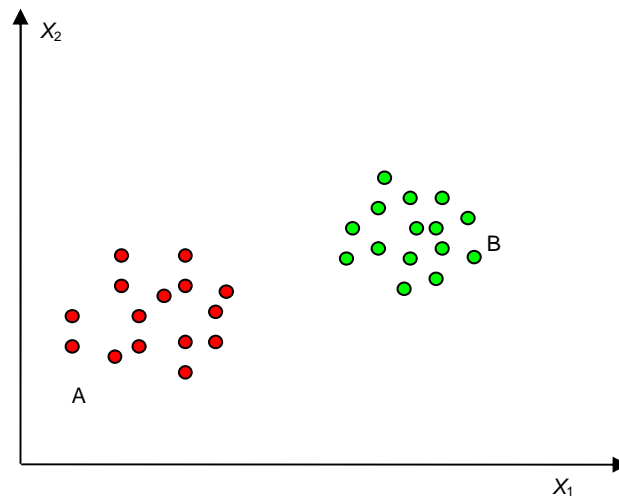
Figure III.5: objects divided in two classes projected onto the bi-dimensional space described by their variables (adapted from [41]).
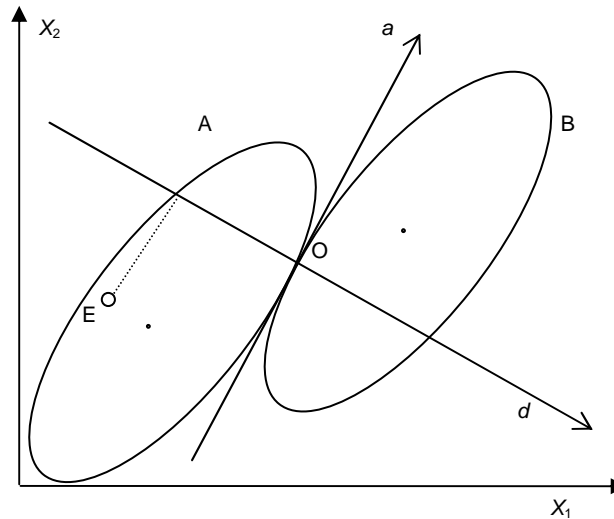
Figure III.6: Confidence limits around the centroids of classes A and B. These limits touches in point O; a is a line
tangential to both ellipses; d is the optimal discriminating direction; E is a new unknown object
(adapted from [41]).

The weights w_1 and w_2 are defined in such a way that D=0 in point O, D>0 for objects of class
B and D<0 for objects of class A. D is a latent variable (such as principal components in
PCA). However the difference is that LDA selects the direction that maximises the separation
between the classes. D is then called *canonical variate* and for *m* classes, *m*-1 canonical
variates can be determined.

3.5.   *k-Nearest Neighbour algorithm (k-NN) [41]*

The *k*-NN algorithm is a simple classification technique that uses the Euclidian distance (eq 2) between the objects.
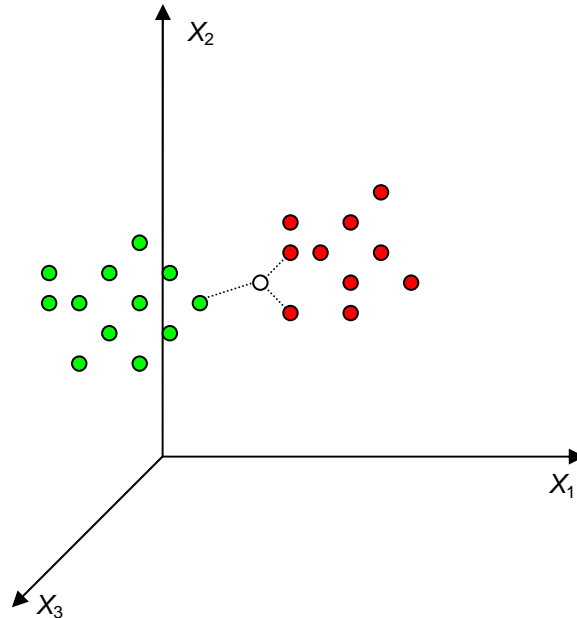
Figure III.7: 3-NN classification of a new object (white circle). The green and the red circles are two groups of objects projected onto the three-dimensional space described by their variables. (adapted from [41]).

As an example we can consider Figure III.7. Figure III.7 shows a dataset with 20 objects (12 of class A and 8 of class B) described in a three-dimensional space (x_1, x_2 and x_3). One must select the optimal number of *k* objects to be considered. Usually, small values (from 3 to 5) are to be preferred.

A new object E is projected in the three-dimensional space. Its Euclidian distance with all objects is computed and the *k* nearest objects are retained. E will be classified in the class to which belongs the majority of the *k* nearest objects (to the red class in FigureIII.7).

3.6.   *Soft Independent Modelling of Class Analogy (SIMCA) [41]*

The SIMCA algorithm emphasises more on the similarity within a class rather than on the discrimination between classes. Those methods called *disjoint class modelling* methods model each class separately. In comparison with LDA or *k*-NN which always classifies an object in a group, SIMCA considers this object as an outlier if it is not included in any class. SIMCA also works with latent variables instead of manifest variables. First of all, the optimal

number of latent variables needed to describe a group of objects is determined by means of leave-one-out cross-validation (LOOCV). LOOCV uses a single observation from the original dataset as the test set, and the remaining observations as the training set. This is repeated in such a way that each observation of the dataset is used once as the test set.
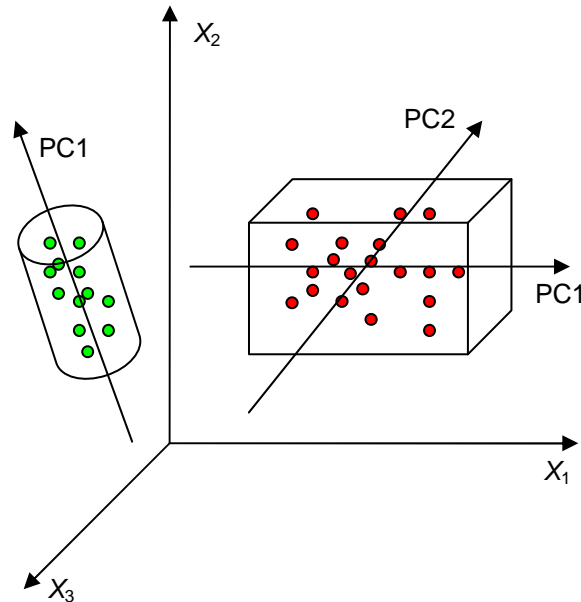
Figure III.8: SIMCA defines boxes around the object of a same class. The green circles are described by a single principal component while the red circles are described by two principal components.
(adapted from [41])

Figure III.8 shows two classes of objects projected onto the three-dimensional space described by the variables (x_1, x_2 and x_3). The class A is described only by one principal component while the class B is described by two principal components.

A critical value of the distance towards the model s_{crit} defines a confidence limit around the objects. The confidence limit is often set at 95% as probability level. This first criterion defines an open boundary around the principal components (open cylinder for class A and two infinite planes for class B of Figure III.8). A second criterion is needed to close the space around the objects. This criterion defines score limits along the principal components describing the objects:

$$t_{max} = \max(t_A) + 0{,}5 s_t \qquad \text{(eq III.5)}$$

$$t_{min} = \min(t_A) - 0{,}5 s_t \qquad \text{(eq III.6)}$$

where $\max(t_A)$ is the highest score of the objects of the training set of class A on the considered PC and s_t is the standard deviation of the scores along that PC.

Objects with a Euclidian distance $s < s_{crit}$ and scores $t_{min} < t < t_{max}$ are said to belong to the studied class otherwise they are considered as outliers. Once each class has been modelled alone, all class models are assembled. This constitutes the predictive model to be validated.

3.7.   *Classification And Regression Trees (CART)*

CART is a non-parametric statistical method used to solve classification and regression problems with categorical and continuous variables by means of a decision tree. It was first described by Breiman et al. [44] in 1984. Classification trees are used for categorical variables while regression trees are used for continuous variables.

For more details see chapter IV section 3.2.

References :

[1] http://www.who.int/medicines/services/counterfeit/faqs/en/index.html (last accessed 14-04-2011)

[2] Clift C., Combating Counterfeit, Falsified and Substandard Medicines Defining the Way Forward?, Chatham House Briefing Papers, November 2010

[3] http://www.europarl.europa.eu/sides/getDoc.do?pubRef=-//EP//TEXT+TA+P7-TA-2011-0056+0+DOC+XML+V0//EN (last accessed 14-04-2011)

[4] Venhuis B.J., Barends D.M., Zwaagstra M.E., de Kaste D., Recent developments in counterfeit and imitations of Viagra®, Cialis® and Levitra®, RIVM Report 370030001/2007, Bilthoven, 2007

[5] Schoen C., Bachmann G., Sildenafil citrate for female sexual arousal disorder: a future possibility?, Nature Review Urology (2009) 6, 216-22

[6] Viagra European public assessment report, Viagra -EMEA/H/C/000202 -II/0064, last update 13-07-2010

[7] Revatio European public assessment report, Revatio -EMEA/H/C/000638 -II/0030/G, last update 04-03-2011

[8] Bischoff E., Potency, selectivity and consequences of nonselectivity of PDE inhibition, International Journal of Impotence Research (2004) 16, 11-14

[9] Shin MH., Hong MK., Kim WS., Lee YJ., Jeoung YC., Identification of a new analogue of sildenafil added illegally to a functional food marketed for penile erectile dysfunction, Food Additives and Contaminants (2003) 20, 793-796

[10] Blok-Tip L.,Zomer B., Bakker F., Hartog K.D., Hamzink M., ten Hove J., Vredenbregt M., de Kaste D., Structure elucidation of sildenafil analogues in herbal products, Food Additives and Contaminants (2004) 21, 737-748

[11] Shin C., Hong M., Kim D., Lim Y., Structure determination of a sildenafil analogue contained in commercial herb drinks, Magnetic Resonance in Chemistry (2004) 42, 1060-1062

[12] Hou P., Zou P., Low M-Y., Chan E., Koh H-L., Structural identification of a new acetildenafil analogue from pre-mixed bulk powder intended as a dietary supplement, Food Additives and Contaminants (2006) 23, 870-875

[13] Lai K-C., Liu Y-C., Tseng M-C., Lin J-H., Isolation and identification of a sildenafil analogue illegally added in dietary supplements, Journal of Food and Drug Analysis (2006) 14, 19-23

[14] Lin M-C. Liu Y-C., Lin J-H., Identification of a sildenafil analogues adulterated in two herbal food supplements, Journal of Food and Drug Analysis (2006) 14, 260-264

[15] Reepmeyer J., Woodruff J., Use of liquid chromatography-mass spectrometry and a

chemical cleavage reaction for the structure elucidation of a new sildenafil analogue detected as an adulterant in an herbal dietary supplement, Journal of Pharmaceutical and Biomedical Analysis (2007) 44, 887-893

[16] Lin M-C, Liu Y-C., Lin Y-L., Lin J-H., Isolation and identification of a novel sildenafil analogue adulterated in dietary supplements, Journal of Food and Drug Analysis (2008) 16, 15-20

[17] Zou P., Hou P., Oh S.S-Y., Chong Y.M., Bloodworth B.C., Low M-Y., Koh H-L., Isolation and identification of thiohomosildenafiland thiosildenafil in health supplements, Journal of Pharmaceutical and Biomedical Analysis (2008) 47, 279-284

[18] Venhuis B.J., Zomer G., de Kaste D., Structure elucidation of a novel synthetic thiono analogue of sildenafil detected in an alleged herbal aphrodisiac, Journal of Pharmaceutical and Biomedical Analysis (2008) 46, 814-817

[19] Reepmeyer J., André d'Avignon D., Structure elucidation of thioketone analogues of sildenafil detected as adulterants in herbal aphrodisiacs, Journal of Pharmaceutical and Biomedical Analysis (2009) 49, 145-150

[20] Gratz S., Zeller M., Mincey D., Flurer C., Structural characterization of sulfoaildenafil, an analogue of sildenafil, Journal of Pharmaceutical and Biomedical Analysis (2009) 50, 228-231

[21] Venhuis B.J., Zomer G., Hamzink M., Meiring H.D., Aubin Y., de Kaste D.,The identification of a nitrosated prodrug of the PDE-5 inhibitor aildenafil in a dietary supplement: a Viagra with a pop, Journal of Pharmaceutical and Biomedical Analysis (2011) 54, 735-741

[22] Venhuis B.J., Zomer G., Vredenbregt M.J., de Kaste D., The identification of (-)-trans-tadalafil and sildenafil in counterfeit Cialis® and the optical purity of tadalafil stereoisomers, Journal of Pharmaceutical and Biomedical Analysis (2010) 51, 723-727

[23] Häberli A., Girard P., Low M-Y., Ge X., Isolation and structure elucidation of an interaction product of aminotadalafil found in an illegal health food product, Journal of Pharmaceutical and Biomedical Analysis (2010) 53, 24-28

[24] Reepmeyer J., Woodruff J., Use of liquid chromatography-mass spectrometry and a hydrolytic technique for the detection and structure elucidation of a novel synthetic vardenafil designer drug added illegally to a "natural" herbal dietary supplement, Journal of Chromatography A (2006) 1125, 67-75

[25] Lai K-C., Liu Y-C., Tseng M-C., Lin Y-L., Lin J-H., Isolation and identification of a vardenafil analogue in a dietary supplement, Journal of Food and Drug Analysis (2007) 15, 220-227

[26] Lam Y-H., Poon W-T., Lai C-K., Chan A Y-W., Mak T W-L., Identification of a novel vardenafil analogue in herbal product, Journal of Pharmaceutical and Biomedical Analysis (2008) 46, 804-807

[27] Lee H-M., Kim C.S., Jang Y.M., Kwon S.W., Lee B-J., Separation and structural elucidation of a novel analogue of vardenafil included as an adulterant in a dietary supplement by liquid chromatography-electrospray ionization mass spectrometry, infrared spectroscopy and nuclear magnetic resonance spectroscopy (2011) 54, 491-496

[28] Hasegawa T., Takahashi K., Saijo M., Ishii T., Nagata T., Kurihara M., Haishima Y., Goda Y., Kawahara N., Isolation and structural elucidation of cyclopentynafil and N-octylnortadalafil found in dietary supplement, Chemical and Pharmaceutical Bulletin (2009) 57, 185-189

[29] Ge X., Low M-Y., Zou P., Lin L., Yin S.O.S., Bloodworth B.C., Koh H-L.? Structural elucidation of a PDE-5 inhibitor detected as an adulterant in a health supplement, Journal of Pharmaceutical and Biomedical Analysis (2008) 48, 1070-1075

[30] Medsafe, classification of analogues of sildenafil, vardenafil and tadalafil, Report for the 41st MCC meeting, February 2009

[31] Vredenbregt M.J., Blok-Tip L., Hoogerbrugge R., Barends D.M., de Kaste D., Screening suspected counterfeit Viagra and imitations of Viagra with near-infrared spectroscopy, Journal of Pharmaceutical and Biomedical Analysis (2006) 40, 840-849

[32] Reddy T.S., Reddy A.S., Devi P., Quantitative determination of sildenafil citrate in herbal medicinal formulations by high-performance thin-layer chromatography, Journal of Planar Chromatography - Modern TLC (2006) 19, 427-431

[33] Park H.J., Jeong H.K., Chang M.I., Im M.H., Jeong J.Y., Choi D.M., Park K., Hong M.K., Youm J., Han S.B., Kim D.J., Park J.H., Kwon S.W., Structure determination of new analogues of vardenafil and sildenafil in dietary supplements, Food Additives and Contaminants (2007) 24, 122-129

[34] Sacré P-Y, Deconinck E., De Beer T., Courselle P., Vancauwenberghe R., Chiap P., Crommen J., De Beer J.O., Comparison and combination of spectroscopic techniques for the detection of counterfeit medicines, Journal of Pharmaceutical and Biomedical Analysis (2010) 53 445-53

[35] de Veij M., Deneckere A., Vandenabeele P., de Kaste D., Moens L., Detection of counterfeit Viagra with Raman spectroscopy, Journal of Pharmaceutical and Biomedical Analysis (2008) 46, 303-309

[36] Trefi S., Routaboul C., Hamieh S., Gilard V., Malet-Martino M., Martino R., Analysis of illegally manufactured formulations of tadalafil (Cialis) by ^{1}H NMR, 2D DOSY ^{1}H NMR and Raman spectroscopy, Journal of Pharmaceutical and Biomedical Analysis (2008) 47, 103-113

[37] Maurin J.K., Pluciński F., Mazurek A.P., Fijałek Z., The usefulness of simple X-ray powder diffraction analysis for counterfeit control - the Viagra example, Journal of Pharmaceutical and Biomedical Analysis (2007) 43, 1514-1518

[38] Amin A.S., Moustafa M.E., El-Dosoky R., Colorimetric determination of sildenafil citrate (Viagra) through ion-associate complex formation, Journal of AOAC International (2009) 92, 125-130

[39] Rodomonte A.L., Gaudiano M.C., Antoniella E., Lucente D., Crusco V., Bartolomei M., Bertocchi P., Manna L., Valvo L., Muleri N., Counterfeit drugs detection by measurement of tablets and secondary packaging colour, Journal of Pharmaceutical and Biomedical Analysis (2010) 53, 215-220

[40] Wawer I., Pisklak M., Chilmonczyk Z., ^{1}H, ^{13}C, ^{15}N NMR analysis of sildenafil base and citrate (Viagra) in solution, solid state and pharmaceutical dosage forms, Journal of Pharmaceutical and Biomedical Analysis (2005) 38, 865-870

[41] Vandeginste B.G.M., Massart D.L., Buydens L.M.C., De Jong S., Lewi P.J., Smeyers-verbeke J.: Handbook of Chemometrics and Qualimetrics-Part B, Elsevier Science, Amsterdam, 1997

[42] Massart D.L., Vandeginste B.G.M., Buydens L.M.C., De Jong S., Lewi P.J., Smeyers-verbeke J.: Handbook of Chemometrics and Qualimetrics-Part A, Elsevier Science, Amsterdam, 1997

[43] Kennard R.W., Stone L.A., Computer aided design of experiments, Technometrics (1969) 11, 137-148

[44] Breiman L., Friedman J.H., Olshen R.A., Stone C.J., Classification and regression trees; Wadsworth & Brooks, Monterey, 1984

IV. Spectroscopic techniques

1. Introduction:

When analyzing suspect medicines, one wants to have quick results, reliable information and avoid the destruction of the sample in order to be able to re-analyse it later or if necessary with another technique. These requests are met with the NIR and Raman spectroscopic techniques. However, as these techniques are not already present in every control laboratory, the usefulness of the Fourier-Transformed Infrared Spectroscopy has also been investigated in the frame of this thesis.

2. Theory:

2.1. The electromagnetic radiation [1,2]

Spectroscopic techniques study the interaction between an electromagnetic radiation and the matter. These techniques are classified according to the region of the electromagnetic spectrum measured (Figure IV.1).
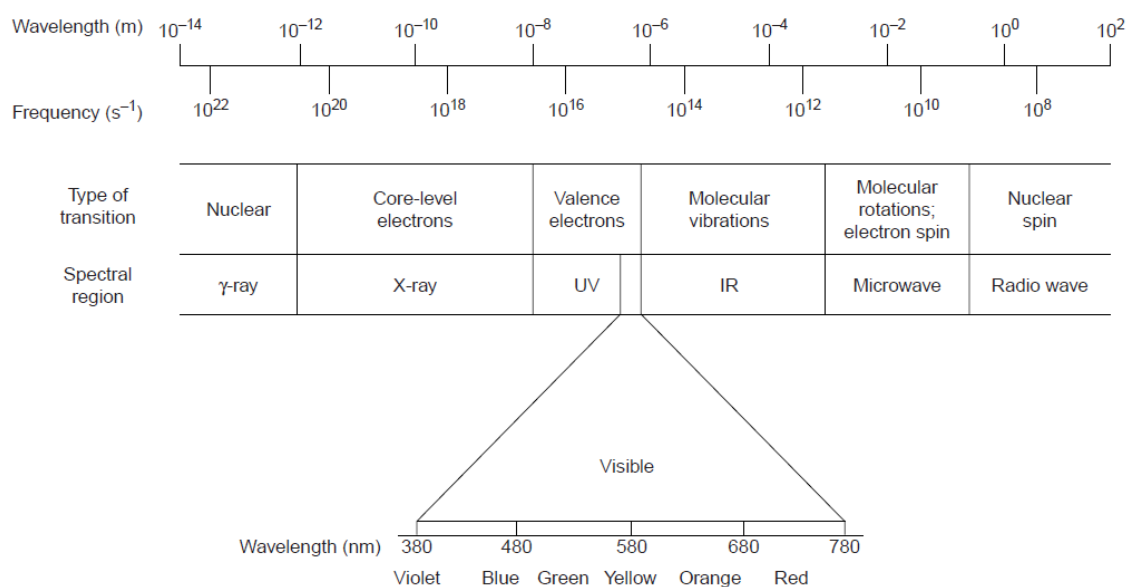
Figure IV.1: Electromagnetic spectrum (reproduced from [1]).

Electromagnetic radiation is a form of energy that consists of oscillating electric and magnetic fields that propagate through space along a linear path with a constant velocity (Figure IV.2). It has the properties of both particles and waves.

As a wave, light has characteristics of wavelength, frequency, amplitude and velocity.
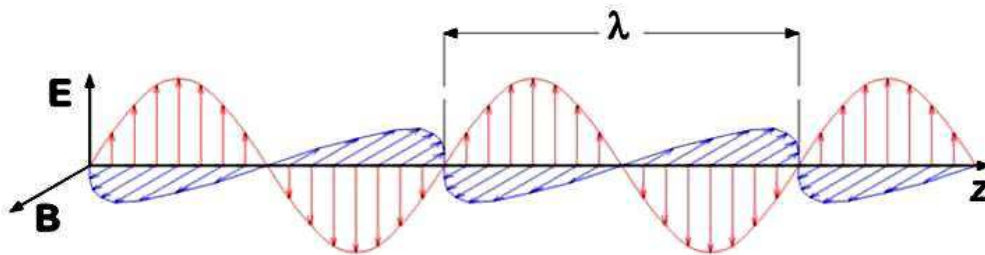
Figure IV.2: Electromagnetic wave. E is the electric component (red) in plane of drawing; B is the magnetic component (blue) in orthogonal plane. The wave propagates to the right with a wavelength λ.
(Source http://commons.wikimedia.org/wiki/File:Electromagnetic_wave.png; 11/05/2011)

The wavelength is the distance between two successive maxima (or minima) and is represented by the Greek letter λ. In the UV/visible region, λ is expressed in nanometres while in the infrared region it is expressed in micrometers. However, when working in the infrared region of the electromagnetic spectrum, one works with wavenumbers (expressed in cm^{-1}) rather than with wavelengths. The wavenumber ($\bar{\nu}$) represents the number of finished cycle per centimetre.

$$\bar{\nu} = \frac{1}{\lambda}$$
(eq IV.1)

Most of the interactions between the electromagnetic radiation and the matter are better described considering light as a particle (photon). The energy (E) of these photons is proportional to the frequency:

$$E = \frac{hC}{\lambda} = hC\bar{\nu}$$
(eq IV.2)

where h is the Planck's constant (6.63×10^{-34} Js) and C is the velocity of light in vacuum.

2.2. *Fourier-transformed Infrared spectroscopy (FT-IR) [5]*

2.2.1. *Fundamental concepts:*

When irradiating a sample with a mid-IR radiation (wavenumbers of 4000-400 cm^{-1}), a part of the energy is absorbed by the molecules. If the energy is sufficient, the molecular bonds go up to an excited state of energy. This excitation results in bending (change in angle) and stretching (change length) vibrations of the electron cloud (molecular bond) (Figure IV.3).
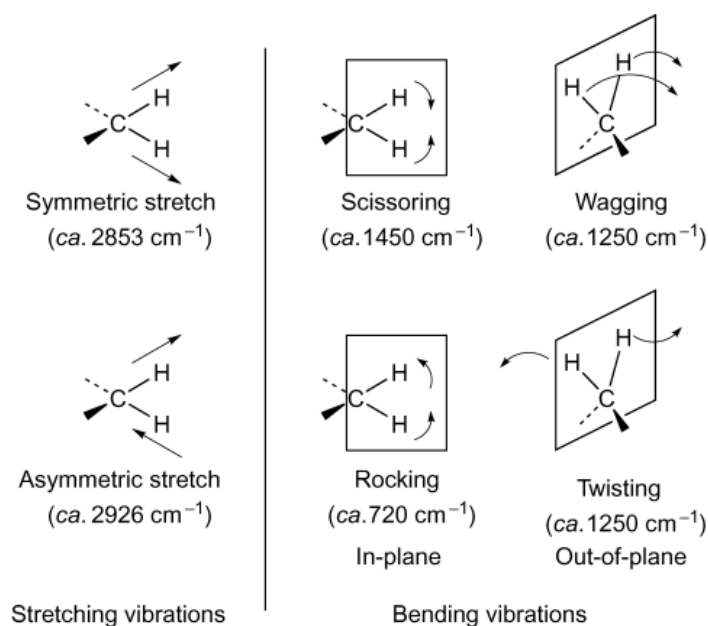
Figure IV.3: Different types of molecular vibrations of the methylene group (reproduced from [5])

After being excited, the molecular bonds return to their ground state of energy. When returning to a lower state of energy, photons are emitted. These photons are detected by spectrometers and transformed in electric signal.

The amount of energy needed to excite a molecular bond depends on the atoms involved and the strength of the bond. This is very useful to detect the existence of functional groups in a molecule. Indeed, a specific wavelength radiation will excite specific bonds. This opportunity to identify functional groups in a molecule is only possible within the 4000-1800cm^{-1} region. Indeed, in the 1800-400 cm^{-1} region (*fingerprint region*), too many peaks are present and are therefore hardly assigned to specific functional groups. It may, on the other hand, be used as a specific fingerprint of the analysed molecule for the identification of pure compounds or the identification of specific mix of compounds (such as tablets).

2.2.2. *Apparatus:*

A scheme describing a FT-IR spectrometer is represented in Figure IV.4. The initial laser beam (A) goes through the beam splitter (or Michelson interferometer) and is split in two beams (B and C). These two beams are reflected by mirrors (M_1 and M_2) and gather in a single beam F. M_1 is an oscillating mirror which means that the distance travelled by B and D changes in function of the M1 position. If M_1 and M_2 are at the same distance to the interferometer, the association of D and E is called *fully constructive* and the intensity of F is maximal. If M_1 moves and leads to beam D being a half wave ahead of beam E, their association becomes *fully destructive*.
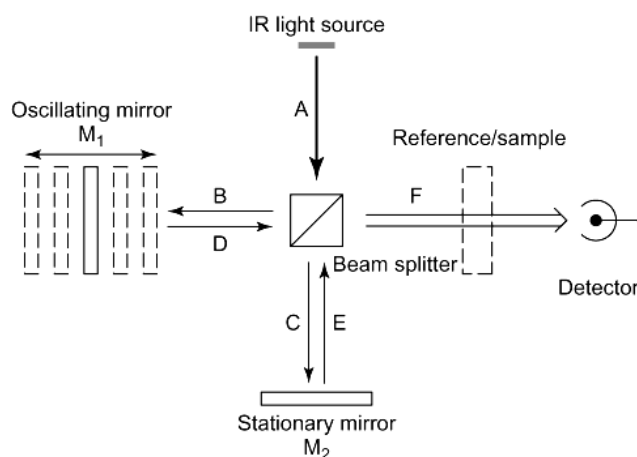
Figure IV.4: FT-IR spectrometer. For details about letters, see text. (reproduced from [5]).

The intensity of F becomes then zero. As M_1 is oscillating, the signal detected is called interferogram (Figure IV.5a). The Fourier transformation is applied on the signal of the interferogram transforming it in an interpretable signal, the FT-IR spectrum (Figure IV.5b).

a)

b)
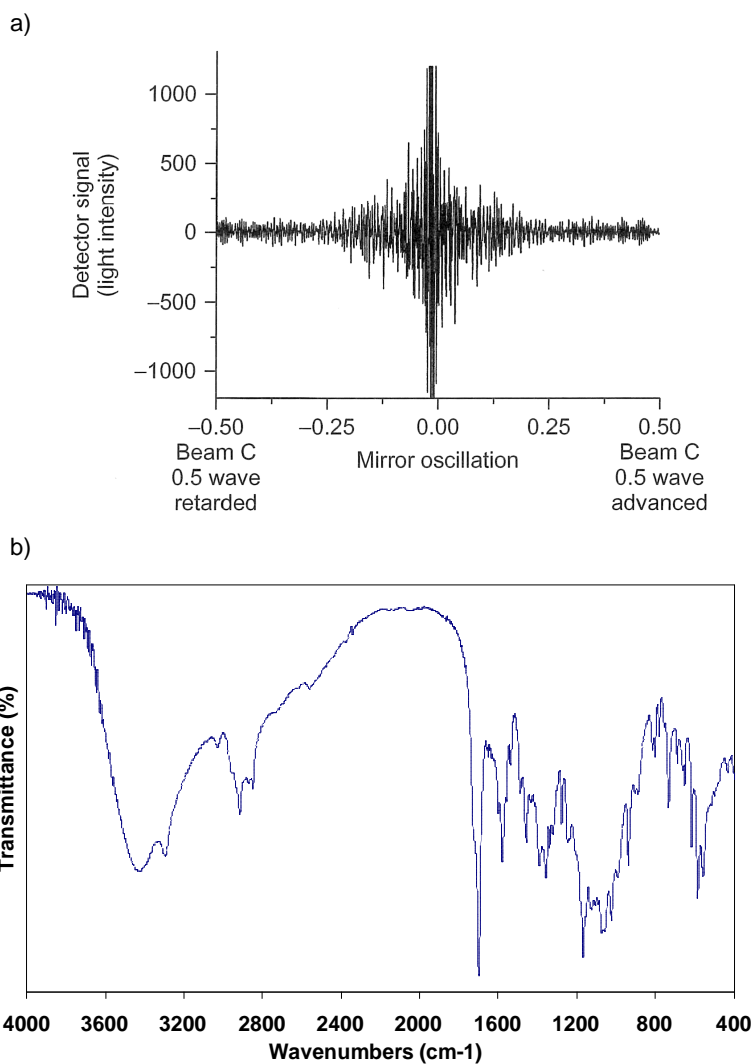
Figure IV.5: a) interferogram produced by a single mirror oscillation; b) resulting FT-IR spectrum of a genuine Viagra® tablet after Fourier transformation was applied. (Figure IV.5a reproduced from [5]).

The most widely used pyroelectric detector is the DTGS (deuterated triglycine sulphate).

The samples may be analysed qualitatively and quantitatively under their solid, liquid or gaseous form. For each of these forms, limitations and specific instrumentations exist.

For solid samples, the KBr disk is the most commonly used technique. One mixes about 1mg of the sample (beforehand finely powdered and dried) with about 250mg of dry KBr in an agate mortar. The mixture is pressed under 10-20 tons pressure. The resulting disk is placed in the laser radiation and its spectrum is recorded. The KBr disk has many disadvantages: difficulty to avoid the presence of water, chemical reactions between the sample and KBr, degradation of the original product due to pressure or heat. To avoid many of these problems, KCl may be used instead of KBr.

For liquid samples or solutions, a drop of the sample is placed between two IR transparent plates (or in a cell for volatile solvents). These plates are often made with NaCl but other materials may be used. Working with solutions has many advantages such as sharper peaks, no difference between solid states (amorphous or crystalline). However, the samples must be soluble in the solvent which must absorb as little as possible without dissolving the plates.

Gaseous samples are rarely analysed by mid-IR spectroscopy. However, special cells with NaCl windows exist.

2.3. *Near Infrared spectroscopy (NIR) [4]*

2.3.1. *Fundamental concepts:*

The NIR region of the electromagnetic spectrum is comprised between 12500 and 4000 cm^{-1} (800-2500 nm). While the mid-IR absorbances correspond mainly to fundamental vibrations, the NIR absorbances correspond to overtones (excitation of a vibration to a double or higher frequency) and combinations of molecular vibrations. This is why the interpretation of NIR spectra is more difficult than mid-IR spectra.

The NIR spectra are essentially used for qualitative analysis because of their fingerprint nature and the fact that the NIR spectra contain both chemical and physical information. For qualitative analysis, the spectra are always measured by reflectance.

The reflected radiation is made up of two main components, the specular and the diffuse radiation. The specular radiation (I_{rs}) is simply reflected from the surface of the sample. It contains thus little information. The diffuse reflected radiation (I_{rdr}) penetrates deeper in the sample (0,1-1 mm for a tablet) and undergoes several reflections within the sample before re-emerging (Figure IV.6). The way of the diffuse reflected radiation depends on many

factors such as the particle size, the compaction, the particle shape, etc. This allows analysts to obtain physical information about the sample that often makes possible the differentiation between samples with the same chemical composition but from different sources. This physical information together with the chemical information make the NIR spectrum a very complete but difficult to interpret fingerprint.
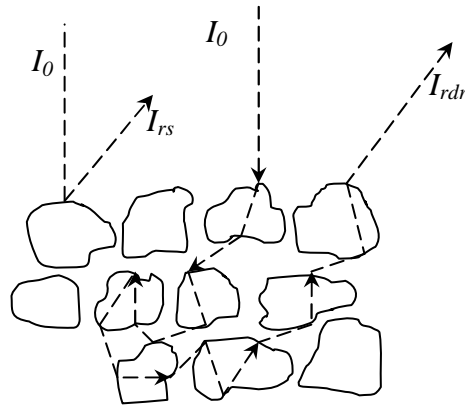
Figure IV.6: Reflectance of a radiation by the particles of the surface of a tablet. I_0, intensity of incoming radiation; I_{rs}, intensity of the specular radiation; I_{rdr} intensity of the diffuse reflectance radiation (adapted from [4]).

The NIR spectrum (Figure IV.7) is reported as a plot of absorbance (calculated as $\log\left(\dfrac{1}{R}\right)$) against wavenumber. Reflectance (R) is given by the ratio of the intensity of the reflected light ($I_{rs} + I_{rdr}$) to the intensity of the incident light (I_0) (eq IV.3).

$$R = \left(\frac{(I_{rs} + I_{rdr})}{I_0}\right) \qquad\qquad \text{(eq IV.3)}$$
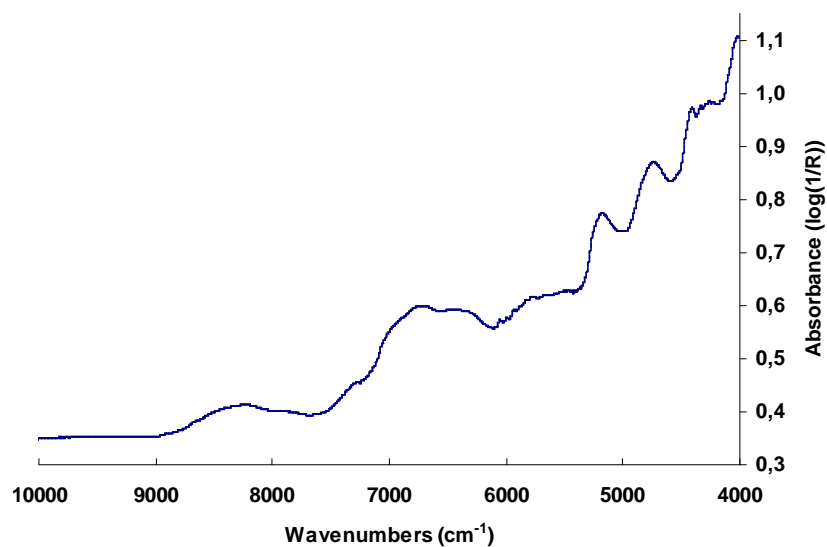
Figure IV.7: NIR reflectance spectrum of a genuine tablet of Viagra[®]

2.3.2. Apparatus:

There exist fixed wavelength, dispersive or interferometer NIR spectrometers. The system used during this thesis is an FT-NIR (Nicolet Antaris II near-IR analyzer, Thermo Fisher Scientific, Waltham, MA, USA) equipped with an indium gallium arsenide detector and a quartz halogen lamp as energy source. As an interferometer designed system, it functions with the same principles as the FT-IR spectrometers. If the measurements may be performed by both reflectance and transmittance, the reflectance mode is the easiest and widest used one.

NIR spectroscopy is commonly used in the pharmaceutical analysis. It may be used to follow the fabrication of tablets at many steps [6], to detect counterfeit products [7] or to perform assays [8].

2.4. Raman spectroscopy [3]

2.4.1. Fundamental concepts:

Raman spectroscopy studies the radiation scattered by a sample when irradiated with a monochromatic radiation.

If the incident radiation is sufficiently energetic, absorption process may occur. If the incident radiation is of insufficient energy to attain an excited energy level S_1, the molecule goes to a *virtual state* of energy. The molecule then returns to a lower level of energy and if it relaxes to the original vibrational state of energy, photons are emitted with the same frequency as the incident radiation. These scattered photons represent the *elastic* (or *Rayleigh*) *scattering* and constitute the majority of the scattered light (Figure IV.8., transition A).
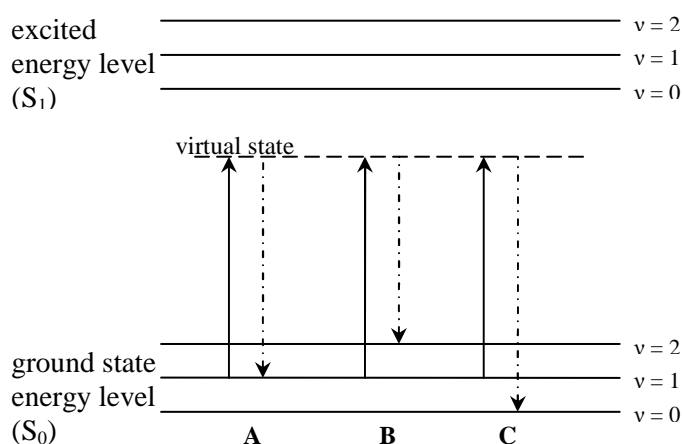
Figure IV.8: Energy level diagram showing the different scattering processes. A, Rayleigh scattering; B, Stokes Raman scattering; C, anti-Stokes Raman scattering. (adapted from [3])

Besides this elastic scattering, a few proportion of photons are scattered at frequencies above or below the original energy level (*inelastic scattering*). If the molecule relaxes to a higher energy level than the original one, the emitted photon is of lower energy (lower frequency) than the original radiation. This constitutes the *Stokes Raman scattering* (Figure IV.8, transition B). On the other hand, if the molecule relaxes to a lower energy level than the original one, the emitted photon is of higher energy (higher frequency) than the original radiation. This constitutes the *anti-Stokes Raman scattering* (Figure IV.8, transition C). The inelastic scattering is explained by the fact that the polarisability of the electron cloud (molecular bond) may change when the position of the atoms involved in the bond change because of their vibration induced by the incident radiation. These changes in polarisability of the chemical bond influence the frequency at which the photons are emitted when the molecule relaxes. Thus, to be Raman active, a molecule must undergo a change in polarisability of its bonds (called the Raman selection rule).

As a fewer proportion of photons are scattered by anti-Stokes Raman scattering (Maxwell-Boltzmann distribution), the Stokes lines are of higher intensities. Then, the Raman spectrum (Figure IV.9) is often constructed by plotting the Raman intensities (arbitrary units) against Stokes shifts (or Raman shift, cm^{-1}).
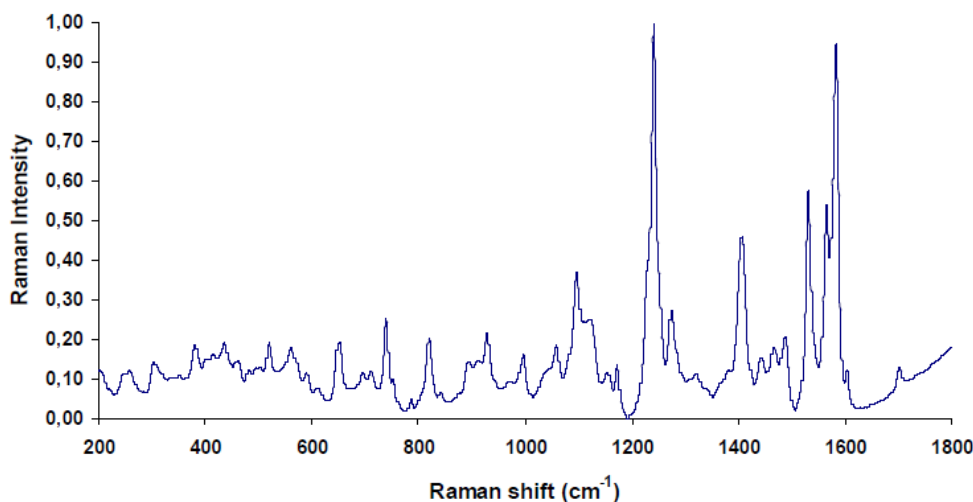
Figure IV.9: Raman spectrum of a genuine tablet of Viagra[®].

Raman spectroscopy may be used in the elucidation of a molecular structure. Raman spectroscopy is a complementary technique to mid-IR spectroscopy. Indeed, a vibrational mode is Raman active when there is a change in polarisability during the vibration whether it is mid-IR active when there is a change in the molecular dipole moment during the vibration. Thus, a vibrational mode that is highly Raman active will be weakly mid-IR active and vice versa.

The amount of energy required by a bond to vibrate is given by the equation IV.4:

$$E = h\nu = h\nu' + \Delta E_{vib} \tag{Eq IV.4}$$

where h is the Planck's constant, ν is the excitation frequency, ν' is the scattered light frequency and ΔE_{vib} is the vibrational energy.

2.4.2. Apparatus:

There exist two types of Raman spectrometers: dispersive and interferometric spectrometers. The spectrometer used during this thesis was a dispersive system (RamanRxn 1, Kaiser Optical systems, Ann Arbor, MI, USA). The source of the monochromatic radiation is a laser (the used spectrometer has a 785 NIR laser source). This wavelength is a good compromise between fluorescence (more frequent at lower wavelengths) and sensitivity (higher intensities at low wavelengths).

In a dispersive system (Figure IV.10), the scattering radiation is collected in a 180° or 90° configuration. The scattered light goes then through a laser-line filter to remove the Rayleigh component of the scattering. Finally a charge-coupled detector (CCD) is used to measure the intensity of the incoming light.
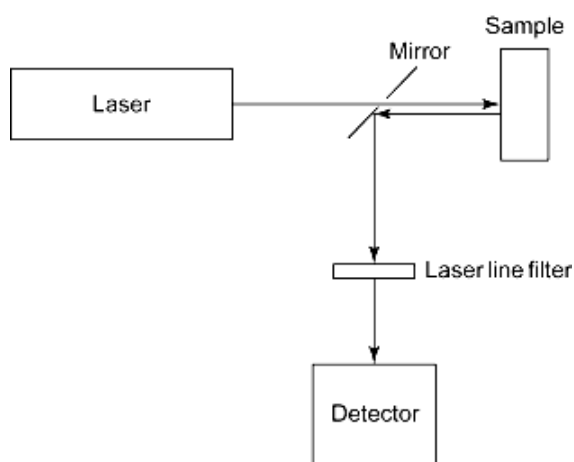
Figure IV.10: Dispersive Raman spectrometer (reproduced from [3])

The spectrometers may also be connected to a microprobe. The scattered light is thus collected in a 180° configuration.

Raman spectroscopy has many applications in the pharmaceutical domain for both qualitative and quantitative analysis [6,9].

References

[1] David H, *in* Modern Analytical Chemistry, Mc Graw Hill, international editions, 2000, 368-446

[2] Skoog D.A., West D.M., Holler F.J., Crouch S.R., *in* Fundamentals of analytical chemistry, Thomson Brooks/Cole, Belmont, 2004, 710-819

[3] Bugay, D.E., Martoglio Smith, P.A. (2004) Raman spectroscopy *in* Moffat A.C., Osselton M.D., Widdop B. (Ed.), *Clarke's analysis of drugs and poisons*, Pharmaceutical Press, London, UK.

[4] Jee, R.D. (2004) Near-infrared spectroscopy. *in* Moffat A.C., Osselton M.D., Widdop B. (Ed.), *Clarke's analysis of drugs and poisons*, Pharmaceutical Press, London, UK.

[5] Drake, A. (2004) Infra-red spectroscopy *in* Moffat A.C., Osselton M.D., Widdop B. (Ed.), *Clarke's analysis of drugs and poisons*, Pharmaceutical Press, London, UK.

[6] De Beer T., Burggraeve A., Fonteyne M., Saerens L., Remon J.P., Vervaet C., Near infrared and Raman spectroscopy for the in-process monitoring of pharmaceutical production processes, International Journal of Pharmaceutics (2011) 412, 32-47

[7] Rodionova O.Y., Pomerantsev A.L., NIR-based approach to counterfeit-drug detection, Trends in Analytical Chemistry (2010) 29, 795-803

[8] Ziémons E., Mantanus J., Lebrun P., Rozet E., Evrard B., Hubert Ph., Acetaminophen determination in low-dose pharmaceutical syrup by NIR spectroscopy, Journal of Pharmaceutical and Biomedical Analysis (2010) 53, 510-516

[9] Wartewig S., Neubert R.H.H., Pharmaceutical applications of Mid-IR and Raman spectroscopy, Advanced Drug Delivery Reviews (2005) 57, 1144-1170

3. <u>Results</u>

3.1. Comparison and combination of spectroscopic techniques for the detection of counterfeit medicines.

The interest of NIR and Raman spectroscopy to detect counterfeit medicines has been assessed in numerous previous researches. However, these studies consider each technique separately. It was therefore decided to evaluate whether each technique provides comparable discrimination and if a combination of these techniques would be useful.

Fifty five samples of counterfeit and imitations of Viagra® and thirty nine samples of counterfeit and imitations of Cialis® were analysed by NIR, FT-IR and Raman spectroscopy. These samples mainly belong to the RIVM professional imitations class. This constitutes a limitation to the present study since the RIVM classes are used to obtain the different conclusions.

The recorded spectra were pre-processed and analysed by PCA. This unsupervised analysis did not provide a sufficient discrimination. To enhance the discrimination between illegal and genuine preparations, a PLS analysis has been performed. This supervised analysis allowed a clear distinction between illegal and legal tablets with each technique and combination of techniques. The comparison between the techniques and their combination has been performed according to the number of unclassified samples and the homogeneity of the clusters according to the RIVM class of the samples.

Besides this visual cluster classification, a predictive and classifying algorithm has been employed. A predictive model has been built using CART algorithm. This allows predicting if a new unknown sample is genuine or not. Furthermore, CART has been used to predict the class of new samples following RIVM classification based on their spectroscopic data.

Methods and results are described in the following publications:

Sacré P-Y, Deconinck E, De Beer T, Courselle P, Vancauwenberghe R, Chiap P, Crommen J, De Beer J, Comparison and combination of spectroscopic techniques for the detection of counterfeit medicines, Journal of Pharmaceutical and Biomedical Analysis (2010), 53, 445-453

Deconinck E, Sacré P-Y, Coomans D, De Beer J, Classification trees based on infrared spectroscopic data to discriminate between genuine and counterfeit medicines, Journal of Pharmaceutical and Biomedical Analysis (2012), 57, 68-75

Comparison and combination of spectroscopic techniques for the detection of counterfeit medicines

Pierre-Yves Sacré[a,c], Eric Deconinck[a], Thomas De Beer[b], Patricia Courselle[a],

Roy Vancauwenberghe[d], Patrice Chiap[c], Jacques Crommen[c], Jacques O. De Beer[a]

[a] Laboratory of Drug Analysis, Scientific Institute of Public Health, Brussels, Belgium

[b] Laboratory of Pharmaceutical Process Analytical Technology, Ghent University, Ghent, Belgium.

[c] Department of Analytical Pharmaceutical Chemistry, Institute of Pharmacy, University of Liège,

Liège, Belgium.

[d] Federal Agency for Medicines and Health Products, Brussels, Belgium

Abstract

During this study, Fourier transform infrared spectroscopy (FT-IR), near infrared spectroscopy (NIR) and Raman spectroscopy were applied to 55 samples of counterfeit and imitations of Viagra[®] and 39 samples of counterfeit and imitations of Cialis[®]. The aim of the study was to investigate which of these techniques and associations of them were the best for discriminating genuine from counterfeit and imitation samples. Only the regions between 1800-400 cm^{-1} and 7000-4000 cm^{-1} were used for FT-IR and NIR spectroscopy respectively. Partial Least Square analysis has been used to allow the detection of counterfeit and imitation tablets. It is shown that for the Viagra[®] samples, the best results were provided by a combination of FT-IR and NIR spectroscopy. On the other hand, the best results for the Cialis[®] samples were provided by the combination of NIR and Raman spectroscopy (1400-1190 cm^{-1}). These techniques permitted a clear discrimination between genuine and counterfeit or imitation samples but also the distinction of clusters among illegal samples. This might be interesting for forensic investigations by authorities.

Keywords:

counterfeiting; phosphodiesterase type 5 inhibitors; IR-spectroscopy; partial least squares.

1. **Introduction**

Counterfeit medicines are more and more present since the last decade. This is mostly due to the extension of the internet and the apparition of numerous fraudulent websites where anyone can easily and anonymously buy prescription only medicines [1,2]. In developed countries, the most popular counterfeit drugs are lifestyle medicines like, among others, the phosphodiesterase type 5 (PDE-5) inhibitor drugs: sildenafil citrate (Viagra®), tadalafil (Cialis®) and more recently vardenafil hydrochloride (Levitra®) [3].

The internationally recognized definition of a counterfeit medicine is the one of the World Health Organization (WHO) [4]:

> "A counterfeit medicine is one which is deliberately and fraudulently mislabelled with respect to identity and/or source. Counterfeiting can apply to both branded and generic products and counterfeit products may include products with the correct ingredients or with the wrong ingredients, without active ingredients, with insufficient active ingredient or with fake packaging."

However, the most encountered illegal drugs in Belgium do not exactly correspond to this definition because most of them do not copy the packaging and brand names of the genuine products. This is why the classification proposed by the Dutch National Institute for Public Health and the Environment (RIVM) [3] was applied. They make the distinction between counterfeits, which appearance is in conformity with genuine medicines and imitations which do not look like genuine (table1). In fact these imitations come in most cases from Asia (mainly India and China) where they do not recognize European and American patent laws. So they are legally manufactured in those countries but illegally imported in Europe.

Several techniques have been used for the analysis of erectile dysfunction drugs [5]. Among these, colorimetry [6,7], TLC [8], NMR (^{1}H, ^{13}C, ^{15}N) [9], NMR (^{1}H, [2]D DOSY ^{1}H) [10], HPLC-UV [11], LC-ESI-MS-MS [12], extracted ion LC–MS/TOF [13], LC-DAD-CD [14]. For the specific detection of counterfeit drugs, spectroscopic techniques are preferred because they are fast and need only a little sample preparation or no preparation at all. Raman spectroscopy has been used to detect counterfeit Viagra® by de Veij et al. [15], counterfeit Cialis® by Trefi et al. [10] Roggo et al. [16] used Raman spectroscopy for the identification of pharmaceutical tablets and Vajna et al. [17] used Raman spectroscopy for the identification of different manufacturing technologies. Vredenbregt et al. [8] used the near infrared (NIR) spectroscopy to check the homogeneity of a batch of genuine Viagra® and to screen for the presence of sildenafil citrate. Storme-Paris et al. [18] and Chong et al. [19] also used the NIR spectroscopy for the detection of counterfeit drugs and the identification of antibiotics

respectively. A comparison of NIR and Raman spectroscopy for the detection of counterfeit Lipitor® has been realised by de Peinder et al. [20]. It has been demonstrated that NIR-Chemical imaging was able to detect counterfeit medicines [21, 22, 23]. Finally, Maurin et al. [24] permitted the prediction of the presence of sildenafil citrate and/or particular excipients in counterfeit Viagra® by the mean of X-ray powder diffraction (XRD).

Table 1: Classification of illegal medicines according to the RIVM [3]

Main category	Subcategory	Inclusion and exclusion criteria
Counterfeit	Accurate	Appearance in conformity with genuine medicine; Content of correct API within 90 - 110 % of declared value; No other APIs; not genuine medicine.
	Non-accurate	Appearance in conformity with genuine medicine; Content of correct API outside 90 - 110 % of declared value; No other APIs.
	Mixed	Appearance in conformity with genuine medicine; Contains correct API and another, known API
	Fraudulent	Appearance in conformity with genuine medicine; Contains a different, known API.
	Analog	Appearance in conformity with genuine medicine, Contains other, unapproved API
	Placebo	Appearance in conformity with genuine medicine; Does not contain APIs.
Imitation or Food supplement	Accurate	Appearance not in conformity with genuine medicine; Content of correct API within 90 - 110 % of declared value; No other APIs.
	Non-accurate	Appearance not in conformity with genuine medicine; Content of declared API outside 90 - 110 % of declared value; No other APIs.
	Mixed	Appearance not in conformity with genuine medicine; Contains declared API and another API.
	Fraudulent	Appearance not in conformity with genuine medicine; Contains an undeclared API.
	Analog	Appearance not in conformity with genuine medicine; Contains other, unapproved API
	Placebo	Appearance not in conformity with genuine medicine; Does not contain APIs.

In this study, 55 counterfeit and imitations of Viagra®, 9 genuine Viagra®, 39 counterfeit and imitations of Cialis® and 4 genuine Cialis® were analysed by Raman-, NIR- and FT-IR-spectroscopy. It has been investigated which technique or combination of these techniques was the best to (1) detect counterfeit Viagra® and counterfeit Cialis® and (2) to make clusters in illegal medicines which can be useful for forensic investigations by authorities.

2. __Experimental__
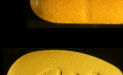
2.1. *Samples*

The counterfeit and imitation tablets of Viagra[®] and Cialis[®] were donated by the Federal Agency for Medicines and Health Products in Belgium (AFMPS/FAGG). They all come from postal packs ordered by individuals via internet sites. All samples were delivered in blisters or closed jars with or without packaging. All samples, once received, were stored at ambient temperature and protected from light. The samples have been divided in groups according to their visual aspect. Table 2 and 3 shows the groups of Viagra[®]-like and Cialis[®]-like samples respectively.

Table 2: Viagra[®]-like samples. (For RIVM classes see table 1)

Group number	Sample photo	Symbol in plots	RIVM Class	Number of Samples
1		●	Non-accurate counterfeits	6
2		X	Accurate imitation	8
3		□	Accurate imitations and one non-accurate imitation	4
4		*	accurate imitation	23
5		Δ	Accurate imitation	4
6		☆	accurate imitation and one mixed imitation	5
Other		◊	Non-accurate imitation and one accurate imitation	5
genuine		○		9

Table 3: Cialis®-like samples. (For RIVM classes see table 1)

Group number	Sample photo	Symbol in plots	RIVM Class	Number of samples
1		●	Mixed counterfeits	5
2		X	Accurate imitation	4
3		□	Accurate imitation	5
4		*	Non-accurate imitation	3
5		Δ	accurate imitation	13
6		☆	Non-accurate imitation and two mixed imitations	4
7		✡	Non-accurate imitation	2
other		◊	accurate imitation and mixed imitations	3
genuine		○		4

Pfizer SA/NV (Belgium) kindly provided one batch of each different dosage of Viagra® (25mg, 50mg, 100mg). Two other batches of each dosage were purchased in a local pharmacy in Belgium.

Eli Lilly SA/NV (Benelux) kindly provided one batch of commercial packaging of Cialis® (10mg and 20mg). Two other batches of Cialis® 20mg were purchased in a local pharmacy in Belgium.

All references were delivered in closed blisters with packaging and were stored protected from light at ambient temperature.

2.2.   Instrumental

2.2.1. Raman spectroscopy

A RamanRxn1 spectrometer (Kaiser Optical Systems, Ann Arbor, MI, USA), equipped with an air-cooled charge coupled device (CCD) detector (back-illuminated deep depletion design) was used in combination with a fiber-optic non-contact probe to collect Raman spectra from the core of the tablets. The laser wavelength during the experiments was the

785 nm line from a 785 nm Invictus NIR diode laser. All spectra were recorded in the range of 0-3500cm^{-1} with a resolution of 4 cm^{-1} using a laser power of 400 mW. Data collection, data transfer, and data analysis were automated using the HoloGRAMS^{TM} (Kaiser Optical Systems, USA, version 2.3.5) data collection software, the HoloREACT^{TM} (Kaiser Optical Systems, USA, version 2.3.5) reaction analysis and profiling software, the Matlab software (The Matworks, Natick, MA, USA, version 7.7), and the Grams/AI-PLSplusIQ software (Thermo Fisher Scientific, Waltham, MA, USA, version 7.02). Ten second exposures were used for spectral acquisition. Spectra were collected at 3 locations per tablet. Spectra were preprocessed by baseline correction (Pearson's method, [25]), mean centered and averaged before data-analysis.

2.2.2. NIR spectroscopy

Diffuse reflectance NIR spectra were collected per tablet using a Fourier-Transform NIR spectrometer (Thermo Fisher Scientific, Nicolet Antaris II near-IR analyzer) equipped with an InGaAS detector, a quartz halogen lamp and an integrating sphere, which was used for NIR spectra collection from the tablets. Data analysis was done using Thermo Fisher Scientific's Result software, SIMCA-P (Umetrics AB, Kinnelon, NJ, USA, version 11) and Matlab (The Matworks, Natick, MA, USA, version 7.7). Each spectrum was collected in the 10 000 – 4000 cm^{-1} region with a resolution of 16 cm^{-1} and averaged over 16 scans. All spectra were preprocessed using standard normal variate transformation (SNV) and mean centered before data-analysis. Each spectrum was performed on the core of the tablet.

2.2.3. FT-IR spectroscopy

A Spectrum 1000 (Perkin Elmer, Waltham, MA, USA) FT-IR spectrometer with a DTGS detector was used. All spectra were recorded from the accumulation of 16 scans in 4000-400 cm^{-1} range with a 4 cm^{-1} resolution. Samples were prepared by compressing a 0.3% mixture of pulverised tablet with spectral grade KBr (Merck, Germany). Three spectra of each sample were obtained, normalized and averaged.

Once recorded, the spectra were normalized with the Spectrum software (Perkin Elmer, Waltham, MA, USA, version 5.0.1.).

2.3. Chemometrics

2.3.1. PCA

PCA is a variable reduction technique, which reduces the number of variables by making linear combinations of the original variables. These combinations are called the principal components and are defined in such way that they explain the highest (remaining) variability in the data and are by definition orthogonal.

The importance of the original variables in the definition of a principal component is represented by its loading and the projections of the objects on to the principal components are called the scores of the objects. [26] In this investigation, it was decided to conduct the research only on the three first PC's, since in all cases more than 95% of the variation in the data was explained by them.

2.3.2. PLS

PLS is based on exactly the same principles as PCA. The difference is situated in the definition of the latent variables, here called PLS-factors. The PLS-factors, also linear combinations of the original explanatory variables in the data set, are defined in such a way that they maximize the covariance with the response variable. In this way latent variables are obtained that are more directly related to the response variable than, for example, those obtained in PCA. In this study, a discrete response variable was chosen (0 for illegal samples and 1 for genuine samples). This is justified since the genuinity of the reference samples is certified.

The scores of the objects on the different PLS-factors were used in this study as tool to distinguish clusters of the different samples. [26]

2.3.3. Data processing

The data pre-processing was performed using HoloREACT^{TM} software. For NIR and FT-IR spectroscopy, the three spectra of a sample were normalized and averaged. For Raman spectroscopy, the three spectra of a sample were baseline corrected using the Pearson's method. All calculations were done with Matlab (The Matworks, Natick, MA, version 7.9.0). The Principal component analysis (PCA) of the data has been performed with algorithms based on Kernel PCA [27]. The Partial Least Squares (PLS) analysis of the data has been performed with the algorithms described by de Jong [28]. The algorithms are part of the ChemoAC toolbox (Freeware, ChemoAC Consortium, Brussels, Belgium, version 4.0). For

each method, the dataset consists of a matrix with a number of columns equal to the number of wavelengths measured and a number of rows equal to the number of samples studied. The combination of the techniques has been performed by addition of the matrices obtained for each technique. The combination matrix was then autoscaled in order to eliminate the influence of the differences of scaling.

3. **Results and Discussion**

3.1. *Measurements*

All IR measurements were performed in triplicate on the pulverised tablet. All NIR measurements were performed once on the core of three different tablets of each sample and all Raman measurements were performed on three different locations of the core of one tablet of each sample. Only the fingerprint region of the IR spectra (1800-400 cm^{-1}) and the 7000-4000 cm^{-1} region of the NIR spectra were used because of their high variability and their richness of information. The Raman spectra were taken with an exposure time of ten seconds on the core of the tablets at three different locations per tablet.

3.2. *Case one: Viagra*®

3.2.1. *PCA*

First, a PCA analysis was performed on all types of measurement results (FT-IR, NIR, Raman and combinations). No separation or not enough separation was seen between genuine and counterfeit or imitation samples. FT-IR provided the best results for the PCA analysis. It was decided to perform a PLS analysis. This choice was based on the supervised character of this chemometric method.

3.2.2. *PLS*

3.2.2.1. *FT-IR spectroscopy*

Figure 1 shows the three dimensional PLS plot of the analysis of the FT-IR spectra of the Viagra®-like samples. As can be seen, a good distinction between genuine and counterfeit or imitations is obtained. Previous inspection of the loading plots confirms that almost the complete fingerprint region is needed for classification. Most of the separation is probably

due to the differences in chemical composition of the tablets: combinations of different API, differences in excipients used, presence of contaminants or both of them.
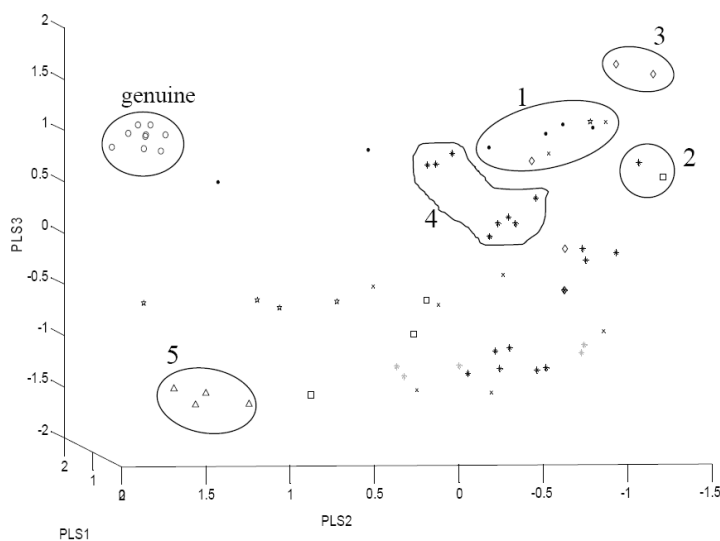
Figure 1: 3D PLS score plot of the FT-IR spectra (region between 1800-400 cm^{-1}) of the Viagra$^{®}$-like samples. For symbol caption see table 2.

The counterfeit samples are quite close to each other (cluster 1) except two of them. Cluster one contains also 4 imitations; this indicates that their chemical composition is presumably similar to the one of the counterfeits. Among the different clusters identified, cluster 3 is very far from the other ones (along the axes PLS 2 and PLS 3 on Figure 2). No reason has been identified for that huge separation. But it can be observed that cluster 3 is always separated from other samples by each technique or combination of techniques except for Raman spectroscopy and the combination of Raman and FT-IR spectroscopy. Clusters 4 and 5 can easily be confirmed by visual examination. Each cluster contains tablets originating from the same manufacturer. Cluster 2 contains two samples visually different but having the same packaging (same brand name and dosage: Nizagara 25mg). The fact that these two samples are close to each other indicates that they probably have the same chemical composition. They may be manufactured in two different laboratories but with the same raw material.

Other samples are widespread and no relationship between these samples is seen. After inspection of the loading plots, no specific wavenumbers corresponding to an excipient or the sildenafil were correlated to the separation.

3.2.2.2. NIR spectroscopy

Figure 2 shows the three dimensional PLS plot of the analysis of the NIR spectra of the Viagra$^{®}$-like samples. As with FT-IR, a good separation between genuine and imitations or

counterfeit is obtained. Some clusters are observed. No obvious reason has been found as an explanation of these clusters except for clusters 4 and 5. NIR cluster 4 contains the same samples as the FT-IR cluster 5 and these samples are from the same manufacturer. NIR cluster 5 contains chewing tablets of three different manufacturers. Their classification in the same cluster is probably the consequence of a same manufacturing process. This is in line with the principle of NIR spectroscopy which is dependant of the physical properties of the sample such as particle size, density and morphology [29]. After visual inspection of the NIR spectra, it appears that the major variability is present between 5500-5000 cm^{-1}.
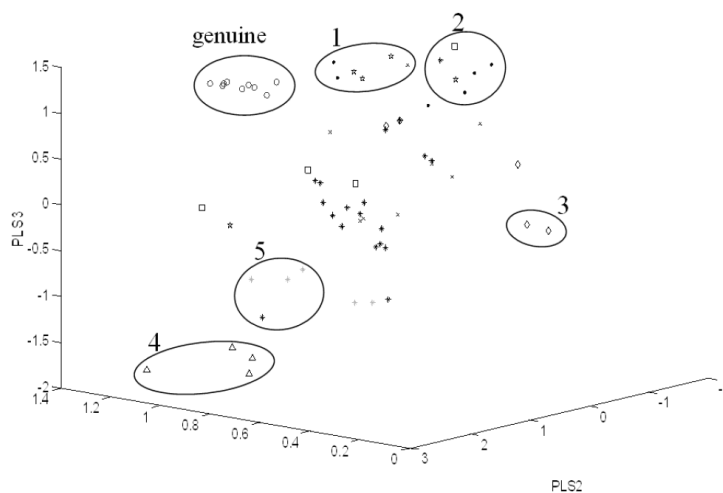
Figure 2: 3D PLS score plot of the NIR spectra (region between 7000-4000 cm^{-1}) of the Viagra$^{®}$-like samples. For symbol caption see table 2.

3.2.2.3.   *Raman spectroscopy*

Raman spectroscopy was able to distinguish genuine from illegal medicines (Figure 3). Illegal samples were widespread and no cluster has been identified except two samples that are apart from other ones. One of these two samples may be separated from other ones because it contains both sildenafil and tadalafil. No satisfying explanation has been found for the separation of the other sample and the loading plots do not give more information.

The Raman spectra also have been evaluated in smaller spectral regions, but the conclusions were similar.

Figure 3: 3D PLS score plot of the Raman spectra (region between 1800-200 cm^{-1}) of the Viagra$^®$-like samples. For symbol caption see table 2.

3.2.2.4.   Combination of techniques

The association of Raman and FT-IR spectroscopy and the association of Raman and NIR spectroscopy allow the distinction of 5 and 6 clusters respectively (results not shown). No reason has been found for this distinction. Neither the visual aspect nor the loading plots permits an explanation.

Figure 4 shows the three dimensional PLS plot of the analysis of the combination of the NIR and FT-IR spectra of the Viagra$^®$ samples. A good separation between genuine and counterfeit or imitation samples can be observed. The illegal samples are divided in 4 clusters. These clusters are the most relevant for a forensic investigation because the classification realised by the combination of the two techniques shows clusters that are the most different according to both physical and chemical properties. These differences should be relatively little among samples from the same manufacturer. Cluster 3 contains the same samples as cluster 3 in Figures 1 and 2. Cluster 4 contains some samples from group 2 and 4 (see table 2). Samples from group 2 are all manufactured by Axon Drugs Pvt Ltd. No reason has been found for the presence of samples from group 4 because no manufacturer name was present. They may be manufactured by Axon Drugs but this can not be confirmed. No satisfying reason has been found to explain the cluster 2. Once again, no specific wavenumbers corresponding to an excipient of the genuine tablets or the sildenafil were correlated to the separation according to the loading plots.

Once Raman spectroscopy data are introduced in the analysis, clusters are no more coherent with the visual aspect of the tablets. As it cannot be ruled about the relevance of the

information provided by the Raman spectroscopy, the combination of NIR and FT-IR spectroscopy will be preferred.
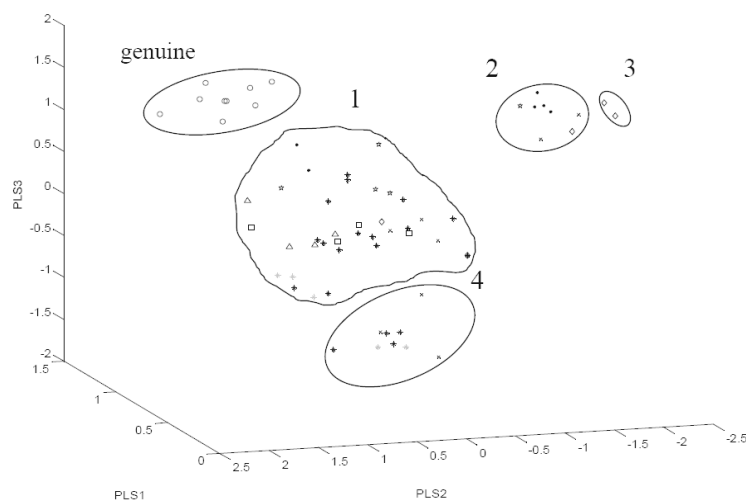
Figure 4: 3D PLS score plot of the association of the FT-IR spectra (region between 1800-400 cm^{-1}) and the NIR spectra (region between 7000-4000 cm^{-1}) of the Viagra$^®$-like samples. For symbol caption see table 2.

3.3.   *Case two: Cialis$^®$*

3.3.1. *PCA*

As for Viagra$^®$, the PCA analysis of Raman spectroscopy did not allow to distinguish genuine from imitations or counterfeit samples. So this technique was abandoned to the advantage of NIR and FT-IR.

PCA analysis of the Cialis$^®$ FT-IR dataset (Figure 5) permitted to clearly separate the counterfeit samples (cluster 2 in Figures 5 and 6) from the imitations and from the genuine samples. Cluster 3 contains the remaining samples. However, a group of imitations is not separated from genuine samples (cluster 1 in Figures 5 and 6). The same observation is done with the NIR dataset (Figure 6). The imitations (group 5 in table 3) have different brand names but are visually similar and can be easily identified as being only one group. The qualitative and quantitative analysis by HPLC and dissolution of some of them indicates that they are of good quality. This might result of a chemical composition and a manufacturing process very close to the original Cialis$^®$. So, the PLS analysis was needed to distinguish these imitations from the originals.

The samples of clusters 4 are coherent with visual inspection. Cluster 3 and 5 in Figure 6 cannot formally be explained. Cluster 2 contains the counterfeit samples.
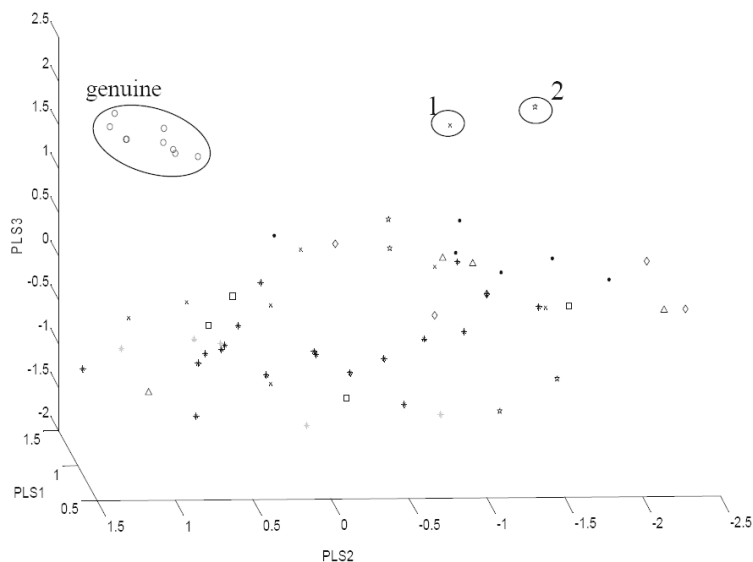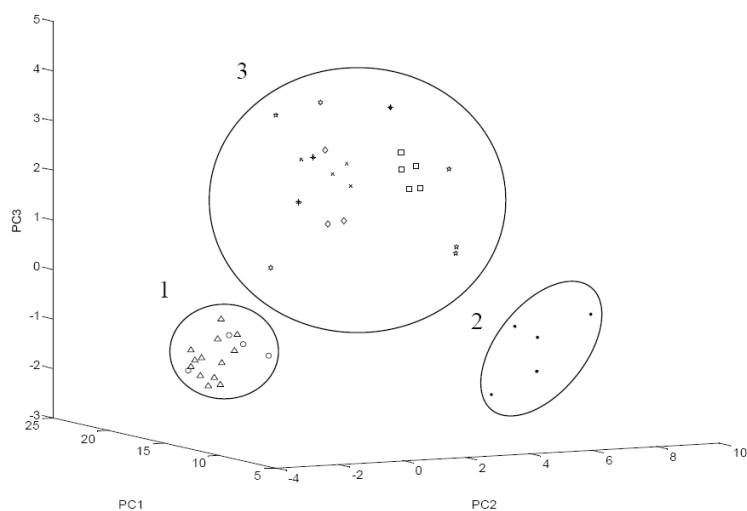
Figure 5: 3D PCA score plot of the FT-IR spectra (region between 1800-400 cm^{-1}) of the Cialis®-like samples. For symbol caption see table 3.
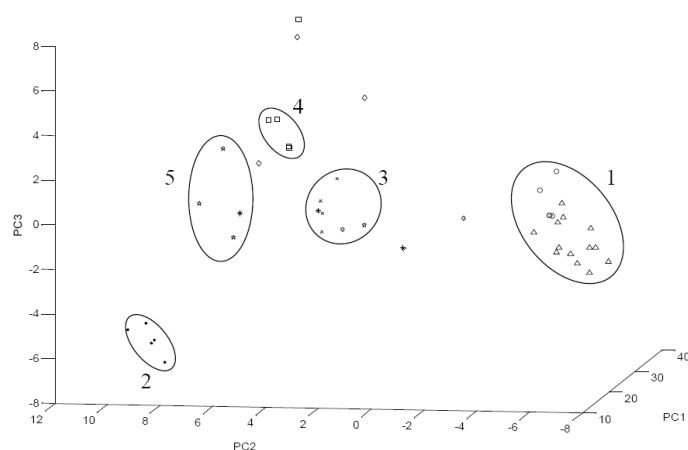
Figure 6: 3D PCA score plot of the NIR spectra (region between 7000-4000 cm^{-1}) of the Cialis®-like samples. The results show no separation of genuine samples. For symbol caption see table 3.

3.3.2. PLS

3.3.2.1.   FT-IR spectroscopy

The PLS analysis permitted a very good separation of the imitations and the counterfeits from the genuine samples. FT-IR also permitted to see 5 clusters of samples (Figure 7). Cluster 1 shows the imitations samples that were not separated from the genuine samples by PCA. It contains imitations that are visually similar: oval shape with E20 embossed; without distinction between conventional tablets and chewable tablets (see Table 3). It can therefore be postulated that only few chemical differences are present (flavouring agents such as menthol). After qualitative and quantitative HPLC analysis and according to the classification of the RIVM [3], they can be called "professional imitations".

Figure 7: 3D PLS score plot of the FT-IR spectra (region between 1800-400 cm^{-1}) of the Cialis®-like samples. For symbol caption see table 3.

Cluster 2 contains the counterfeit samples. It is very clearly separated from other samples. A HPLC analysis showed that they contain both sildenafil and tadalafil. So they can be called "mixed counterfeit" according to the RIVM classification [3]. This combination of API may explain this clear separation. Cluster 3 contains samples from the same manufacturer (according to the packaging) that are visually similar: round, orange and without film-coat. In this case, the chewable tablets were separated from other samples (arrow 3).

Cluster 4 contains samples that are neither counterfeit nor imitation samples. Their packaging is totally different from genuine samples but their shape, film-coat colour and engraving C20 are similar. However, they really seem manufactured by amateurs so we classed them among imitations. Once again, the chewable version of these tablets is not comprised in the cluster (arrow 4).

Cluster 5 contains the other samples except three of them that are widespread in the plot. They are not similar between them but quite close to each other. They probably have the same chemical composition and the same manufacturer.

The examination of the loading plots did not permit to identify which component was correlated with this separation. After visual inspection of the FT-IR spectra of each cluster, it can be observed that almost the whole spectrum is different between each sample except between cluster one and genuine samples which is in agreement with the fact that they were not separated by PCA.

3.3.2.2. NIR spectroscopy

NIR spectroscopy shows a clear separation between genuine samples and counterfeit or imitation ones (Figure 8). Clusters 1 and 2 are very clearly separated from other samples but the clustering of the illegal samples is not clear (clusters 3, 4). These 2 clusters are very close to each other. Once again, the counterfeit samples (cluster 2) are clearly separated from other samples. The visual inspection of the NIR spectra of each cluster shows no clear difference between the different clusters.
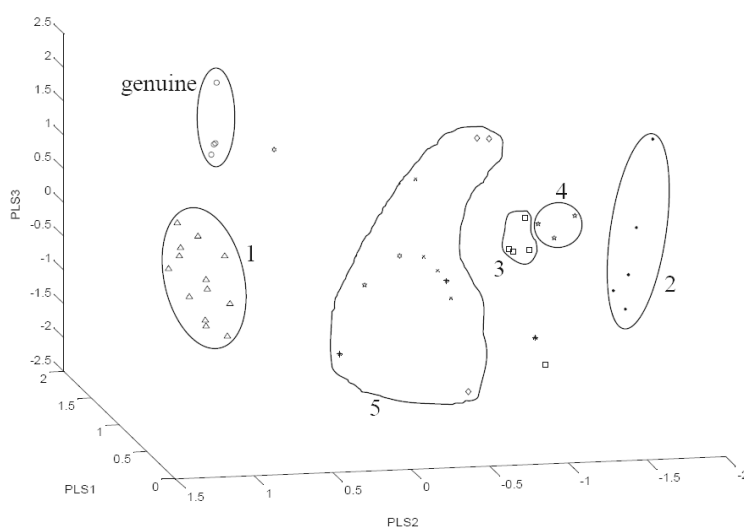
Figure 8: 3D PLS score plot of the NIR spectra (region between 7000-4000 cm^{-1}) of the Cialis$^{®}$-like samples. For symbol caption see table 3.

3.3.2.3. Raman spectroscopy

Raman spectroscopy permits the distinction between genuine and illegal samples. This distinction was greater when the region between 1400-1190 cm^{-1} was studied. So this region has been selected for the rest of the analysis with Raman spectroscopy on Cialis$^{®}$-like samples. Figure 9a shows the separation of the illegal samples in 3 clusters. Cluster 1 contains the imitations from the group 5 (see table 3) and one sample from the group 7. This sample was not classified in any cluster by both NIR and FT-IR spectroscopy. Cluster 3 contains two samples from the same group but no reason has been found for their separation from the other ones. The loading plots did not permit to identify which component was correlated with these clusters. As shown on Figure 9b, the Raman spectra of the three clusters are different in particular in the studied region (grayed area).
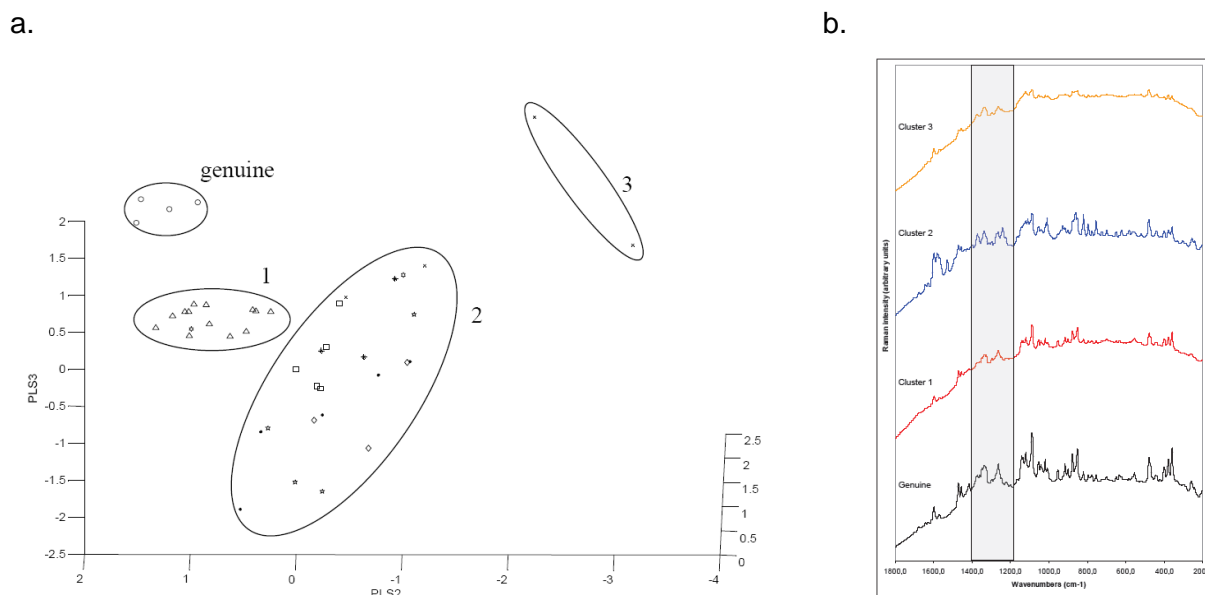
a.   b.
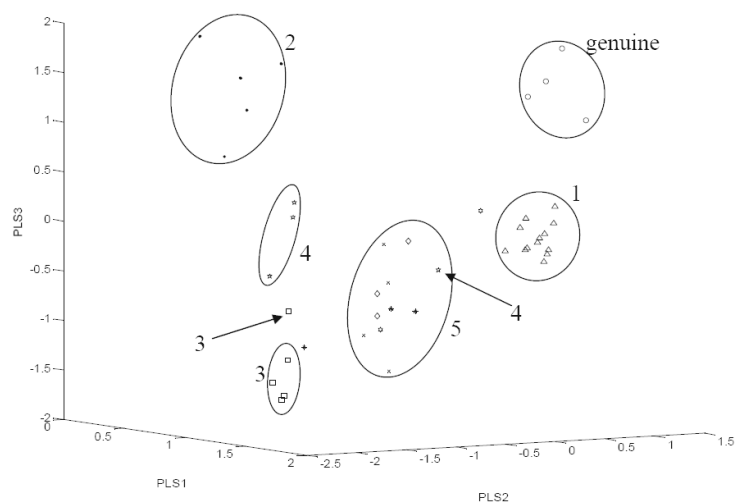

Figure 9:

    a.   3D PLS score plot of the Raman spectra (region between 1400-1190 cm^{-1}) of the Cialis$^{®}$-like samples. For symbol caption see table 3.

    b.   Mean Raman spectrum of each cluster. The region between 1400-1190 cm^{-1} is grayed.

3.3.2.4. Combination of techniques

The NIR and the FT-IR data were associated to obtain Figure 10. This plot shows a separated cluster of the genuine samples and four other clusters. Cluster 1 contains the professional imitations identified by both FT-IR and NIR (group 5 of table 3) and it contains also a sample that was not included in a cluster by each technique separately except by the Raman spectroscopy. Cluster 2 contains the counterfeit samples and cluster 3 contains the remainder samples. Only one sample stand alone (cluster 4), this sample was included in cluster 5 by both techniques separately (Figures 7 and 8). It could not be explained why the association of the techniques isolated it.

Figure 11 shows the combination of the NIR and the Raman spectra. Three clusters are observed. These clusters are the same as for the association of NIR and FT-IR spectroscopy except that the sample from group 7 that was in cluster one is now separated in cluster 5. The sample of cluster 4 in Figure 10 is still isolated.

Figure 12 shows the association of the FT-IR and the Raman spectra. This time, illegal samples are divided into 4 clusters. Clusters 2 and 3 are coherent with visual inspection of the tablet. Cluster 4 contains all the samples from group 3 except a tablet from group 4. This sample was already classified close to group 3 by FT-IR spectroscopy (see Figure 7). Cluster 1 contains the remainder samples.

The association of the three techniques permitted exactly the same separation as the association of NIR and Raman spectroscopy.
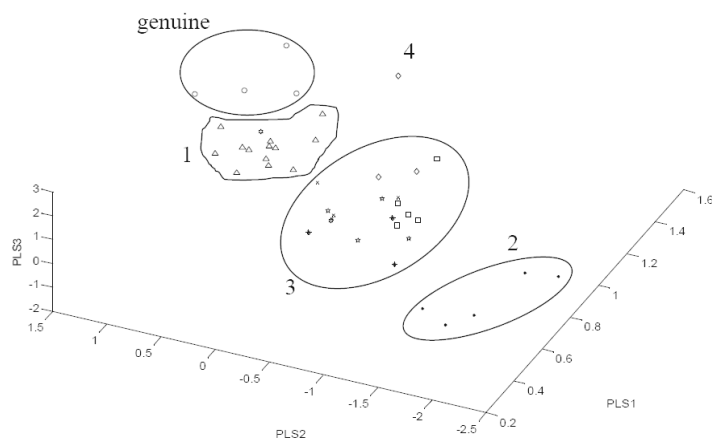
Figure 10: 3D PLS score plot of the association of the FT-IR spectra (region between 1800-400 cm^{-1}) and the NIR spectra (region between 7000-4000 cm^{-1}) of the Cialis$^®$-like samples. For symbol caption see table 3.
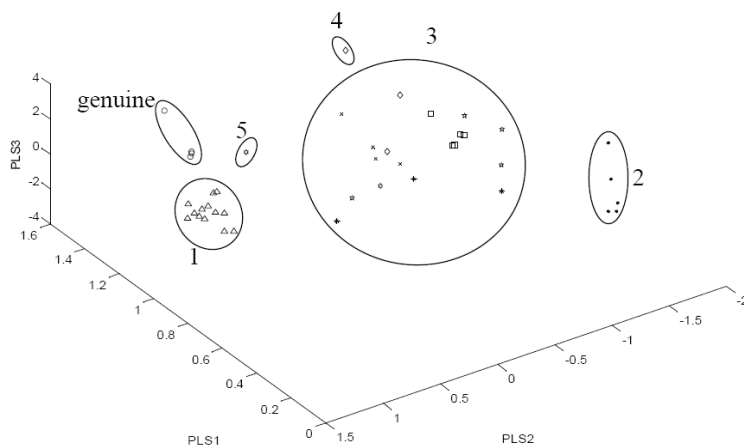
Figure 11: 3D PLS score plot of the association of the Raman spectra (region between 1400-1190 cm^{-1}) and the NIR spectra (region between 7000-4000 cm^{-1}) of the Cialis$^®$-like samples. For symbol caption see table 3.
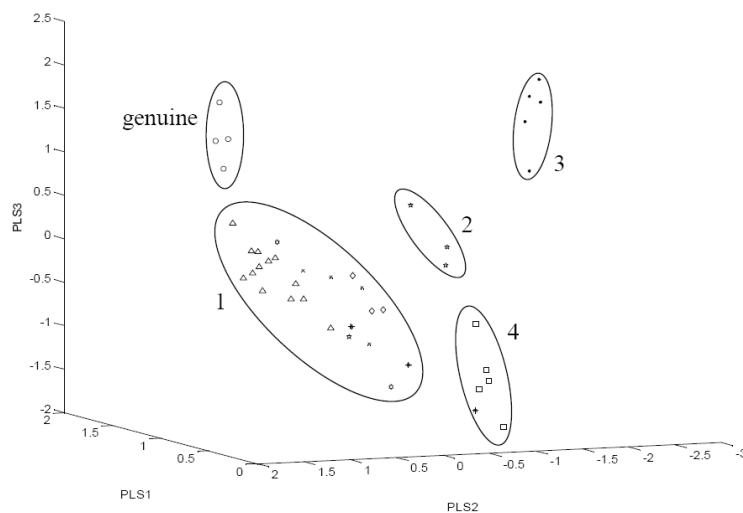
Figure 12: 3D PLS score plot of the association of the FT-IR spectra (region between 1800-400 cm^{-1}) and the Raman spectra (region between 1400-1190 cm^{-1}) of the Cialis®-like samples. For symbol caption see table 3.

4. <u>Conclusion</u>

The aim of this study was to establish which technique or combination of techniques was the most powerful to distinguish counterfeits from genuine samples of Viagra® and Cialis®. The spectroscopic techniques investigated comprised FT-IR, NIR and Raman spectroscopy.

FT-IR is a widely spread and relatively cheap technique, used for decades and present in each analytical laboratory. The main drawback of this technique is its destructive character.

NIR and Raman techniques are more and more used in the pharmaceutical industry because of their easiness of use, their rapidity and the fact that it is non-destructive. So, any further analysis can still be done on the tablets analysed by NIR or Raman spectroscopy which is very important for an official analytical laboratory.

The ability of NIR and Raman spectroscopy separately to make the distinction between genuine and counterfeit or imitation samples has already been demonstrated [8,10,15]. PCA analysis of the data was insufficient to achieve complete separation of the samples. Hence, PLS analysis was preferred because it is a powerful tool for a discrimination study with reference samples.

For the Viagra® samples, after investigation, the conclusion is that the association of NIR and FT-IR spectroscopy provides the best results (see Table 4a). Indeed, the many clusters observed with NIR and FT-IR alone were reduced to 4 clusters showing the most variability between the samples. This variability is correlated to both physical and chemical information. This is very useful for a forensic investigation because it takes into account both chemical

composition and the manufacturing process. This information is useful for characterizing a manufacturer.

Table 4: (a) Summary table of the results obtained with the different techniques and associations analysed by PLS for the Viagra®-like samples. The best method is in bold font.

Viagra®-like samples	Genuine discrimination	Counterfeit-Imitations discriminations	Clusters number	Explained clusters	Unclassified samples
FT-IR (1800-400 cm^{-1})	Yes	No	5	4	33
NIR (7000-4000 cm^{-1})	Yes	No	5	2	31
Raman (1800-200 cm^{-1})	Yes	No	-	-	55
FT-IR+NIR	**Yes**	**No**	**4**	**2**	**0**
FT-IR+Raman	Yes	No	5	1	2
NIR+Raman	Yes	No	6	1	2
FT-IR+NIR+Raman	Yes	No	6	1	2

Table 4: (b) Summary table of the results obtained with the different techniques and associations analysed by PLS for the Cialis®-like samples. The best method is in bold font.

Cialis®-like samples	Genuine discrimination	Counterfeit-Imitations discriminations	Clusters number	Explained clusters	Unclassified samples
FT-IR (1800-400cm^{-1})	Yes	Yes	5	4	3
NIR (7000-4000cm^{-1})	Yes	Yes	5	4	3
Raman (1400-1190cm^{-1})	Yes	Yes	3	2	1
FT-IR+NIR	Yes	Yes	3	2	1
FT-IR+Raman	Yes	Yes	4	3	0
NIR+Raman	**Yes**	**Yes**	**3**	**2**	**2**
FT-IR+NIR+Raman	Yes	Yes	3	2	2

For the Cialis®-like samples, each technique separately permitted a classification of the samples and the distinction between genuine and illegal samples (see Table 4b). But this classification was insufficient for the Raman spectroscopy or incomplete for the FT-IR and the NIR spectroscopy. It is concluded that the association of NIR spectroscopy (region between 7000-4000 cm^{-1}) and Raman spectroscopy (region between 1400-1190 cm^{-1}) was the most useful association of techniques. This association permitted a very good separation between genuine and counterfeit or imitation samples. The classification performed allows the distinction between very bad counterfeits, very good imitations and other samples from genuine samples. This classification is also very easy even by visual inspection of a non-trained operator. This is useful for its application in control laboratory. The association of FT-IR and Raman spectroscopy has not been considered as optimal because some groups were not separated and there were samples misclassified. For these reasons, this association seems to be less useful than the association of NIR and Raman spectroscopy.

This study was performed on a limited number of samples. If those techniques are applied to a routine forensic laboratory working on counterfeits drugs, it is clear that the constitution of a library of genuine and illegal samples would allow a sharper classification of samples.

The use of spectroscopic tools allows an objective distinction between legal and illegal tablets based on chemical and physical information of the tablets. This distinction sometimes confirms the visual classification of the samples but most of the time it completes this classification. As it has been demonstrated, it is frequent that many visually similar samples are finally classified in the same cluster which indicates that they have similar physico-chemical properties. That kind of objective classification is the most useful for any further investigation.

References

[1] Weiss A., Buying prescription drugs on the internet: promises and pitfalls, Cleveland Clinic Journal of Medicine (2006)73, 282-288

[2] Veronin M., Youan B.-B., Magic bullet gone astray: medications and the internet, Science (2004) 305, 481

[3] Venhuis B.J., Barends D.M., Zwaagstra M.E., de Kaste D., Recent developments in counterfeit and imitations of Viagra, Cialis and Levitra, RIVM Report 370030001/2007, Bilthoven, 2007

[4] WHO, sixty-second world health assembly item 12.9, counterfeit medical products, April 2009. http://aps.who.int/gb/ebwha/pdf_files/A62/A62_13-en.pdf

[5] Singh S., Prasad B., Savaliya A., Shah R.P., Gohil V.M., Kaur A., Strategies for characterizing sildenafil, vardenafil, tadalafil and their analogues in herbal dietary supplements, and detecting counterfeit products containing these drugs, Trends in Analytical Chemistry (2009) 28, 13-28

[6] Amin A.S., Moustafa M.E., El-Dosoky R., Colorimetric determination of sildenafil citrate (Viagra) through ion-associate complex formation, Journal of AOAC International (2009) 92, 125-130

[7] Rodomonte A.L., Gaudiano M.C., Antoniella E., Lucente D., Crusco V., Bartolomei M., Bertocchi P., Manna L., Valvo L., Muleri N., Counterfeit drugs detection by measurement of tablets and secondary packaging colour, Journal of Pharmaceutical and Biomedical Analysis (2010) 53, 215-220

[8] Vredenbregt M.J., Blok-Tip L., Hoogerbrugge R., Barends D.M., de Kaste D., Screening suspected counterfeit Viagra and imitations of Viagra with near-infrared spectroscopy, Journal of Pharmaceutical and Biomedical Analysis (2006) 40, 840-849

[9] Wawer I., Pisklak M., Chilmonczyk Z., 1H, 13C, 15N NMR analysis of sildenafil base and citrate (Viagra) in solution, solid state and pharmaceutical dosage forms, Journal of Pharmaceutical and Biomedical Analysis (2005) 38, 865-870

[10] Trefi S., Routaboul C., Hamieh S., Gilard V., Malet-Martino M., Martino R., Analysis of illegally manufactured formulations of tadalafil (Cialis) by 1H NMR, 2D DOSY 1H NMR and Raman spectroscopy, Journal of Pharmaceutical and Biomedical Analysis (2008) 47, 103-113

[11] Aboul-Enein H.Y., Ali I., Determination of tadalafil in pharmaceutical preparation by HPLC using monolithic silica column, Talanta (2005) 65, 276-280.

[12] Bogusz M.J., Hassan H., Al-Enazi E., Ibrahim Z., Al-Tufail M., Application of LC-ESI-MS-MS for detection of synthetic adulterants in herbal remedies, Journal of Pharmaceutical and Biomedical Analysis (2006) 41, 554-564

[13] Savaliya A.A., Shah R.P., Prasad B., Singh S., Screening of Indian aphrodisiac ayurvedic/herbal healthcare products for adulteration with sildenafil, tadalafil and/or vardenafil using LC/PDA and extracted ion LC-MS/TOF, Journal of Pharmaceutical and Biomedical Analysis (2010) 52, 406-409

[14] Venhuis B.J., Zomer G., Vredenbregt M.J., de Kaste D., The identification of (-)-trans-tadalafil, tadalafil, and sildenafil in counterfeit Cialis and the optical purity of tadalafil stereoisomers, Journal of Pharmaceutical and Biomedical Analysis (2010) 51, 723-727

[15] de Veij M., Deneckere A., Vandenabeele P., de Kaste D., Moens L., Detection of counterfeit Viagra with Raman spectroscopy, Journal of Pharmaceutical and Biomedical Analysis (2008) 46, 303-309

[16] Roggo Y., Degardin K., Margot P., Identification of pharmaceutical tablets by Raman spectroscopy and chemometrics, Talanta (2010) 81, 988-995

[17] Vajna B., Farkas I., Szabó A., Zsigmond Z., Marosi G., Raman microscopic evaluation of technology dependent structural differences in tablets containing imipramine model drug, Journal of Pharmaceutical and Biomedical Analysis (2010) 51, 30-38

[18] Storme-Paris I., Rebiere H, Matoga M., Civade C., Bonnet P.-A., Tissier M.H., Chaminade P., Challenging near infrared spectroscopy discriminating ability for counterfeit pharmaceuticals detection, Analytica Chimica Acta (2010) 658, 163-174

[19] Chong X.-M., Hu C.-Q., Feng Y.-C., Pang H.-H., Construction of a universal model for non-invasive identification of cephalosporins for injection using near-infrared diffuse reflectance spectroscopy, Vibrational Spectroscopy (2009) 49, 196-203

[20] de Peinder P., Vredenbregt M.J., Visser T., de Kaste D., Detection of Lipitor counterfeits: a comparison of NIR and Raman spectroscopy in combination with chemometrics, Journal of Pharmaceutical and Biomedical Analysis (2008) 47, 688-694

[21] Puchert T., Lochmann D., Menezes J.C., Reich G., Near-infrared chemical imaging (NIR-CI) for counterfeit drug identification--a four-stage concept with a novel approach of data processing (Linear Image Signature), Journal of Pharmaceutical and Biomedical Analysis (2010) 51, 138-145

[22] Lopes M.B., Wolff J.C., Investigation into classification/sourcing of suspect counterfeit Heptodintrade mark tablets by near infrared chemical imaging, Analytica Chimica Acta (2009) 633, 149-155

[23] Lopes M.B., Wolff J.C., Bioucas-Dias J.M., Figueiredo M.A., Determination of the composition of counterfeit Heptodin tablets by near infrared chemical imaging and classical least squares estimation, Analytica Chimica Acta (2009) 641, 46-51

[24] Maurin J.K., Pluciński F., Mazurek A.P., Fijałek Z., The usefulness of simple X-ray powder diffraction analysis for counterfeit control--the Viagra example, Journal of Pharmaceutical and Biomedical Analysis (2007) 43, 1514-1518

[25] Pearson G.A., A general baseline-recognition and baseline-flattening algorithm. Journal of Magnetic Resonance (1977) 27, 265–272.

[26] Massart D.L., Vandeginste B.G.M., Buydens L.M.C., De Jong S., Lewi P.J., Smeyers-verbeke J.: Handbook of Chemometrics and Qualimetrics-Part A. Elsevier Science, Amsterdam, 1997

[27] Wu W., Massart D.L., de Jong S., The kernel PCA algorithms for wide data. Part I: Theory and algorithms, Chemometrics and Intelligent Laboratory Systems (1997) 36, 165-172

[28] de Jong S., SIMPLS: An alternative approach to partial least squares regression, Chemometrics and Intelligent Laboratory Systems (1993) 18, 251-263

[29] Reich G., Near-infrared spectroscopy and imaging: Basic principles and pharmaceutical applications, Advanced Drug Delivery Reviews (2005) 57, 1109-1143

3.2. Classification trees based on infrared spectroscopic data to discriminate between genuine and counterfeit medicines.

Classification trees based on infrared spectroscopic data to discriminate between genuine and counterfeit medicines

E. Deconinck [1], P.Y. Sacré [1,2], D. Coomans [3,4], J. De Beer [1]

[1] Division of food, medicines and consumer safety, Section Medicinal Products, Scientific Institute of Public Health (IPH), J. Wytmansstraat 14, B-1050 Brussels, Belgium

[2] Dept. of Analytical Pharmaceutical Chemistry, Institute of Pharmacy, University of Liège, Liège, Belgium.

[3] Dept. of Biostatistics and Medical Informatics, Vrije Universiteit Brussel, Laarbeeklaan 103, B-1090 Brussels, Belgium

[4] Dept. of Analytical Chemistry and Pharmaceutical Technology , CePhaR, Vrije Universiteit Brussel-VUB, Laarbeeklaan 103, B-1090 Brussels, Belgium

Abstract:

Classification trees built with the Classification And Regression Tree algorithm were evaluated for modelling infrared spectroscopic data in order to discriminate between genuine and counterfeit drug samples and to classify counterfeit samples in different classes following the RIVM classification system.

Models were built for two data sets consisting of the Fourier Transform Infrared spectra, the Near Infrared spectra and the Raman spectra for genuine and counterfeit samples of respectively Viagra® and Cialis®.

Easy interpretable models were obtained for both models. The models were validated for their descriptive and predictive properties. The predictive properties were evaluated using both cross validation as an external validation set. The obtained models for both data sets showed a 100% correct classification for the discrimination between genuine and counterfeit samples and 83.3% and 100% correct classification for the counterfeit samples for the Viagra® and the Cialis® data set respectively.

1. Introduction

Due to the extension of the internet, counterfeit drugs represent a growing threat for public health in the developing countries but also more and more in the industrial world [1,2]. The European Agency for Access to Safe Medicines (EAASM) claims that about 50% of the medicines sold through non identified/recognized websites are counterfeit and that 10% of the market in the developing countries and about 1% of the European market is covered by counterfeits [3]. In Europe and the United States one of the most popular group of medicines bought through the internet are the phosphodiesterase type 5 (PDE-5) inhibitors, i.e. sildenafil citrate (Viagra®), tadalafil (Cialis®) and vardenafil hydrochloride (Levitra®).

The World Health Organization (WHO) [4] defines a counterfeit drug as: "one which is deliberately and fraudulently mislabelled with respect to identity and/or source. Counterfeiting can apply to both branded and generic products and counterfeit products may include products with the correct ingredients or with the wrong ingredients, without the active ingredients, with insufficient active ingredient or with fake packaging."

Even if this is the internationally accepted definition of a counterfeit medicine, it does not apply to the majority of the illegal products encountered on the European market, since they do not copy the packaging and brand names of the genuine products. Therefore it was chosen to follow the classification proposed by the Dutch National Institute for Public Health and the Environment (RIVM) [5]. This classification (table 1) distinguishes counterfeits, which appearance corresponds to the one of the genuine products, and imitations, which do not. Most of these imitations originate from Asia, where European and American patents are not recognized.

In literature several analytical techniques were proposed to discriminate between counterfeit and genuine medicines. Savaliya et al. proposed to use HPLC and LC-MS for the screening of aphrodisiacs on the Indian market [6]. Infrared-spectroscopy showed to be a valuable instrument for the identification of counterfeit medicines. Y. Roggo et al. [7] and Vajna et al. [8] made use of Raman spectroscopy for the identification of pharmaceutical tablets and investigate their structural differences, while de Veij et al. [9] used Raman spectroscopy to detect counterfeit Viagra®. Storme-Paris et al. [10], De Peinder et al. [11] Puchert et al. [12] and Lopes et al. [13,14] all demonstrated the usefulness of near infrared spectroscopy in the distinction of genuine and counterfeit medicines. Other techniques found for this purpose are colorimetry [15,16], TLC [17], NMR [18,19] and X-ray powder diffraction [20]. An overview of all these techniques can be found in reference [21].

Table 1: Classification of illegal medicines according to the RIVM [5]

Main category	Subcategory	Inclusion and exclusion criteria
Counterfeit	Accurate	Appearance in conformity with genuine medicine; Content of correct API within 90 - 110 % of declared value; No other APIs; not genuine medicine.
	Non-Accurate	Appearance in conformity with genuine medicine; Content of correct API outside 90 - 110 % of declared value; No other APIs.
	Mixed	Appearance in conformity with genuine medicine; Contains correct API and another, known API
	Fraudulent	Appearance in conformity with genuine medicine; Contains a different, known API.
	Analogue	Appearance in conformity with genuine medicine, Contains other, unapproved API
	Placebo	Appearance in conformity with genuine medicine; Does not contain APIs.
Imitation or Food supplement	Accurate	Appearance not in conformity with genuine medicine; Content of correct API within 90 - 110 % of declared value; No other APIs.
	Non-Accurate	Appearance not in conformity with genuine medicine; Content of declared API outside 90 - 110 % of declared value; No other APIs.
	Mixed	Appearance not in conformity with genuine medicine; Contains declared API and another API.
	Fraudulent	Appearance not in conformity with genuine medicine; Contains an undeclared API.
	Analogue	Appearance not in conformity with genuine medicine; Contains other, unapproved API
	Placebo	Appearance not in conformity with genuine medicine; Does not contain APIs.

One thing all these techniques have in common is that they generate a huge amount of data, which is often difficult to interpret in order to see differences between the different samples and to determine the cause of the differences. The majority of the authors make use of explorative chemometric tools to visualise the differences in the data obtained for the different samples: Principal Component Analysis, Partial Least Squares, Projection Pursuit, Multiple Factor Analysis and clustering techniques as hierarchical clustering, Generative topographic mapping and auto-associative multivariate regression trees are examples of methods that were and can be used for such purpose [9,22-24]. Even if some of the applied methods could be able to give a model with predictive ability, only a few authors created a model able to predict if a sample is counterfeit or not. Storme-Paris et al. [10] applied SIMCA to obtain a predictive model. The SIMCA model is a PCA-based model and the interpretation of the predictions is not always clear.

In this paper we evaluated the use of Classification And Regression Trees (CART) to build an easily interpretable predictive model to distinguish between counterfeit and genuine

medicines and to classify the counterfeit samples based on the RIVM definitions [5]. The first aim was to discriminate between genuine and counterfeit samples with at least 0% of genuine classified as counterfeits. The secondary aim was to be able to classify the counterfeit samples in their respective RIVM classes or at least get an idea about the type of the class.

To do so the data acquired by Sacré et al. [24] was used. The different samples were classified, following their visual aspects and the results obtained after identification and dosage of the active components, applying the RIVM classification system. The classes were used as response variable, while the spectroscopic data (FT-IR, NIR and Raman) were used as descriptive variables.

The results were compared to the results obtained by Sacré et al. [24]. In this paper the exploratory chemometric tools PCA and PLS were used for discrimination purposes. The results obtained with CART were also compared with the ones obtained with a more classic discrimination method, k-nearest neighbours (*k*NN). Due to the limited number of samples of some RIVM classes, SIMCA was not applied, since this will result in non representative classification rates for the counterfeit samples. This is due to the fact that in SIMCA each class is modelled separately.

2. Theory

2.1. Classification And Regression Trees (CART)

CART is a non-parametric statistical technique, developed by Breiman et al. [25] in 1984, which is able to solve classification (categorical dependent variables) as well as regression problems (continuous dependent variables). In both cases the method builds a decision tree, describing a response variable as a function of different explanatory variables (figure 1).
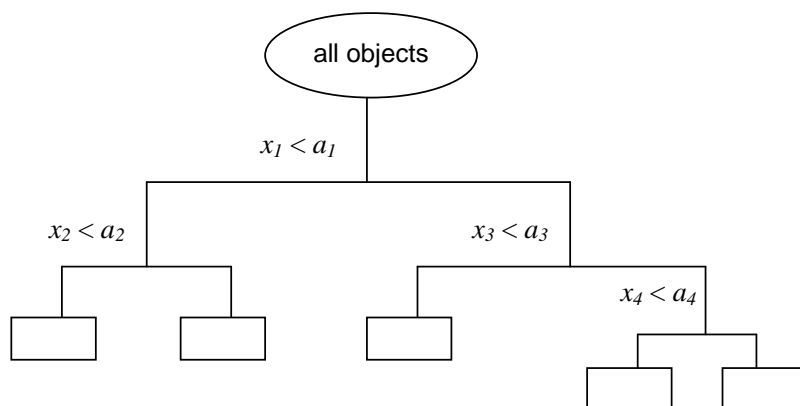
Figure 1: General structure of a CART-model. x_i = selected split variable, a_i = selected split value

A CART analysis generally consists of three steps. In a first step the maximum tree is build, using a binary split-procedure. The maximum tree is overgrown and closely describes the training set, usually resulting in overfitting. In a second step this overfitted model is pruned. This procedure results in a series of less complex trees, derived from the maximum tree. In the third and final step the optimal tree is selected using a cross validation procedure [25-27].

2.1.1. Building the maximum tree

The maximum tree is built using a binary split procedure, starting at the tree root, consisting of all objects in the training set. In every step of the procedure a mother group is considered and split into two daughter groups. The split is chosen in such a way that the impurity of the daughter groups is lower than that of the mother group. This means that the daughter groups become more homogeneous in the response variable (class numbers). In the following step each daughter group is considered a mother group. Every split is defined by one value of one explanatory variable. For continuous explanatory variables the splits are defined by "$x_i < a_j$" where x_i is the selected variable and a_j its split value [25-27].

To choose the most appropriate variable and split value, CART uses an algorithm in which all descriptors and all possible split values are considered. The split resulting in the highest decrease in impurity between the mother group (t_p) and the daughter groups (t_L and t_R) is selected. Mathematically this is expressed as:

$$\Delta i(S, t_p) = i_p(t_p) - p_L i(t_L) - p_R i(t_R) \qquad \text{(eq 1)}$$

where i is the impurity, S the candidate split value, and p_L and p_R the fractions of the objects in the left and right daughter groups, respectively [25-27].

For classification trees the impurity can be defined by different split criteria [25]. The three commonly used split criteria are the Gini index, the Twoing index and the Information index. In this work CART models were built using the Gini index. The Information index and the Twoing index were not used since these measures were not found useful in solving the considered classification problem.

The Gini index is defined as

$$\Delta i = 1 - \sum_{j=1}^{k} (p_j(t))^2 \qquad \text{(eq 2)}$$

where j = 1, 2, 3,…, k is the number of classes of the categorical response variable and $p_j(t)$ the probability of correct classification for class j at node t.

2.1.2. Tree pruning

The obtained maximum tree usually overfits the training set, therefore the model is pruned by successively cutting terminal branches. This procedure results in a series of smaller sub trees derived from the maximum tree. The different sub trees with the same complexity are then compared to find the optimal. This comparison is based on a cost-complexity measure $R_\alpha(T)$, in which both tree accuracy and complexity are considered [25-27]. For each sub tree complexity T it is defined as:

$$R_\alpha(T) = R(T) + \alpha \left| \breve{T} \right| \qquad \text{(eq 3)}$$

with $R(T)$ the average within-node sum of squares, $\left| \breve{T} \right|$ the tree complexity, defined as the total number of nodes of the sub tree, and α the complexity parameter, which is a penalty for each additional terminal node.

During the pruning procedure, α is gradually increased from 0 to 1 and for each value of α, the tree is selected which minimizes $R_\alpha(T)$. For a value of α equal to zero, $R_\alpha(T)$ is minimized by the maximum tree. By gradually increasing α a series of trees with decreasing complexity is obtained [25-27].

2.1.3. Selection of the optimal tree

From the obtained sequence of sub trees, the optimal has to be selected. The selection is usually based on the evaluation of the predictive error of the models using a cross validation procedure. In this paper a 10-fold cross validation procedure [26, 28] was used. The predictive error is then given as the overall misclassification rate for each of the sub trees [25]. The optimal model is the simplest model with a predictive error within one standard error (SE) of the minimal predictive error. This rule, generally referred to as the one SE-rule, allows the selection of a less complex model than the one with the minimal misclassification rate, without a significant loss of information and accuracy [25]. The algorithm allows the selection of all tree complexities. If previous knowledge about the data set justifies it, one can deviate from the one SE-rule and select another tree as optimal model.

2.2. k Nearest Neighbours (kNN)

The *k*-NN algorithm [28] was applied on the training set. The algorithm computes the minimal Euclidian distances between an unknown object and each of the objects of the training set.

For a training set of n samples, n distances are calculated. Then it selects the k nearest objects to the unknown one. The unknown object is classified in the group to which the majority of the k objects belong. The number of nearest neighbours is optimised using a cross validation procedure. The main advantages of this method are its mathematical simplicity and the fact that it is free from statistical assumptions.

3. **Methods and materials**

3.1. *Data*

The data for the Viagra® like samples consists of the Fourier-transformed infrared, the near-infrared and the Raman spectra for 55 counterfeit samples and 9 genuine samples. For the Cialis® like samples the data consists of the same type of spectra for 39 counterfeit and 4 genuine samples. All spectra were measured in triplicate. For more details about how this data was acquired we refer to Sacré et al. [24]. During the study of Sacré et al. it was seen that the variability in spectral data between the genuine samples is very low. The limited number of genuine samples should therefore be enough to represent the genuine class in the models. The more because CART defines the classes based on the improvement of homogeneity from mother to daughter leaves and therefore should isolate the small class of genuine relatively early in the building of the tree.

All counterfeit and imitation samples were donated by the Federal Agency for Medicines and Health Products in Belgium (AFMPS/FAGG). One batch of each dosage of genuine Viagra® (25mg, 50mg and 100mg) was kindly provided by Pfizer SA/NV (Belgium). Eli Lilly SA/NV (Benelux) kindly provided one batch of each commercial packaging (10 mg and 20 mg) of genuine Cialis®. Two other batches of each dosage of the genuine products were purchased from local pharmacies in Belgium.

The counterfeit samples were classified following the classification proposed by the RIVM [5]. The classification for both data sets is given in table 2

Table 2: Composition of the data sets in function of the RIVM classes [5]

Main category	subcategory	category number	number of Viagra[®] like samples	number of Cialis[®] like samples
Counterfeit	Accurate	1	1	0
	Non-accurate	2	3	0
	Mixed	3	1	5
	Fraudulent	4	0	0
	Analogue	5	0	0
	Placebo	6	0	0
Imitation	Accurate	7	45	27
	Non-accurate	8	4	2
or	Mixed	9	1	5
	Fraudulent	10	0	0
Food supplement	Analogue	11	0	0
	Placebo	12	0	0
Genuine		0	9	4

3.2. Data preprocessing

The data preprocessing was performed using the HoloREACT[TM] software (Kaiser Optical Systems, USA, version 2.3.5). For NIR and FT-IR spectroscopy, the three spectra of a sample were normalized and averaged. For Raman spectroscopy, the three spectra of a sample were baseline corrected using the Pearson's method [29].

In order to evaluate the predictive ability of the models the Viagra[®] and Cialis[®] data sets were divided in training and test sets. It was chosen that the test sets would contain about 20% of the samples. The division in test- and training set was performed using the Duplexx algorithm [30]. This algorithm starts by selecting the two samples with the highest Euclidean distance in the data space for a first set. The next two samples with the highest Euclidean distance are selected for a second set. The procedure continues by selecting iteratively pairs of samples for the first and the second set. The second set was chosen as test set, while the other set combined with the samples not selected by the algorithm formed the training set. During selection of the test sets it was made sure that one genuine sample was selected for the test set, while the others were kept in the training set. This was necessary due to the limited number of genuine samples in the data sets.

From the PCA plots [31] shown in figure 2 and 3 it can be seen that the test sets selected by the Duplexx algorithm cover quite well the data space of the data sets.
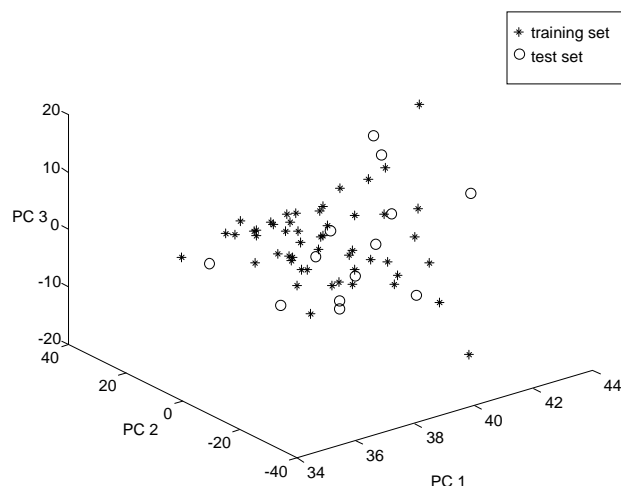
Figure 2: PCA plots representing the spread of the test set for the Viagra® data set over the data space.
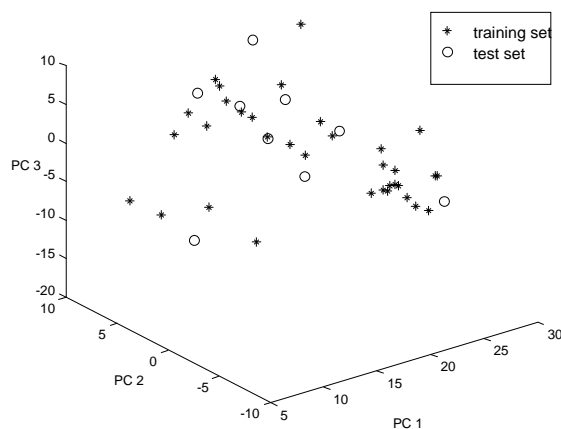
Figure 3: PCA plots representing the spread of the test set for the Cialis® data set over the data space.

3.3.   *Chemometrics*

The data preprocessing and the modelling was performed using Matlab R2009b (The Mathworks, Natick, USA). The programming of the CART algorithm was done according to the original CART algorithm proposed by Breiman [25].

4.   <u>Results and Discussion</u>

4.1.   *Viagra® like samples*

For all data sets used the data was first autoscaled. The signals at the different wavelengths in the respective spectra were used as explanatory variables while the class numbers of the different samples were used as response. The class numbers were assigned to the different samples based on the classification proposed by RIVM (table 2).

The maximal tree was build and pruned. In a next step a 10-fold cross validation was carried out resulting in a graph representing the percentage misclassification as a function of the tree complexity.

4.1.1. Classification tree based on the FT-IR data

Figure 4 shows the graph of the percentage misclassification as a function of the tree complexity obtained with the FT-IR data. As can be seen from the figure the tree with complexity 2 has the smallest cross validation error. Since we have more than two classes and following the general rule that the optimal tree can have each complexity with a cross validation error within one standard deviation of the tree with the smallest error, the tree with complexity five was selected as optimal tree (figure 5). The cross validation error was 0.26 or 11.6%. Even if the cross validation error is quite high, it could be observed that during cross validation all genuine samples were classified correctly and none of the counterfeit or imitation samples were classified as genuine. This was confirmed during external validation, which means that the CART model is able to distinguish between genuine and counterfeit drugs, based on the FT-IR data. When focussing on the classification of the counterfeit or imitation samples over the different classes it was observed that 10 of the 12 counterfeit samples of the external test set were classified correctly while the 2 other were classified as non-accurate imitations (class 8) in stead of professional imitations (class 7). Since the data set of the Viagra$^{®}$ like samples contains representatives of 7 classes, one should select a tree with minimal 7 leafs in order to be able to predict each class. Since our primary goal was to distinguish between counterfeit and genuine and the fact that we chose the optimal tree size based on the cross validation results, the leafs of the selected tree are not homogeneous for some counterfeit classes (class 1,3,9) and so the tree model is only able to give an indication about the sample type for these samples. The inhomogeneity for these classes in the model is probably due to the low number of samples belonging to these classes.
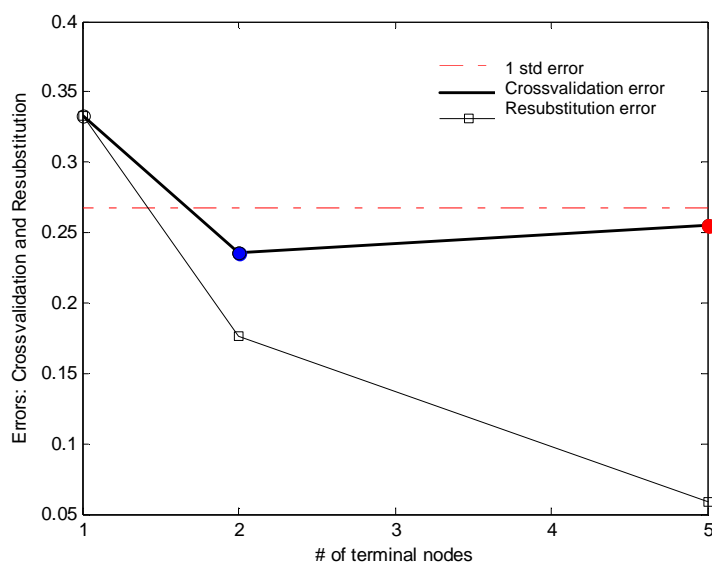
Figure 4: the cross validation error and the resubstitution error in function of the tree complexity for the FT-IR data
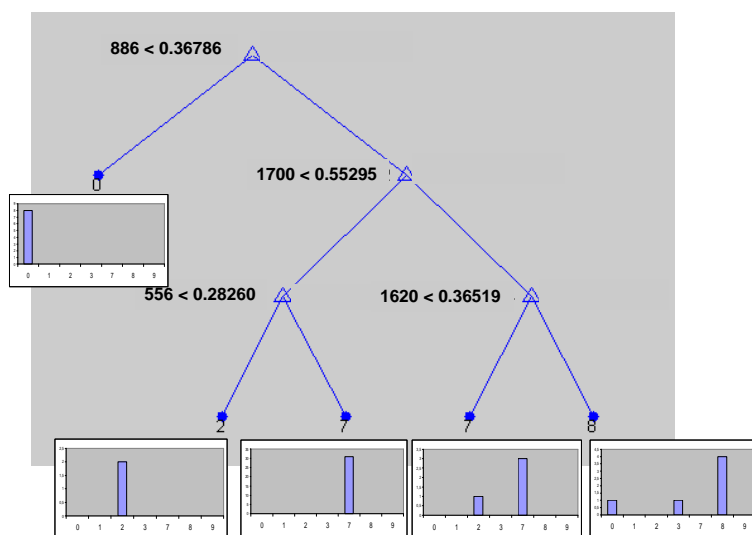
Figure 5: Classification tree based on the FT-IR data for the Viagra® data set. Each split is defined by the selected wavelength and its splitvalue. Each leaf is defined by the class number of the class most represented in the leaf and the graph gives the distribution (homogeneity) of the different samples in the leaf.

One of the main disadvantages of CART, used with spectral data is that it selects only one variable/wavelength to define each split. Since spectral data usually has a signal over a range of wavelengths this causes the difficulty to interpret the significance of the selected wavelengths. In fact for the CART model based on the FT-IR data the wavelengths of 886 cm^{-1} and 1700 cm^{-1} could be related to the concentration of sildenafil present in the samples. For the other selected wavelengths no logical explanation could be found.

4.1.2. *Classification tree based on the NIR data*

From a similar graph as shown in figure 4 it could be concluded that for the NIR data, the tree with complexity 4 has the lowest cross validation error and is the optimal tree (figure 6). The cross validation error was 0.37 or 14.4 %. Investigation of the tree shows that the leaf of the genuine samples is homogeneous and that during cross validation all genuine samples were classified correctly and that none of the counterfeit samples was classified as genuine. These results were also reflected during the external validation. During external validation, ten of the twelve counterfeit samples were classified correctly, while two professional imitations (class 7) were classified as non-professional counterfeits. From these results it can be concluded that the CART model based on NIR-data is comparable to the model obtained with the FT-IR data for its predictive and descriptive properties.

Figure 6: classification tree based on the NIR data for the Viagra® data set. Each split is defined by the selected wavelength and its splitvalue. Each leaf is defined by the class number of the class most represented in the leaf and the graph gives the distribution (homogeneity) of the different samples in the leaf.

Investigation of the selected variables revealed that the selected wavelengths 4150.1 cm^{-1} and 5233.9 cm^{-1} correspond to specific peaks of the NIR spectrum of microcrystalline cellulose. It can therefore be stated that the discrimination of genuine and counterfeit samples by the CART model, based on NIR data, is partly based on the presence of different amounts of microcrystalline cellulose in the counterfeit and the genuine samples.

4.1.3. *Classification tree based on the Raman spectroscopy data*

For the Raman spectroscopic data the tree with complexity 3 was selected as the optimal tree (figure 7). The cross validation error was 0.25 or 11.5 %. Investigation of the tree and

the cross validation results show that the leaf representing the genuine samples (0) is homogeneous and that no genuine samples are classified in another leaf. Also during cross validation all genuine samples are correctly classified and none counterfeit sample is classified as genuine. The external validation reflects the same, all genuine are classified as genuine and no counterfeits are classified as genuine. When focussing on the classification of the counterfeit samples of the external test set, the model gives a correct classification for 8 of the 12 samples, which is significantly worse compared to the previous 2 models.
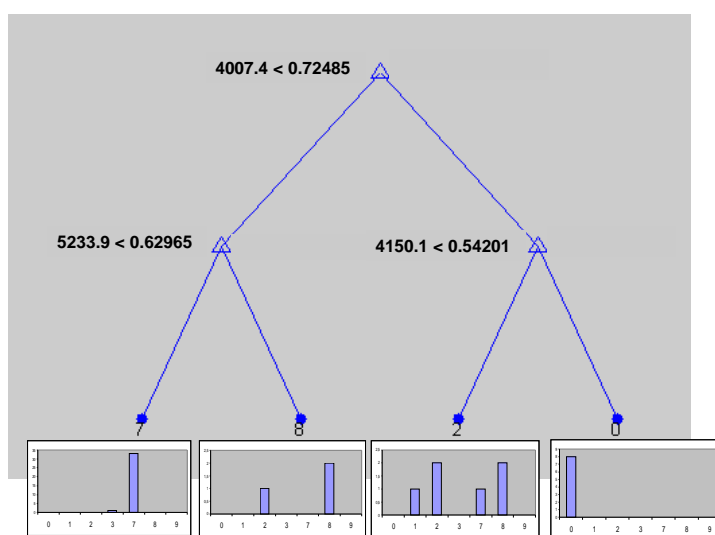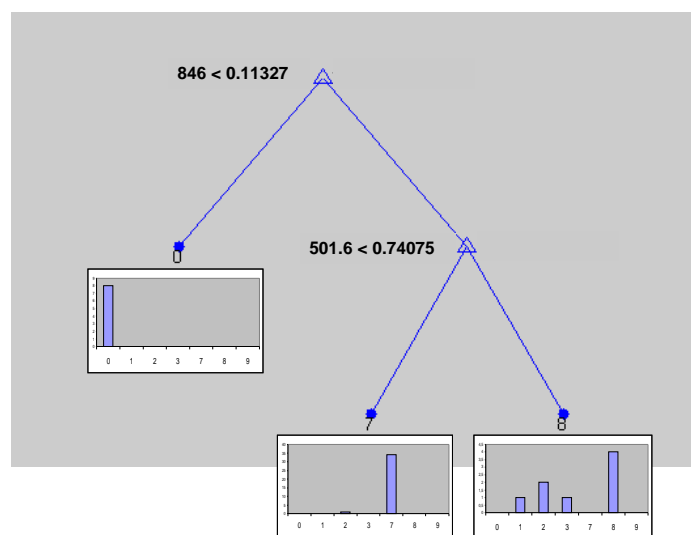

Figure 7: classification tree based on the Raman data for the Viagra® data set. Each split is defined by the selected wavelength and its splitvalue. Each leaf is defined by the class number of the class most represented in the leaf and the graph gives the distribution (homogeneity) of the different samples in the leaf.

The selected wavelengths could be linked to the presence of excipients. The wavelength of 501.6 cm^{-1} is a characteristic signal for the Raman spectrum of calcium hydrogenophosphate while 846 cm^{-1} is a wavelength corresponding to a signal characteristic for hydroxypropylcellulose. Calcium hydrogenophosphate is present in the genuine samples, but not or in different amounts in the counterfeit samples. Hydroxypropylcellulose on the other hand is not present in the genuine samples. Again it can be stated that the discrimination of the CART model is based on the presence of secondary components and excipients.

4.1.4. *Classification trees based on the combination of the spectral data*

Tree models were built using combinations of the data. One model was built using the FT-IR and the NIR data, one using the FT-IR and the Raman data, one using NIR and Raman and one using the combination of the three.
None of these models led to satisfying results, therefore it was decided not to discuss them in detail.

The models obtained with the combination of the FT-IR and the NIR data as well as the one based on the three types of spectral data, did not result in a satisfying model since a number of counterfeit samples was classified as genuine during both cross validation as external validation. Since the models based on each technique separately were able to make this distinction, it seems that combining the two data sets introduces noise in the model.

The other two models (combination FT-IR-Raman and NIR-Raman respectively) were able to distinguish counterfeit from genuine samples, since no genuine sample were classified as counterfeit and no counterfeit as genuine, during both cross validation as external validation. During external validation it was seen that the models had higher misclassification rates (4/12 and 5/12) than the models discussed in section 4.1.1 and 4.1.2.

From these results it has to be concluded that the combination of different types of spectral data, does not result in better models for the Viagra® data set.

4.2. Cialis® like samples

Exactly the same approach as described for the Viagra® data set was followed. The assignment of the class numbers, based on the RIVM classification, for the Cialis® data set is given in table 2.

4.2.1. Classification trees based on the FT-IR and the NIR data

From the graphs of percentage misclassification in function of the tree complexity the trees of complexity three and five were selected as optimal trees for respectively the FT-IR and the NIR data. Since cross validation and external validation showed that both models were not able to distinguish between genuine and counterfeit samples, these models are not further discussed.

4.2.2. Classification tree based on the Raman spectroscopy data

The tree of complexity five was selected as the optimal model obtained using the Raman spectroscopy data for the Cialis® data set (figure 8). A cross validation error of 0.62 or 28 % was obtained, which is high if it is compared to the errors obtained for the models for the Viagra® data set. Investigation of the leafs shows that the group of the genuine samples is homogeneous and that no genuine is classified with counterfeit samples. Also during cross validation all genuine samples are correctly classified and no counterfeit samples are classified as genuine. During external validation on the other hand it could be observed that

despite the fact that all genuine samples are correctly classified, two counterfeit samples are wrongly classified from which one is classified as genuine.

Three of the selected wavelengths (1109.1 cm^{-1}, 1119.0 cm^{-1} and 1120.2 cm^{-1}) could be linked to the Raman spectrum of lactose, an excipient present in both genuine as counterfeit samples. Probably the differences in amounts partly account for the discrimination.
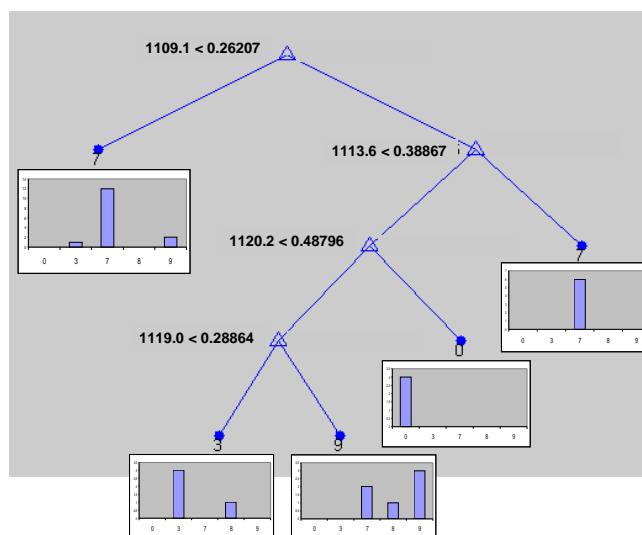
Figure 8: classification tree based on the Raman data for the Cialis® data set. Each split is defined by the selected wavelength and its splitvalue. Each leaf is defined by the class number of the class most represented in the leaf and the graph gives the distribution (homogeneity) of the different samples in the leaf.

4.2.3. Classification trees based on the combination of the spectral data

Tree models were built using a combination of the different types of spectral data. The only model able to distinguish between counterfeit and genuine samples was the one combining the NIR and the Raman spectroscopic data. The tree with complexity six was selected as the optimal tree (Figure 9). A cross validation error of 0.50 or 22.5 % was obtained. Investigation of the leafs showed that the leaf representing the genuine samples is homogeneous and that no genuine samples are classified with counterfeit ones. Also during cross validation and external validation all genuine are classified correctly and no counterfeit samples are classified as genuine. It has also to be mentioned that during external validation all counterfeit samples were classified correctly.

Three of the selected NIR wavelengths (4215.6 cm^{-1}, 5997.5 cm^{-1} and 6730.3 cm^{-1}) could be linked to excipients, present in the genuine Cialis® tablets. 4215.6 cm^{-1} corresponds to a characteristic peak of lactose, 5997.5 cm^{-1} to a characteristic peak of carmellose and 6730.3 cm^{-1} to one of microcrystalline cellulose. The two other wavelengths could not be linked to compounds, present or not in counterfeit samples.

Since three of the five wavelengths could be linked to excipients present in the genuine tablets, the discrimination is again probably due to the differences in amounts.
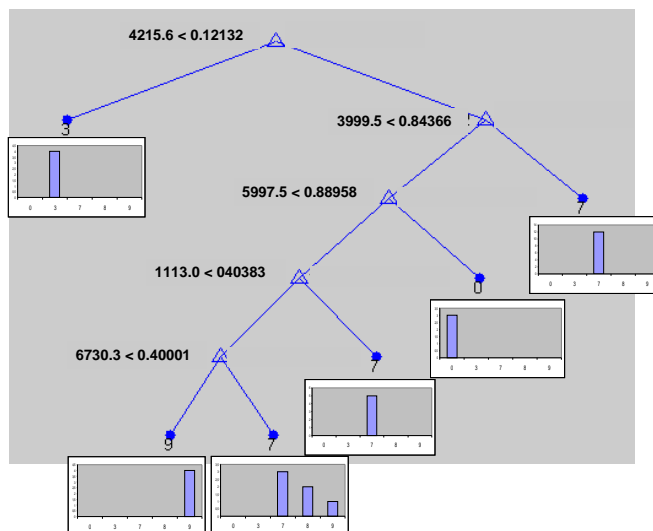
Figure 9: classification tree based on the combination of the NIR and the Raman data for the Cialis[®] data set. Each split is defined by the selected wavelength and its splitvalue. Each leaf is defined by the class number of the class most represented in the leaf and the graph gives the distribution (homogeneity) of the different samples in the leaf.

4.3.   Results obtained with kNN

*k*NN was applied to the same data sets as described in sections 4.1 and 4.2. In a first step the optimal number of nearest neighbours was chosen, for each data set, using a leave-one-out cross validation procedure. The models were evaluated based on the correct classification rate (CCR) obtained during cross validation and the prediction of the external test set.

Two kind of *k*NN models were built, one using only the classes 0 for genuine samples and 1 for counterfeit samples and one using the different classes as used for the CART models. The reason is the fact that the theory of the algorithms (CART and *k*NN) are completely different. While CART will isolate the genuine group in a early phase of the model building and continue further classification of the counterfeits without influence of the genuine group, *k*NN will model the data set as a whole, resulting in a higher influence of the unbalanced numbers of samples in the different classes.

In general it can be stated that the results obtained with *k*NN are unsatisfying.

For the Viagra® dataset CCR values of 90% (optimal number of k = 3), 100% (optimal number of k = 3) and 98,04% (optimal number of k = 3) were obtained for respectively the FT-IR, the NIR- and the Raman data, using cross validation when using the binary class (genuine vs. counterfeit) approach. Only the model based on the NIR data was able to discriminate between genuine and counterfeit, which was reflected by the 100 % CCR for both cross validation as external validation. In the models based on the FT-IR data and the Raman data at least one genuine was classified as counterfeit, which is unacceptable since it is a false positive. When using the different RIVM classes CCR values of 55% (optimal number of k = 5), 61% (optimal number of k = 5) and 43% (optimal number of k = 9) were obtained for respectively the FT-IR, the NIR- and the Raman data, using cross validation. For the external validation CCR values were obtained of 31%, 23% and 23% respectively. The more in all models some originals were classified as counterfeit and some counterfeits as original.

For the Cialis® dataset it was not possible to discriminate between original and counterfeit samples using *k*NN. Probably due to the fact that the number of genuine samples in this data set is too low for the algorithm.

5. <u>Conclusions</u>

The use of classification trees as easy interpretable models for the distinction of counterfeit and genuine drugs as well as the classification of counterfeit drugs, following the RIVM classification, was evaluated. All models were based on spectroscopic data. Models were built for two data sets, one consisting of the spectroscopic data for genuine and counterfeit samples of Viagra® and one consisting of the spectroscopic data for genuine and counterfeit samples of Cialis®. An overview of the obtained correct classification rates for the different models proposed is given in table 3. Only models with a 100% correct classification rate for the discrimination between genuine and counterfeit, during cross validation, are present in the table, since only these models are of interest.

For the Viagra® data set, two comparable models could be proposed, one based on the FT-IR data and one on the NIR data. The models have cross validation errors of 11.6% and 14.4% respectively and equal misclassification rates of 2/12 after external validation. Since both models are comparable the choice is based on the equipment present in the laboratories. For the both models the classification/discrimination could partly be explained by the differences in amounts of active substance (FT-IR model) and excipients (NIR model). The combination of the different types of spectroscopic data did not result in better models compared to the ones obtained with only FT-IR or NIR data.

Table 3: Overview of the prediction errors of the proposed models

	Data used	CCR genuine/counterfeit (cross-validation) (%)	Overall CCR (cross validation) (%)	CCR genuine/counterfeit	Overall CCR
Viagra® like samples	FT-IR	100	88,4	13/13	11/13
	NIR	100	85,6	13/13	11/13
	Raman	100	88,5	13/13	9/13
Cialis® like samples	Raman	100	72	8/9	6/9
	Raman-NIR	100	77,5	9/9	9/9

For the Cialis® data set the best model was obtained by combining the NIR and the Raman spectroscopic data. All other models were not able to make the distinction between counterfeit and genuine samples. Only the model based on the Raman spectroscopy data was able to classify all genuine samples correctly, but also classified a counterfeit sample as genuine.

The proposed model has a cross validation error of 22.5%, but showed a 100% correct classification rate during external validation. Again the majority of the selected wavelengths could be linked to differences in amounts of excipients between the different samples.

The obtained results show that the application of CART to spectroscopic data result in easy interpretable models, which are able to discriminate between counterfeit and genuine drug samples and which are able to classify the counterfeit samples in their corresponding RIVM class and this with low misclassification rates, evaluated with an external test set. The classification of the counterfeits in their respective RIVM class, can allow an easy and fast evaluation of the risk for public health of a considered counterfeit sample.

Further it was shown that the results obtained with this tree based method are far better than the ones obtained with the more traditional discriminating method *k*NN. If the results of the CART models are compared to the results obtained with PLS by Sacré et al. [24], it can be seen that both methods are able to discriminate between genuine and counterfeit products, but that CART also allows a clear discrimination of the counterfeit samples in different classes. The more CART has the advantage to be able to classify the samples in a discriminating and easy interpretable model. Though the models are limited by the nature of the data set and they should be adapted and updated each time new samples/classes are encountered.

References

[1] Weiss A., Buying prescription drugs on the internet: promises and pitfalls, Cleveland Clinic Journal of Medicine (2006)73, 282-288

[2] Veronin M., Youan B.-B., Magic bullet gone astray: medications and the internet, Science (2004) 305, 481

[3] European Alliance For Acces to Safe Medicines: www.eaasm.eu

[4] WHO, sixty-second world health assembly item 12.9, counterfeit medical products, April 2009. http://aps.who.int/gb/ebwha/pdf_files/A62/A62_13-en.pdf

[5] Venhuis B.J., Barends D.M., Zwaagstra M.E., de Kaste D., Recent developments in counterfeit and imitations of Viagra, Cialis and Levitra, RIVM Report 370030001/2007, Bilthoven, 2007

[6] Savalyia A.A., Shah R.P., Prasad B., Singh S., Screening of Indian aphrodisiac ayurvedic/herbal healthcare products for adulteration with sildenafil, tadalafil and/or vardenafil using LC/PDA and extracted ion LC–MS/TOF, Journal of Pharmaceutical and Biomedical Analysis (2010) 52, 406-409

[7] Roggo Y., Degardin K., Margot P., Identification of pharmaceutical tablets by Raman spectroscopy and chemometrics, Talanta (2010) 81, 988-995

[8] Vajna B., Farkas I., Szabó A., Zsigmond Z., Marosi G., Raman microscopic evaluation of technology dependent structural differences in tablets containing imipramine model drug, Journal of Pharmaceutical and Biomedical Analysis (2010) 51, 30-38

[9] de Veij M., Deneckere A., Vandenabeele P., de Kaste D., Moens L., Detection of counterfeit Viagra with Raman spectroscopy, Journal of Pharmaceutical and Biomedical Analysis (2008) 46, 303-309

[10] Storme-Paris I., Rebiere H, Matoga M., Civade C., Bonnet P.-A., Tissier M.H., Chaminade P., Challenging near infrared spectroscopy discriminating ability for counterfeit pharmaceuticals detection, Analytica Chimica Acta (2010) 658, 163-174

[11] de Peinder P., Vredenbregt M.J., Visser T., de Kaste D., Detection of Lipitor counterfeits: a comparison of NIR and Raman spectroscopy in combination with chemometrics, Journal of Pharmaceutical and Biomedical Analysis (2008) 47, 688-694

[12] Puchert T., Lochmann D., Menezes J.C., Reich G., Near-infrared chemical imaging (NIR-CI) for counterfeit drug identification--a four-stage concept with a novel approach of data processing (Linear Image Signature), Journal of Pharmaceutical and Biomedical Analysis (2010) 51, 138-145

[13] Lopes M.B., Wolff J.C., Investigation into classification/sourcing of suspect counterfeit Heptodintrade mark tablets by near infrared chemical imaging, Analytica Chimica Acta (2009) 633, 149-155

[14] Lopes M.B., Wolff J.C., Bioucas-Dias J.M., Figueiredo M.A., Determination of the composition of counterfeit Heptodin tablets by near infrared chemical imaging and classical least squares estimation, Analytica Chimica Acta (2009) 641, 46-51

[15] Amin A.S., Moustafa M.E., El-Dosoky R., Colorimetric determination of sildenafil citrate (Viagra) through ion-associate complex formation, Journal of AOAC International (2009) 92, 125-130

[16] Rodomonte A.L., Gaudiano M.C., Antoniella E., Lucente D., Crusco V., Bartolomei M., Bertocchi P., Manna L., Valvo L., Muleri N., Counterfeit drugs detection by measurement of tablets and secondary packaging colour, Journal of Pharmaceutical and Biomedical Analysis (2010) 53, 215-220

[17] Vredenbregt M.J., Blok-Tip L., Hoogerbrugge R., Barends D.M., de Kaste D., Screening suspected counterfeit Viagra and imitations of Viagra with near-infrared spectroscopy, Journal of Pharmaceutical and Biomedical Analysis (2006) 40, 840-849

[18] Wawer I., Pisklak M., Chilmonczyk Z., 1H, 13C, 15N NMR analysis of sildenafil base and citrate (Viagra) in solution, solid state and pharmaceutical dosage forms, Journal of Pharmaceutical and Biomedical Analysis (2005) 38, 865-870

[19] Trefi S., Routaboul C., Hamieh S., Gilard V., Malet-Martino M., Martino R., Analysis of illegally manufactured formulations of tadalafil (Cialis) by 1H NMR, 2D DOSY 1H NMR and Raman spectroscopy, Journal of Pharmaceutical and Biomedical Analysis (2008) 47, 103-113

[20] Maurin J.K., Pluciński F., Mazurek A.P., Fijałek Z., The usefulness of simple X-ray powder diffraction analysis for counterfeit control--the Viagra example, Journal of Pharmaceutical and Biomedical Analysis (2007) 43, 1514-1518

[21] Martino R., Malet-Martino M., Gilard V., Counterfeit drugs: Analytical techniques for their identification, Analytical and Bioanalytical Chemistry (2010) 398, 77-92.

[22] Deconinck E., van Nederkassel A.M., Stanimirova I., Daszykowski M., Bensaid F., Lees M., Martin G.J., Desmurs J.R., Smeyers-Verbeke J., Vander Heyden Y., Isotopic ratios to detect infringements of patents or proprietary processes of pharmaceuticals: two case studies, Journal of Pharmaceutical and Biomedical Analysis (2008) 48, 27-41.

[23] Dumarey M., van Nederkassel A.M., Stanimirova I., Daszykowski M., Bensaid F., Lees M., Martin G.J., Desmurs J.R., Smeyers-Verbeke J., Vander Heyden Y., Recognizing paracetamol formulations with the same synthesis pathway based on their trace-enriched chromatographic impurity profiles, Analytica Chimica Acta. (2009) 655, 43-51.

[24] Sacré P-Y, Deconinck E., De Beer T., Courselle P., Vancauwenberghe R., Chiap P., Crommen J., De Beer J.O., Comparison and combination of spectroscopic techniques for the detection of counterfeit medicines, Journal of Pharmaceutical and Biomedical Analysis (2010) 53, 445-53

[25] Breiman L., Friedman J.H., Olshen R.A., Stone C.J., Classification and regression trees; Wadsworth & Brooks, Monterey, 1984.

[26] Deconinck E., Hancock T., Coomans D., Massart D.L., Vander Heyden Y., Classification of drugs in absorption classes using Classification And Regression Trees (CART)-methodology, Journal of Pharmaceutical and Biomedical Analysis (2005) 39, 91-103.

[27] Deconinck E., Zhang M.H., Coomans D., Vander Heyden Y., Classification tree models for the prediction of blood-brain barrier passage of drugs, Journal of Chemical Information and Modeling (2006) 46, 1410-1419.

[28] Vandeginste B.G.M., Massart D.L., Buydens L.M.C., De Jong S., Lewi P.J., Smeyers-verbeke J.: Handbook of Chemometrics and Qualimetrics-Part B, Elsevier Science, Amsterdam, 1997

[29] Pearson G.A., A general baseline-recognition and baseline flattening algorithms, Journal of Magnetic Resonance (1977) 27, 265-272.

[30] Snee R.D.: Validation of regression models: Methods and examples. Technometrics (1977) 19, 415-428.

[31] Massart D.L., Vandeginste B.G.M., Buydens L.M.C., De Jong S., Lewi P.J., Smeyers-verbeke J.: Handbook of Chemometrics and Qualimetrics-Part A, Elsevier Science, Amsterdam, 1997

3.3.   Detection of counterfeit Viagra® by Raman Microspectroscopy imaging and multivariate analysis.

During the following study, the interest of Raman Microspectroscopy imaging has been evaluated in the frame of counterfeit Viagra® detection. The Raman microscopic maps of 26 counterfeits and imitations of Viagra® tablets and 8 genuine tablets of Viagra® were recorded. The fact that most of the samples belong to the RIVM professional imitations class does not constitutes a limitation to the conclusions since the visual appearance of the samples is not taken into account.

The different maps were pre-processed to allow multivariate analysis. Three different analyses were performed:

- discrimination between genuine and illegal samples based on the whole Raman spectrum (200-1800cm^{-1}).
- discrimination between genuine and illegal samples based on the presence of lactose in the core of the tablets. Indeed, lactose is not present in the core of genuine Viagra® tablets but is a common and cheap filler probably used by counterfeiters.
- discrimination between genuine and illegal samples based on the distribution of sildenafil among the core of the tablets. The counterfeiters have probably less high-performance equipment than Pfizer. It is therefore expected that the spatial distribution of sildenafil is less homogenous in illegal tablets than in genuine ones.

The methods and results are described in the paper:

Sacré P-Y, Deconinck E, Saerens L, De Beer T, Courselle P, Vancauwenberghe R, Chiap P, Crommen J, De Beer J, Detection of counterfeit Viagra® by Raman Microspectroscopy imaging and multivariate analysis, Journal of Pharmaceutical and Biomedical analysis (2011), 56, 454-461

Detection of counterfeit Viagra® by Raman Microspectroscopy imaging and multivariate analysis.

Pierre-Yves Sacré[a,c#], Eric Deconinck[a#], Lien Saerens[b], Thomas De Beer[b], Patricia Courselle[a], Roy Vancauwenberghe[d], Patrice Chiap[c], Jacques Crommen[c], Jacques O. De Beer[a,*]

[a] *Laboratory of Drug Analysis, Scientific Institute of Public Health, Brussels, Belgium*

[b] *Laboratory of Pharmaceutical Process Analytical Technology, Ghent University, Ghent, Belgium.*

[c] *Department of Analytical Pharmaceutical Chemistry, Institute of Pharmacy, University of Liege, Liege, Belgium.*

[d] *Federal Agency for Medicines and Health Products, Brussels, Belgium*

Abstract

During the past years, pharmaceutical counterfeiting was mainly a problem of developing countries with weak enforcement and inspection programs. However, Europe and North America are more and more confronted with the counterfeiting problem. During this study, 26 counterfeits and imitations of Viagra® tablets and 8 genuine tablets of Viagra® were analysed by Raman microspectroscopy imaging.

After unfolding the data, three maps are combined per sample and a first PCA is realised on these data. Then, the first principal components of each sample are assembled. The exploratory and classification analysis are performed on that matrix.

PCA was applied as exploratory analysis tool on different spectral ranges to detect counterfeit medicines based on the full spectra (200-1800 cm^{-1}), the presence of lactose (830-880 cm^{-1}) and the spatial distribution of sildenafil (1200-1290 cm^{-1}) inside the tablet. After the exploratory analysis, three different classification algorithms were applied on the full spectra dataset: linear discriminant analysis, k-nearest neighbour and soft independent modelling of class analogy. PCA analysis of the 830-880cm^{-1} spectral region discriminated genuine samples while the multivariate analysis of the spectral region between 1200-1290 cm^{-1} returns no satisfactory results.

A good discrimination of genuine samples was obtained with multivariate analysis of the full spectra region (200-1800 cm^{-1}). Application of the k-NN and SIMCA algorithm returned 100% correct classification during both internal and external validation.

Keywords:

Raman Microspectroscopy, counterfeit medicines, PCA, discrimination, chemical imaging

[#] These authors contributed equally to this work.

1. Introduction

During the past years, pharmaceutical counterfeiting was mainly a problem of developing countries with weak enforcement and inspection programs. Asia and Latin America are the most contaminated geographical regions. However, Europe and North America are more and more confronted to the counterfeiting problem. [1]

Recently, the Belgian Federal Agency for Medicines and Health Products (AFMPS/FAGG) participated in PANGEA III, an international operation fighting against the online sale of counterfeit and illegal medicines [2]. The most encountered therapeutic categories in Belgium were weight-loss drugs and potency enhancing drugs such as Viagra® (Pfizer).

Since its approval by the American Food and Drug Agency (FDA) [3] and the European Medicines Agency (EMA) [4] in 1998, Viagra® has become one of the most counterfeited medicines in industrialized countries. Several spectroscopic techniques have been used to detect counterfeit Viagra®. Rodomonte et al. used colorimetry to detect counterfeit medicines based on their differences of tablets and second packaging colour [5]. Vredenbregt et al. applied NIR spectroscopy on 103 samples to detect counterfeit Viagra® but also to check the homogeneity of batches and screen the presence of sildenafil citrate [6]. De Veij et al. showed for the first time that Raman spectroscopy was able to detect counterfeit Viagra® [7]. However this study compared 18 illegal samples to only one genuine tablet. Our group concluded that the combination of FT-IR and NIR spectroscopy was more powerful than FT-IR, NIR or Raman spectroscopy alone to discriminate genuine from illegal Viagra® samples [8]. X-ray powder diffraction [9], NMR (^{1}H, ^{13}C, ^{15}N) [10], and NMR (2D DOSY, 3D DOSY-COSY, ^{1}H NMR) [11] were also used to detect counterfeit Viagra®. However, compared to the first cited techniques, X-ray diffraction and NMR necessitate a more elaborated sample preparation and are therefore only performed by well trained analysts.

Chemical imaging is a powerful tool since it provides physico-chemical information and spatial information of the sample. Raman microspectroscopy imaging is widely used in the biomedical field. Among others, it has been recently used to predict the cellular response to cisplatin in lung adenocarcinoma [12] and to study the molecular interactions between zoledronic acid and bone [13]. It is also used in the pharmaceutical field since it necessitates a negligible sample preparation (e.g. for tablet analysis, sample preparation is only cutting tablets in two). It has been mostly used in pharmaceutical technology applications [14-17].

Near infrared chemical imaging (NIR-CI) has also been used in the field of pharmaceutical technology [18-21]. More recently, NIR-CI has been used by Lopes et al. to detect and classify counterfeit antiviral drugs [22] and to determine their chemical composition [23]. Puchert et al. successfully used NIR-CI to detect counterfeit bisoprolol tablets [24].

During this study, 26 counterfeits and imitations of Viagra® tablets and 8 genuine tablets of Viagra® were analysed by Raman microspectroscopy imaging. After an exploratory PCA analysis, linear discriminant analysis (LDA), k-nearest neighbours (k-NN) and soft independent modelling by class analogy (SIMCA) were applied on the full spectra dataset, as classification algorithms. Other spectral ranges were also investigated to detect counterfeit medicines based on the presence of lactose and the spatial distribution of sildenafil inside the tablet. The aim of this study was to discriminate illegal samples and to evaluate which of the three applied classification algorithm was the best suited for purpose. As far as we know, this is the first time that Raman microspectroscopy imaging is used to detect counterfeit medicines.

2. **Theory**

2.1.   Principal component analysis

PCA is a variable reduction technique, which reduces the number of variables by making linear combinations of the original variables. These combinations are called the principal components and are defined in such way that they explain the highest (remaining) variability in the data and are by definition orthogonal.

The importance of the original variables in the definition of a principal component is represented by its loading and the projections of the objects on to the principal components are called the scores of the objects [25].

2.2.   Selection of a test set for external validation.

In order to perform an external validation of the classification models, matrix **B** was split into a training and a test set applying the Kennard and Stone algorithm [25, 26]. Kennard and Stone algorithm is a uniform mapping algorithm that consists of maximizing the minimal Euclidian distance between each selected point and all the other. In this study, the selection of the objects started with the furthest object from the mean point using the Euclidian distance. The second chosen object i_0 is the furthest point from the previous one, i:

$$d_{selected} = \max_{i_0}(\min_{i}(d_{i,i_0}))$$

where $d_{selected}$ is the Euclidian distance between the new selected point i_0 and the previously selected point i.

Then, all the other objects are selected the same way until the selected number of objects of the training set is reached. The remaining objects are included in the test set.

2.3.   Linear Discriminant Analysis (LDA)

Linear discriminant analysis [27,28] is a feature reduction method just like PCA. But when PCA selects a direction which maximises the variance of the data, LDA selects the direction that maximises the between-class variance and so discriminate the given classes. The latent variable obtained is a linear combination of the original variables and is called canonical variate. For *k* classes, *k*-1 canonical variates are determined. To maximize the discriminating power, the algorithm selects a linear function of the variables, D, that maximizes the ratio between the between-class variance and the within-class variance.

2.4.   k-Nearest Neighbour (k-NN)

The k-NN algorithm [27] was applied on the training set. The algorithm computes the minimal Euclidian distances between an unknown object and each of the objects of the training set. For a training set of n samples, n distances are calculated. Then it selects the k nearest objects (here k is set at 3) to the unknown one. The unknown object is classified in the group to which the majority of the k objects belong. The main advantages of this method are its mathematical simplicity and the fact that it is free from statistical assumptions.

2.5.   Soft Independent Modelling by Class Analogy (SIMCA)

SIMCA [27] is not a discriminating algorithm but a classifying algorithm since it decides whether a new object belongs to a certain class or not. If the object does not belong to a class, it is considered as an outlier while with LDA and k-NN it is always classified.
The algorithm also defines latent variables and uses them to classify the objects.

First of all, the algorithm determines the number of eigenvectors needed to describe the training class by applying cross-validation. Then a critical value of the Euclidian distance towards the model, s_{crit}, is defined. Along each eigenvector score limits are defined as:

$$t_{max} = \max(t_K) + 0.5 s_t$$

$$t_{min} = \min(t_K) - 0.5 s_t$$

where $\max(t_K)$ is the largest score of the training objects of the studied class on the eigenvector considered and s_t is the standard deviation of the scores along that eigenvector.

Objects with an Euclidian distance s < s$_{crit}$ and scores t_{min} < t < t_{max} are said to belong to the studied class otherwise they are considered as outliers.

In fact all of the classes are modelled separately and test objects are predicted as belonging or not to the studied class. Afterwards the different models can be assembled. In this case, a test object will be predicted as belonging to the nearest class.

3. <u>Experimental</u>

3.1. *Samples*

3.1.1. *Illegal samples*

A total of 26 counterfeit and imitation tablets of Viagra® were donated by the Federal Agency for Medicines and Health Products in Belgium (AFMPS/FAGG). They all come from postal packs ordered by individuals through internet sites. All samples were delivered in blisters or closed jars with or without packaging. All samples, once received, were stored at ambient temperature and protected from light.

3.1.2. *Reference samples*

Pfizer SA/NV (Belgium) kindly provided one batch of each different dosage of Viagra® (25 mg, 50 mg, 100 mg). Two other batches of each dosage were purchased in a local pharmacy in Belgium. A total of 8 references (3 different batches of 100 mg, 3 different batches of 50 mg and 2 different batches of 25 mg) were used in this study.
All references were delivered in closed blisters with packaging and were stored protected from light at ambient temperature.

3.2. *Raman Microspectroscopy measurements*

Each tablet was radially and sharply cut into two parts. Each part was made as smooth as possible to avoid spectral intensity differences due to differences in sample to probe distance. and a 1700 μm x 1300 μm area of the fracture plane was scanned by a 10x long working distance objective lens (spot size laser = 50 μm) in point-by-point mapping mode with a step size of 100 μm in both the x and y directions (= 221 points per mapping).
The image system was a RamanRxn 1 Microprobe (Kaiser Optical Systems, Ann Arbor, USA), equipped with an air-cooled CCD detector (back-illuminated deep depletion design).

The laser wavelength during the experiments was the 785 nm line from a 785 nm Invictus NIR diode laser. All spectra were recorded at a resolution of 4 cm^{-1} using a laser power of 400 mW and a laser light exposure time of 30 sec per collected spectrum. Data collection was done using HoloGRAMS^{TM} (Kaiser Optical Systems, version 2.3.5) data collection software, HoloMAP^{TM} (Kaiser Optical Systems, version 2.3.5) data analysis software and Matlab software (The Matworks, version 7.7).

Three maps were taken at different positions of the core of the tablet.

3.3. Data analysis

All data treatments were realized with Matlab (The Matworks, Natick, MA, USA, version 7.9.0). SIMCA analysis was performed using the PLS_toolbox (Eigenvector Research, Inc., Wenatchee, WA, USA, version 6.0.1).

3.3.1. Data pre-processing

Each Raman microspectroscopic map is a spectral hypercube (Figure 1a). For a map A, X and Y represent the spatial information and λ the spectral information. First of all, an unfolding step is imperative to convert a three dimensional dataset **A** (λ x X x Y) in a two dimensional exploitable dataset **A$_{unfolded}$** (λ x XY). Thus, starting from the matrix **A** (11612 x 13 x 17) matrix, the matrix **A$_{unfolded}$** (11612 x 221) is obtained after unfolding.

Once each map has been unfolded, the three maps of a same sample are associated and only the spectral region between 200-1800 cm^{-1} is kept (representing 5334 recorded intensities). The resulting **A$_{sample}$** matrix is normalized, a principal component analysis (PCA) is performed per sample and the first principal component (PC1) is retained. The first principal component includes the majority of the information variance of the spectral data over the measured regions of the sample (Table 1).

This pre-processing step allows us to reduce a dataset of (11612 x 13 x 17) x 3 in a column vector of (5334 x 1) representing the sample.

a.
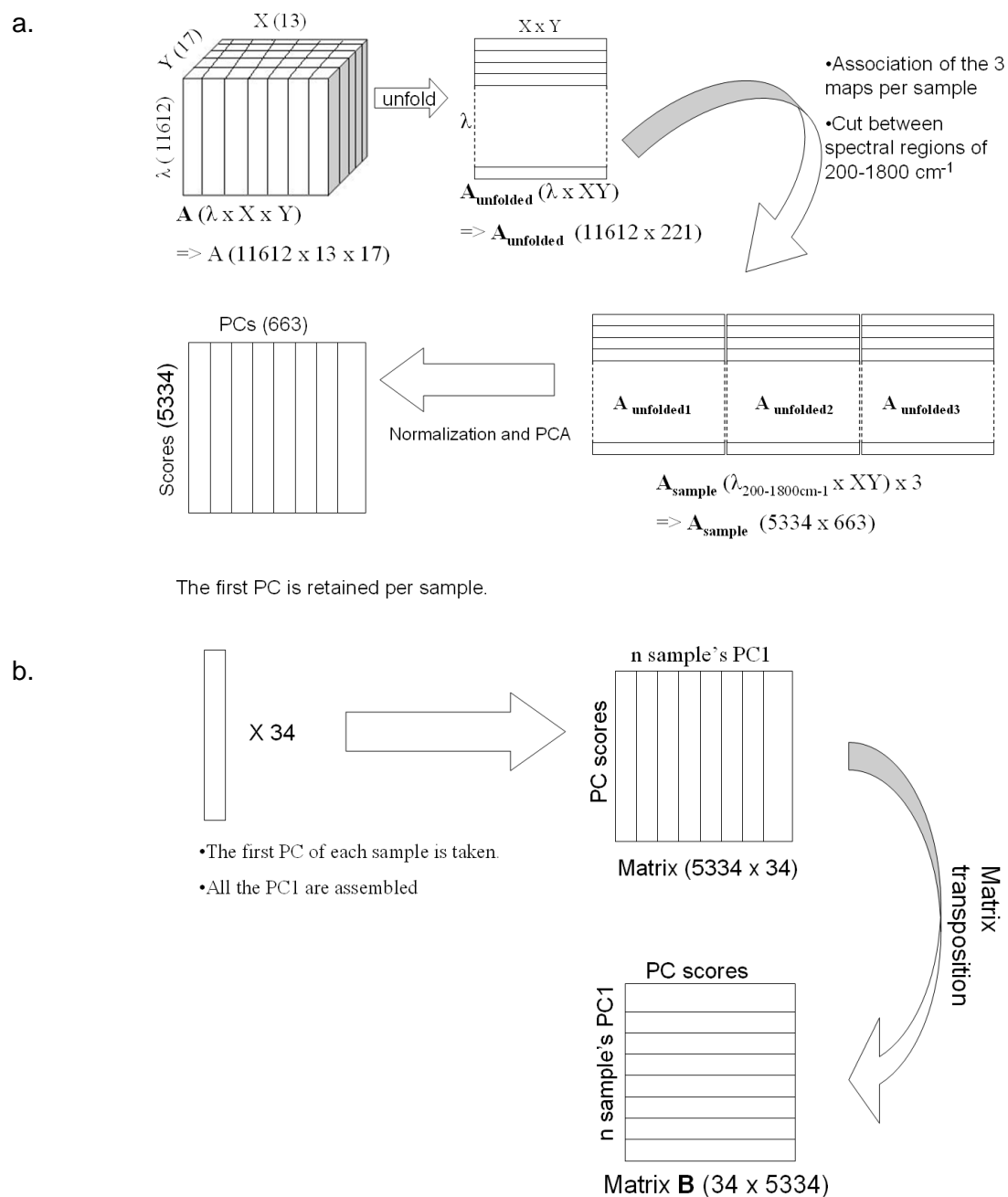
Figure 1: Pre-processing of the Raman Microspectroscopy imaging data. All numbers presented are for the treatment of the 200-1800cm^{-1} spectral range maps.

   a.   Pre-treatment step per sample, from the hyperspectral cube to the first PC.

   b.   Treatment of the data, from the first principal component of each sample to the final PCA discriminating plot.

Table 1: Percentage of variation of matrix **A$_{sample}$** (see 3.3.1.) explained by the three firstprincipal components.

Sample	PC1	PC2	PC3
illegal sample 1	99,71	0,13	0,11
illegal sample 2	99,41	0,45	0,10
illegal sample 3	99,87	0,08	0,03
illegal sample 4	98,64	1,12	0,15
illegal sample 5	99,59	0,23	0,07
illegal sample 6	99,27	0,63	0,07
illegal sample 7	97,47	1,90	0,44
illegal sample 8	99,87	0,09	0,02
illegal sample 9	99,32	0,54	0,10
illegal sample 10	99,98	0,01	0,01
illegal sample 11	99,97	0,02	0,01
illegal sample 12	98,30	1,46	0,15
illegal sample 13	99,54	0,30	0,07
illegal sample 14	99,60	0,21	0,09
illegal sample 15	99,31	0,45	0,09
illegal sample 16	99,55	0,29	0,09
illegal sample 17	99,10	0,67	0,09
illegal sample 18	99,88	0,09	0,01
illegal sample 19	99,36	0,53	0,05
illegal sample 20	99,14	0,34	0,20
illegal sample 21	97,92	1,62	0,28
illegal sample 22	96,41	2,72	0,52
illegal sample 23	99,70	0,28	0,01
illegal sample 24	99,68	0,26	0,05
illegal sample 25	99,61	0,28	0,08
illegal sample 26	98,71	0,96	0,18
Viagra[®] 25mg batch 8268130B	99,79	0,20	0,01
Viagra[®] 50mg batch 8272205B	99,79	0,18	0,01
Viagra[®] 100mg batch 8272604B	99,84	0,13	0,02
Viagra[®] 25mg batch 8333550B	99,87	0,11	0,01
Viagra[®] 100mg batch 8339107B	99,86	0,12	0,01
Viagra[®] 50mg batch 9113106B	99,53	0,36	0,07
Viagra[®] 100mg batch 9114001B	99,91	0,07	0,01
Viagra[®] 50mg batch 9151918B	99,83	0,13	0,02

The column vectors obtained for each sample were assembled in a (5334 x 34) matrix which is transposed resulting in a matrix of dimensions (34 x 5334) where 34 is the number of samples and 5334 the number of wavelengths for which spectral data is available (Figure 1b). This dataset, named matrix **B**, was used in further analysis.

The data pre-processing was the same for the other spectral regions.

4.   <u>Results and Discussion</u>

4.1.   Raman microspectroscopy maps

Figure 2 shows typical genuine Viagra[®] maps at the three dosage forms and Figure 3 shows the maps of 3 illegal samples which are representative of the other illegal samples. There is no visible difference between the dosage forms of the genuine samples at the chosen intensity range (1×10^7 – 10×10^7 Raman counts). However, as can be seen, the spectral intensities are much higher in illegal preparations than in genuine tablets. This is sometimes due to higher sildenafil content but in most cases this is due to a higher background shift. This shift may be caused by high impurity content or the use of other excipients like colored excipients such as sample B in Figure 3 which is a non coated blue tablet. Those excipients may cause fluorescence or be more Raman active and, therefore, be responsible of those higher spectral intensities.

As the aim of this study was to be able to discriminate illegal Viagra[®] from genuine ones, the different shifts were not corrected. Those differences must be kept to perform a correct and complete discrimination based on both spectral intensities, additional peaks and also on the peak intensity distribution.
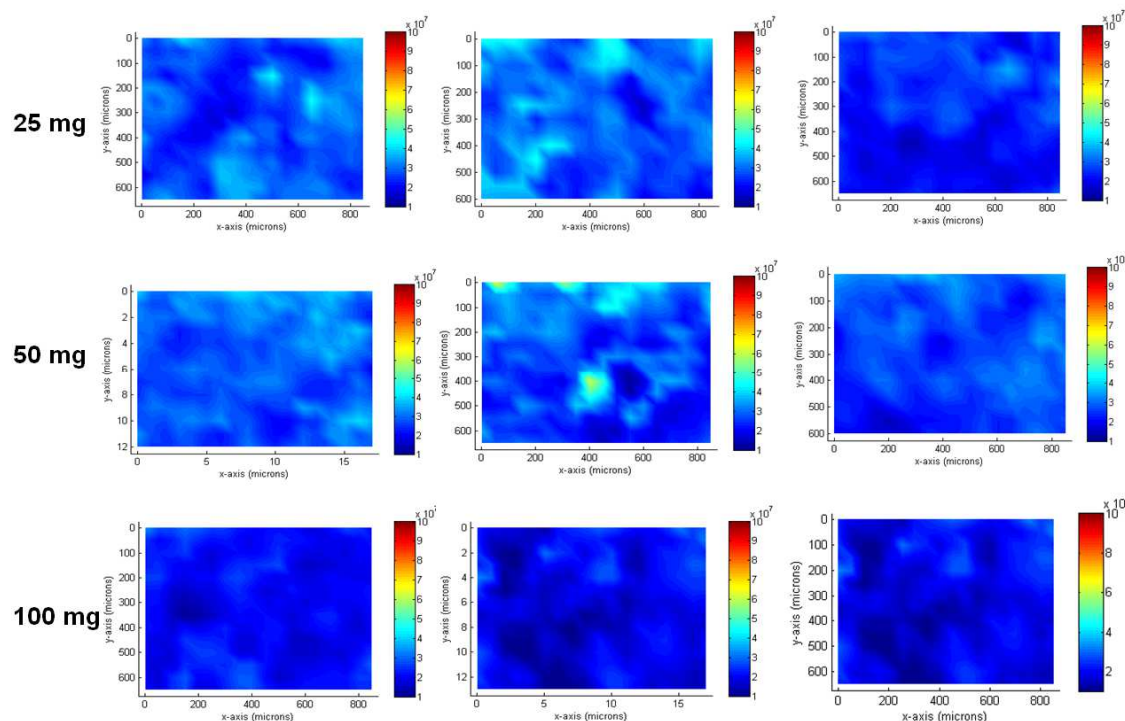
Figure 2: Raman Microspectroscopy imaging maps of representative genuine. Three maps in the spectral region of 200-1800cm^{-1} taken at different positions of the core of three dosage forms of genuine Viagra[®] are presented. Spectral intensity colors are comprised between 1×10^7 and 10×10^7 Raman Counts.
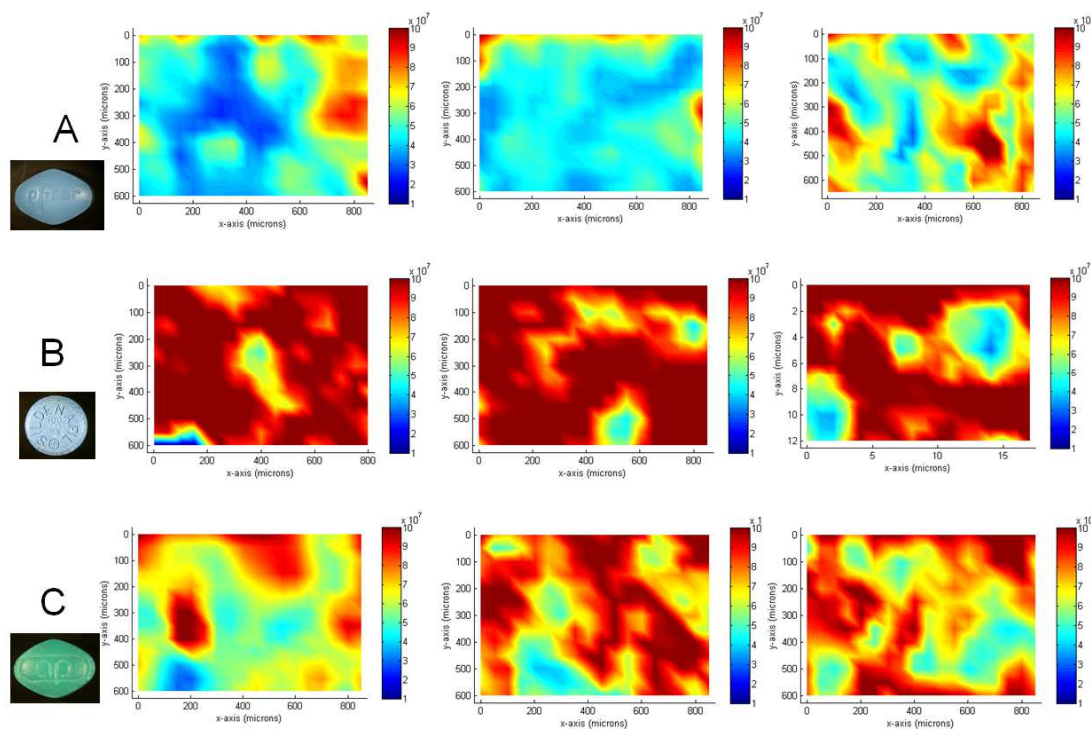
Figure 3: Raman Microspectroscopy imaging maps of representative illegal samples. Three maps in the spectral region of 200-1800cm^{-1} taken at different positions of the core of three illegal samples are presented with the corresponding sample photo. Spectral intensity colors are comprised between 1x10^7 and 10x10^7 Raman Counts.

4.2. PCA

In order to evaluate which of the whole spectrum or specific spectral regions is the best to discriminate genuine samples from illegal ones; principal component analysis was applied as exploratory method.

4.2.1. spectral range 200-1800 cm^{-1}

The PCA analysis has been performed on the matrix **B**. The complete spectral region between 200 cm^{-1} and 1800 cm^{-1} has been chosen because this is the most informative region for pharmaceutical tablet analysis.
As can be seen from Figure 4, a clear discrimination was obtained. This discrimination is mainly due to PC3 which explains only 0.1% of the variance.

No real cluster can be seen but a group of three illegal samples are clearly apart from the other ones. This is explained by the fact that the three samples are non coated colored tablets. This is logical since the colorant results in higher spectral intensities.
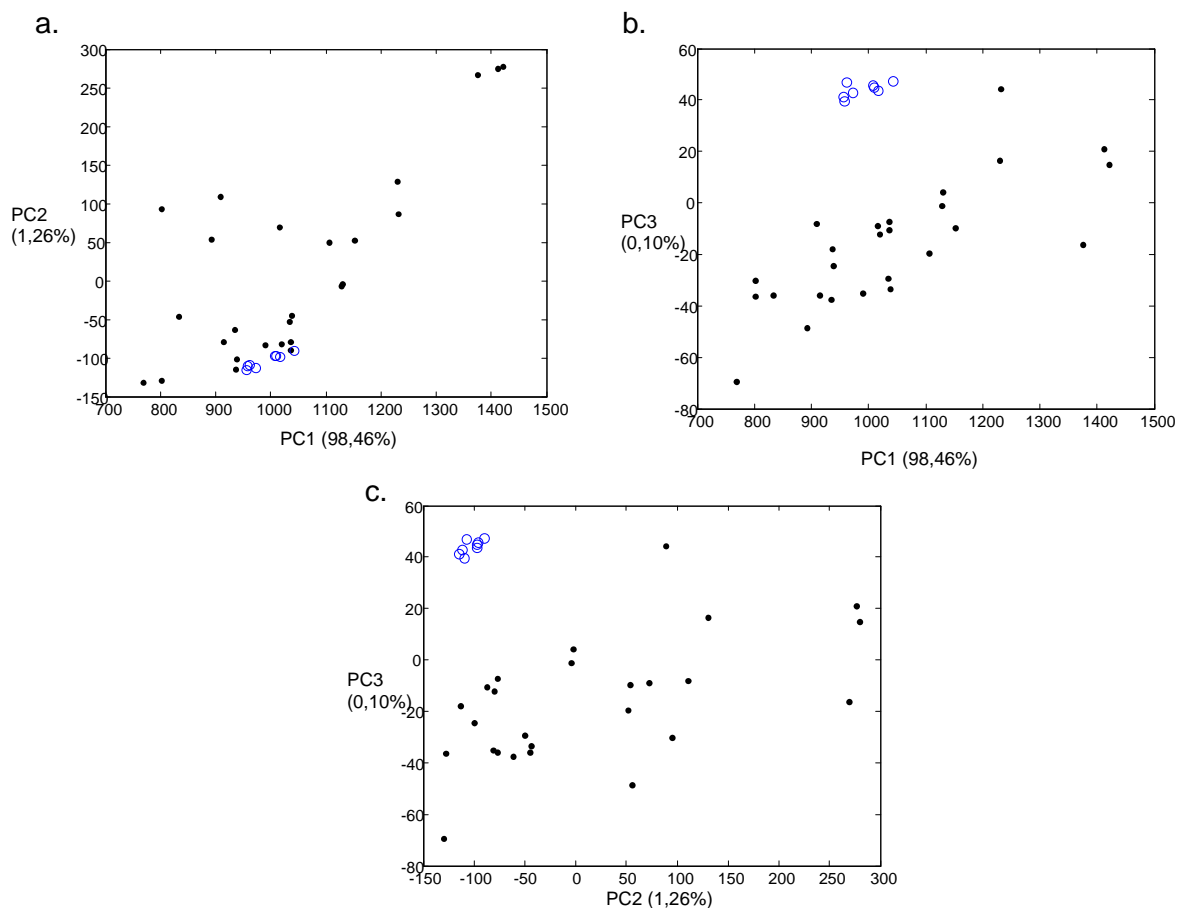
Figure 4: PCA plots of the 200-1800cm-1 spectral range dataset. Black dots are illegal samples and blue circles are genuine Viagra® samples.

    a.   PC1-PC2 plot,
    b.   PC1-PC3 plot,
    c.   PC2-PC3 plot.

4.2.2. Spectral range 830-880 cm^{-1}

A second PCA analysis has been performed between the 830-880 cm^{-1} spectral range. In this region, genuine tablets shows no peak because lactose is not present in the core of genuine Viagra® tablets whereas illegal samples show two peaks at 851 and 876 cm^{-1}. These two peaks are attributed to lactose [7, 29]. As can be seen on Figure 5, a good discrimination between genuine and illegal samples is achieved with the PC2-PC3 plot. These two principal components explain 10% and 7% of the variance respectively. One can then see that counterfeiters do not copy the genuine tablet formulation but use more classical filler excipients such as lactose.

Some clusters or sample regrouping can be observed. However, no clear reason has been found since no full excipients analysis has been performed.

a.

b.

c.
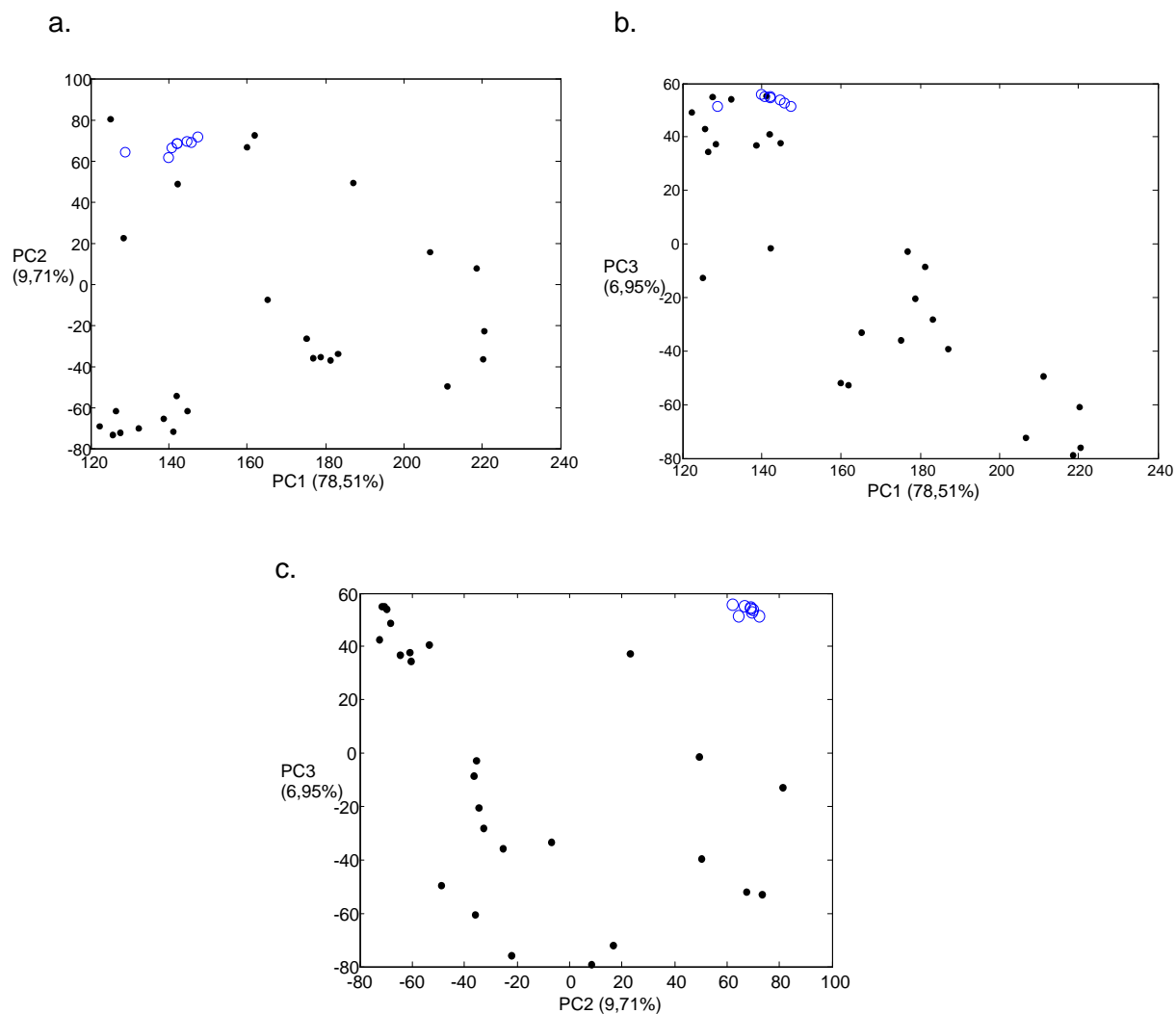
Figure 5: PCA plots of the 830-880cm^{-1} spectral range dataset. This spectral region corresponds to lactose peaks. Black dots are illegal samples and blue circles are genuine Viagra$^®$ samples.

    a.   PC1-PC2 plot,
    b.   PC1-PC3 plot,
    c.   PC2-PC3 plot.

4.2.3. Spectral range 1200-1290 cm^{-1}

A multivariate analysis has been performed keeping only the 1200-1290 cm^{-1} spectral range. This region corresponds to intense peaks at 1238 and 1272 cm^{-1} which are attributed to the C=N bond of sildenafil in Viagra$^®$ tablets [7]. To perform this analysis, the matrix **B** was normalized before the last PCA. This normalization avoided differences due to intensity while keeping only the information related to the distribution of sildenafil in the tablets. This analysis did not discriminate genuine tablets from illegal samples. It indicates that the distribution of the active ingredient is not sufficiently different among the different samples to permit discrimination.

4.3. Classification

After the exploratory analysis, it was found that the whole spectral region was the best to perform the discrimination between genuine and illegal samples. As a result, classification algorithms were applied on the 200-1800 cm^{-1} spectra dataset. For official control laboratories, it is very important to be able to classify correctly an unknown sample in the genuine or in the illegal classes. This is why classification algorithms were applied and their correct classification rate evaluated during both internal and external validation.
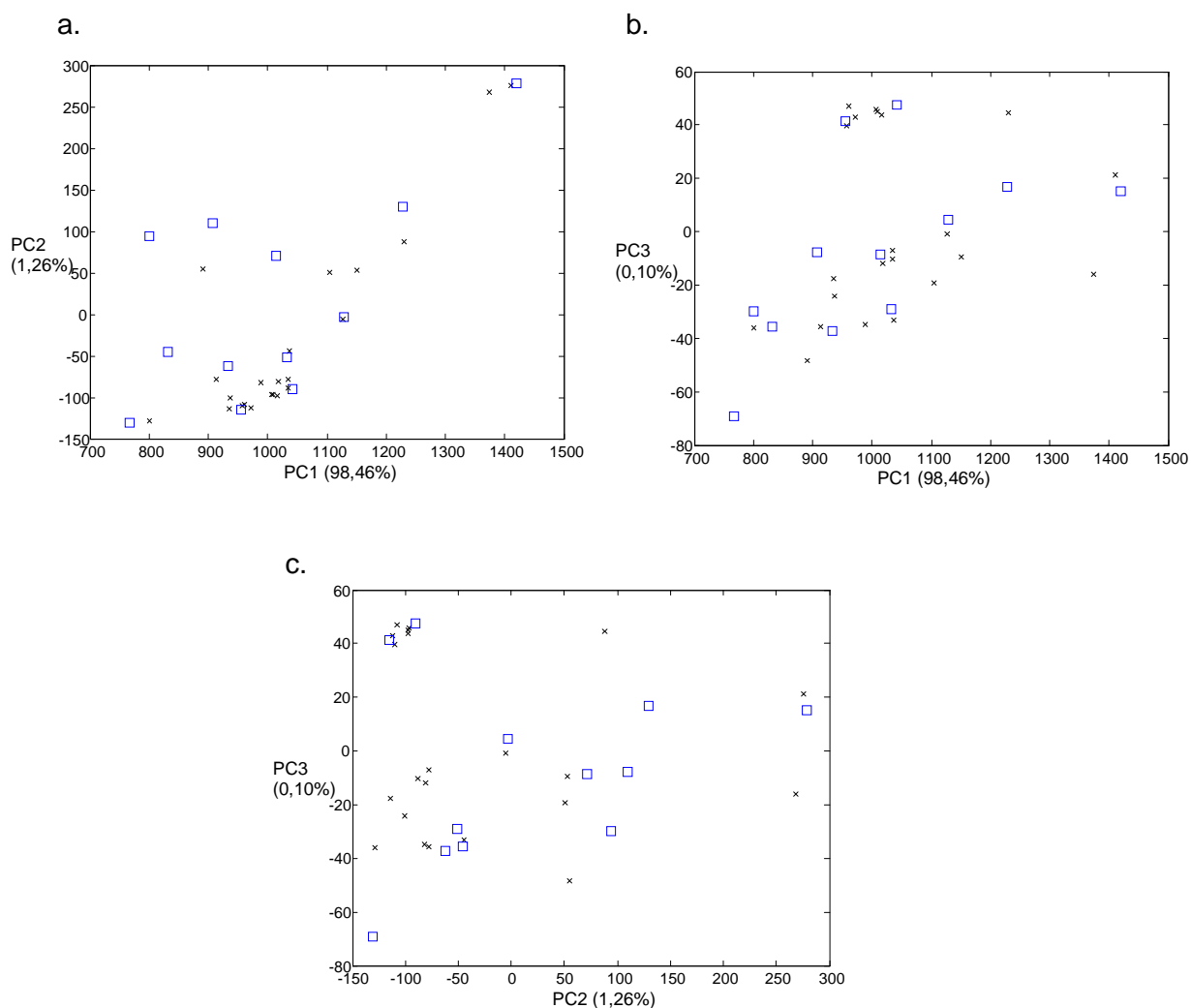
Figure 6: Homogenous distribution of the test set samples (squares) among the training set samples (crosses) selected by the Kennard and Stone algorithm on the 200-1800cm^{-1} spectral range dataset. These datasets were used for the application of the prediction algorithms.

    a.   PC1-PC2 plot,

    a.   PC1-PC3 plot,
    b.   PC2-PC3 plot.

The dataset was split into a training set and a test set for the external validation. The samples of each dataset were chosen applying the Kennard and Stone algorithm on the matrix **B**. Test set size was set at 12 objects and included two reference samples. The training set is composed of the first 22 samples chosen by the algorithm.

Three classification algorithms were tested.

Application of the LDA algorithm gave good results even though not all samples were classified correctly. The correct classification rate was 95,5% for the leave-one-out cross-validation (LOOCV) and 91,2% for the external validation. One illegal sample was misclassified in both internal and external validation.

The k-NN analysis has been performed on the training set using a LOOCV for the internal validation. Both internal and external validations returns 100% correct classification when considering the 3 nearest neighbours to the new sample. This confirms that the method can be used to detect illegal medicines since their spectral intensities are not the same as the ones of genuine samples.

As third a SIMCA analysis was performed. The SIMCA algorithm optimises of the number of principal components used to describe each class of samples by LOOCV. In this case, two and five principal components were respectively used to define a model for the genuine and the illegal samples. Each model separately was not able to classify all samples of the test set correctly, though using the nearest class principle SIMCA returned 100% correct classification in both the internal and external validation.

Comparison of the three algorithms showed that they could all be applied to model this type of data. For our dataset k-NN and SIMCA gave the best results. Based on the easiness of computation and interpretation the k-NN model was preferred and chosen as the best model for this dataset. Though it should be kept in mind that the preferred algorithm is case sensitive and can change in function of the data. For example when data is available for generic products, the model should deal with a multiclass problem. It is possible that in this case better results can be obtained with SIMCA or LDA compared to k-NN.

5. <u>Conclusion</u>

Raman microspectroscopy is a powerful tool allowing a complete mapping of a limited area of a tablet with a limited sample preparation. The analysis of these maps may provide a lot of information about the identification of chemical compounds present, their distribution and their amount [30]. In this study, the core of 26 counterfeit and imitation tablets of Viagra[®] and 8 genuine samples of Viagra[®] were analysed by Raman microspectroscopy over the spectral regions of 200-1800 cm^{-1}, 830-880 cm^{-1} and 1200-1290 cm^{-1}.

After a pre-processing step that made the data suitable for further analysis, a principal component analysis has been performed. The results in the spectral regions of 200-1800 cm^{-1} allowed a clear discrimination between genuine and illegal samples. This discrimination is mainly due to differences in spectral intensities between genuine and illegal samples. These differences may be explained by differences in chemical composition such as the presence of colored excipients in the core of the tablets.

A second PCA analysis of the dataset in the spectral region of 830-880 cm^{-1} allows a detection of illegal samples based on the presence of lactose. This common filler excipient is not present in the core of genuine Viagra tablets.

A third PCA analysis was performed on the spectral region of 1200-1290 cm^{-1} that is correlated with the presence of sildenafil in tablets. The aim of this analysis was to detect illegal samples based on the spatial distribution of sildenafil. No discrimination has been obtained revealing that the spatial distribution of sildenafil between illegal and genuine samples is not sufficiently different.

Three predictive models have been tested on the spectral regions of 200-1800 cm^{-1} dataset. The best results were obtained with k-NN and SIMCA, showing both a correct classification for all samples during internal and external validation steps. Based on its simplicity the k-NN algorithm was chosen as the most suited method for this two class classification.

This feasibility study shows that Raman microspectroscopy is able to discriminate illegal samples from genuine ones using unsupervised chemometrics.

References

[1] PSI, Counterfeit situation: geographic distribution, http://www.psi-inc.org/index.cfm (last accessed 09/05/11)

[2] FAGG/AFMPS, Belgian participation in PANGEA III, an international operation fighting against the online sale of counterfeit and illegal medicines, October 2010, http://www.fagg-afmps.be/fr/news/news_pangea_III.jsp

[3] US FDA, Label and Approval History: Viagra[®], http://www.accessdata.fda.gov/scripts/cder/drugsatfda/index.cfm?fuseaction=Search.DrugDetails (last accessed 09/05/11)

[4] EMA, Authorisation Details: Viagra[®], http://www.ema.europa.eu/ema/index.jsp?curl=pages/medicines/human/medicines/000202/human_med_001136.jsp&mid=WC0b01ac058001d124&murl=menus/medicines/medicines.jsp&jsenabled=true (last accessed 09/05/11)

[5] Rodomonte A.L., Gaudiano M.C., Antoniella E., Lucente D., Crusco V., Bartolomei M., Bertocchi P., Manna L., Valvo L., Muleri N., Counterfeit drugs detection by measurement of tablets and secondary packaging colour, Journal of Pharmaceutical and Biomedical Analysis (2010) 53, 215-220

[6] Vredenbregt M.J., Blok-Tip L., Hoogerbrugge R., Barends D.M., de Kaste D., Screening suspected counterfeit Viagra and imitations of Viagra with near-infrared spectroscopy, Journal of Pharmaceutical and Biomedical Analysis (2006) 40, 840-849

[7] de Veij M., Deneckere A., Vandenabeele P., de Kaste D., Moens L., Detection of counterfeit Viagra with Raman spectroscopy, Journal of Pharmaceutical and Biomedical Analysis (2008) 46, 303-309

[8] Sacré P-Y, Deconinck E., De Beer T., Courselle P., Vancauwenberghe R., Chiap P., Crommen J., De Beer J.O., Comparison and combination of spectroscopic techniques for the detection of counterfeit medicines, Journal of Pharmaceutical and Biomedical Analysis (2010) 53 445-53

[9] Maurin J.K., Pluciński F., Mazurek A.P., Fijałek Z., The usefulness of simple X-ray powder diffraction analysis for counterfeit control--the Viagra example, Journal of Pharmaceutical and Biomedical Analysis (2007) 43, 1514-1518

[10] Wawer I., Pisklak M., Chilmonczyk Z., ^{1}H, ^{13}C, ^{15}N NMR analysis of sildenafil base and citrate (Viagra) in solution, solid state and pharmaceutical dosage forms, Journal of Pharmaceutical and Biomedical Analysis (2005) 38, 865-870

[11] Trefi S., Gilard V., Balayssac S., Malet-Martino M., Martino R., The usefulness of 2D DOSY and 3D DOSY-COSY ^{1}H NMR for mixture analysis: application to genuine and fake formulations of sildenafil (Viagra), Magnetic Resonance in Chemistry (2009) 47, 163-73

[12] Nawaz H., Bonnier F., Knief P., Howe O., Lyng F.M., Meade A.D., Byrne H.J., Evaluation of the potential of Raman microspectroscopy for prediction of chemotherapeutic response to cisplatin in lung adenocarcinoma, Analyst (2010) 135, 3070-3076

[13] Juillard A., Falgayrac G., Cortet B., Vieillard M.H., Azaroual N., Hornez J.C., Penel G., Molecular interactions between zoledronic acid and bone: An in vitro Raman microspectroscopic study, Bone (2010) 47, 895-904

[14] Quinten T., De Beer T., Vervaet C., Remon J.P., Evaluation of injection moulding as a pharmaceutical technology to produce matrix tablets, European Journal of Pharmaceutics and Biopharmaceutics (2009) 71, 145-54

[15] Furuyama N., Hasegawa S., Hamaura T., Yada S., Nakagami H., Yonemochi E., Terada K., Evaluation of solid dispersions on a molecular level by the Raman mapping technique, International Journal of Pharmaceutics (2008) 361, 12-18

[16] Karavas E., Georgarakis M., Docoslis A., Bikiaris D., Combining SEM, TEM, and micro-Raman techniques to differentiate between the amorphous molecular level dispersions and nanodispersions of a poorly water-soluble drug within a polymer matrix, International Journal of Pharmaceutics (2007) 340, 76-83

[17] Vajna B., Farkas I., Szabó A., Zsigmond Z., Marosi G., Raman microscopic evaluation of technology dependent structural differences in tablets containing imipramine model drug, Journal of Pharmaceutical and Biomedical Analysis (2010) 51, 30–38

[18] Burger J., Geladi P., Hyperspectral NIR imaging for calibration and prediction: a comparison between image and spectrometer data for studying organic and biological samples, Analyst (2006) 131, 1152-1160

[19] Roggo Y., Edmond A., Chalus P., Ulmschneider M., Infrared hyperspectral imaging for qualitative analysis of pharmaceutical solid forms, Analytica Chimica Acta (2005) 535, 79-87

[20] Roggo Y., Jent N., Edmond A., Chalus P., Ulmschneider M., Characterizing process effects on pharmaceutical solid forms using near-infrared spectroscopy and infrared imaging, European Journal of Pharmaceutics and Biopharmaceutics (2005) 61, 100-110

[21] El-Hagrasy A.S., Morris H.R., D'Amico F., Lodder R.A., Drennen J.K., Near-infrared spectroscopy and imaging for the monitoring of powder blend homogeneity, Journal of Pharmaceutical Sciences (2001) 90, 1298-1307

[22] Lopes M.B., Wolff J.C., Investigation into classification/sourcing of suspect counterfeit Heptodintrade mark tablets by near infrared chemical imaging, Analytica Chimica Acta (2009) 633, 149–155

[23] Lopes M.B., Wolff J.C., Bioucas-Dias J.M., Figueiredo M.A., Determination of the composition of counterfeit Heptodin tablets by near infrared chemical imaging and classical least squares estimation, Analytica Chimica Acta (2009) 641, 46–51.

[24] Puchert T., Lochmann D., Menezes J.C., Reich G., Near-infrared chemical imaging (NIR-CI) for counterfeit drug identification-a four-stage concept with a novel approach of data processing (Linear Image Signature), Journal of Pharmaceutical and Biomedical Analysis (2010) 51, 138–145.

[25] Massart D.L., Vandeginste B.G.M., Buydens L.M.C., De Jong S., Lewi P.J., Smeyers-verbeke J.: Handbook of Chemometrics and Qualimetrics-Part A, Elsevier Science, Amsterdam, 1997

[26] Kennard R.W., Stone L.A., Computer aided design of experiments, Technometrics (1969) 11, 137-148

[27] Vandeginste B.G.M., Massart D.L., Buydens L.M.C., De Jong S., Lewi P.J., Smeyers-verbeke J.: Handbook of Chemometrics and Qualimetrics-Part B, Elsevier Science, Amsterdam, 1997

[28] Wu W., Mallet Y., Walczak B., Penninckx W., Massart D. L., Heuerding S., Erni F., Comparison of regularized discriminant analysis, linear discriminant analysis and quadratic discriminant analysis, applied to NIR data, Analytica Chimica Acta (1996) 329, 257-265

[29] De Gelder J., De Gussem K., Vandenabeele P., Moens L., Reference database of Raman spectra of biological molecules, Journal of Raman Spectroscopy (2007) 38, 1133-1147.

[30] Balss K.M., Llanos G., Papandreou G., Maryanoff C.A., Quantitative spatial distribution of sirolimus and polymers in drug-eluting stents using confocal Raman microscopy, Journal of Biomedical Materials Research Part A (2008) 85, 258-270.

4. <u>Discussion</u>

In the field of counterfeit medicines detection, spectroscopic techniques are tools of choice. They allow a fast and easy analysis of the samples. Furthermore, these techniques do not request a special sample preparation and enables further analysis with other (i.e. chromatographic) techniques since they are non destructive (NIR and Raman).

The previous studies show that both mid-IR, NIR, Raman spectroscopy and Raman microspectroscopy are able to detect illegal preparations. These techniques offer the possibility to build a predictive model that enables the classification of a new unknown sample as counterfeit or genuine. The CART algorithm is also able to classify illegal samples following the RIVM classification.

These results indicate that control laboratories can, in function of their equipment, implement fast, easy and reliable detection of illegal preparations. However, the reliability of the results is dependent of the database upon which the model is based. The bigger and diversified the database is, the more reliable are the results.

Therefore, before starting to analyse new samples, laboratories must analyse a minimum number of genuine and illegal preparations. As time goes by, each new analysed sample could be included in the database and the models rebuilt. Each laboratory could then have a powerful model of classification adapted to the kind of medication analysed.

V. Chromatographic techniques

1. <u>Introduction:</u>

High Performance Liquid Chromatography (HPLC) has been extensively employed for the detection and quantification of PDE5-i and their analogues. Generally, the mobile phase is a combination of an acidic aqueous phase and acetonitrile as organic modifier while octadecyl bonded silica (C_{18}) is employed as stationary phase [1-21].

During the first part of this chapter, a newly developed and validated reversed phase UHPLC method for the fast analysis of PDE5-i and some of their analogues is described.

In the second part of this chapter, HPLC-UV provides impurity –profiles used as fingerprints for the detection of illegal PDE5-i preparations.

2. <u>Theory:</u>

2.1. *Analytical method validation*

The validation of an analytical method aims to « demonstrate that it (the method) is suitable for its intended purpose » [22]. The purpose of any quantitative analytical method is to provide as accurate results as possible. Thus, the validation process of an analytical method demonstrates that the measured values are precise and close enough to the true value (accuracy) to be accepted. Acceptance limits are defined *a priori* for both precision and accuracy.

2.1.1. *Validation criteria*

2.1.1.1. *Specificity:*

"Specificity is the ability to assess unequivocally the analyte in presence of components which may be expected to be present. Typically these might include impurities, degradants, matrix, etc [22]." For chromatographic methods, specificity depends on the separation quality and the selectivity of the detector: mass spectrometry (LC-MS), ultraviolet diode array detector (LC-DAD), etc [23]

2.1.1.2. *Response function [2]:*

The response function describes the mathematical relation between the measured signal (peak area, absorbance, ion abundance, etc.) and the concentration or quantity of the analyte present in the sample. The response function is linear or non-linear according to the

detection method or the studied concentration range. Fitting models (quadratic, weighted …) exist and allow to obtain reliable results. Analysts should test several fitting models and choose the one that gives the best results.

However, one should be aware that choosing an inadequate fitting model gives significant biases or imprecision. This step is crucial to obtain reliable results and should therefore be tested over a wide range of concentrations.

2.1.1.3. Linearity:

"The linearity of an analytical procedure is its ability to obtain test results which are directly proportional to the concentration (amount) of analyte in the sample [22]." In other words, the linearity is the ability of the analytical procedure to back-calculate the real concentration (or amount) of the analyte in the sample applying the chosen response function.

Linearity of an analytical method (results directly proportional to concentrations) is often confused with the linearity of the response function (signal directly proportional to concentration) [23]. Linearity of the method is required and must be fulfilled by all analytical methods, which is not the case for the linearity of the response function.

2.1.1.4. Trueness

Trueness is the closeness of agreement between the average value from a large series of test results and an accepted reference value (or a conventional true value) [23].

Trueness is related to the systematic part of the error of analytical results. It is expressed in terms of bias:

Relative bias (%) = $\dfrac{\overline{x}_i - \mu_T}{\mu_T} \times 100$ (eq V.1)

where $\overline{x}_i$ is the mean value of the individual results obtained and μ_T is the true analyte concentration.

2.1.1.5. Precision

The precision is related to the random part of the error of analytical results. It is the "closeness of agreement between a series of measurements of the same homogenous sample under prescribed conditions. [23]"

The precision is expressed as standard deviation (s), variance (s^2) or relative standard deviation (RSD). It is also distinguished at three different levels:

- *Repeatability*: "precision under the same operating conditions over a short interval of time (= intra-assay precision) [22]." It involves a repetition of the whole procedure (from the sample preparation to the end of the procedure) and not only instrumental replicates of the same sample.
- *Intermediate precision*: "expresses within-laboratories variations: different days, different analysts, different equipments, etc [22]."
- *Reproducibility*: "expresses the precision between laboratories (collaborative studies) [22]."

All intermediate precision criteria are not to be fulfilled. The laboratory chooses which, among those criteria, are the most relevant keeping in mind the utilisation of the method in routine. For example, if the method will be performed by a single analyst on a single equipment, the validation must only be performed by this analyst on the same equipment. The reproducibility step is optional and only performed when the method will be used in routine in different laboratories.

The RSD acceptable values are calculated with the Horwitz ratio (HorRat) [24]. This parameter reflects the acceptability of an analytical method with respect to precision.

For inter-laboratories studies, HorRat is the ratio of the RSD among laboratories (RSD_R), calculated on experimentally measured concentrations to the predicted RSD calculated as:

$$PRSD_R = 2C^{-0.15}$$ (eq V.2)

where C is the concentration expressed as a dimensionless fraction (for example for a concentration of 1 µg/g, C = 10^{-6} g/g)

Thus, Horwitz ratio during reproducibility tests (HorRat$_r$) is given by:

$$HorRat_R = \frac{RSD_R}{PRSD_R}$$ (eq V.3)

HorRat is also applicable for intra-laboratories study and is therefore named HorRat$_r$.

For intermediate precision, the Horwitz ratio should be situated between 0.3-1.3 HorRat$_r$ while it is situated between 0.5-2.0 HorRat$_R$ for reproducibility tests.

2.1.1.6.   Accuracy [25, 26]:

"The accuracy of an analytical procedure is the closeness of agreement between the value which is accepted either as a conventional true value or an accepted reference value and the value found [22]." In other words, the accuracy of an analytical procedure corresponds to the measurement error.

When applying an analytical method, the measured value x_i is different from the true value μ_T. This difference or error is composed of:

- A random error: the precision or standard deviation that is calculated based on replicate measurements of the same sample.
- A systematic error: the bias or trueness that is calculated as the difference between the average value of a large series of measurements of the same sample and an accepted reference value.

The true values of these errors are never known. However, the validation process gives estimations of their true values.

The total error strategy considers the combination of these two types of error:

$$x_i = \mu_T + \hat{\mu}_M + \hat{\sigma}_M \Leftrightarrow x_i = \mu_T + total\ error \qquad\qquad \text{(eq V.4)}$$

where $\hat{\mu}_M$ is the estimated method bias and $\hat{\sigma}_M$ is the estimated method precision.

Total error defines a region around the reference value where measured analytical results can be found with a defined probability that is the distribution of analytical results linked to a conventional true or reference concentration [27].

2.1.1.7.   Uncertainty [27, 28]:

Uncertainty of measurement is "a parameter, associated with the result of a measurement, that characterises the dispersion of the values that could reasonably be attributed to the measurand".

The numerical value of uncertainty may be determined by two methods:

- Type A uncertainty: determined by statistical methods. This evaluation applies to random and systematic errors and is expressed as a standard deviation.
- Type B uncertainty is determined by other means, usually based on scientific judgement using all relevant information available.

Uncertainty defines a region around the measured analytical results where the conventional true or reference value can be found with a defined probability that is the distribution of reference analytical results linked to an observed analytical result. . Uncertainty and total error concepts are thus related but considered in two different ways.

2.1.2. Decision rule:

At the end of the validation process, one must decide whether the analytical method is valid or not. Two main strategies exist to help analysts decide:

*   The classical strategy evaluates the different parameters (accuracy, linearity, repeatability, intermediate precision, specificity, range of applicability and robustness) separately [22]. Most of these classical strategies are based on the null hypothesis:

    H_0 : relative bias = 0%. Relative bias is described in equation 1.

    This kind of approach is hazardous since it may declare as valid an unacceptable method and vice versa. Indeed, the greater the method's variance, the more likely the method will be declared valid since the 0 bias value will be included in the confidence interval.

    This strategy involves the descriptive approach, the difference approach and the equivalence approach. These approaches are described in [29].

*   The accuracy profile strategy.

2.1.2.1. Accuracy profiles [25, 26, 30-32]

The goal of the validation of an analytical method is to ensure that the expected proportion E of future measurements that will fall within the acceptance limits ($\lambda = \pm 5\%$ for determination of active ingredients in pharmaceutical specialities) is higher than a predefined proportion level β (often fixed at 95%):

$$E_{\hat{\mu},\hat{\sigma}} \left\{ P\left[\left| x_i - \mu_T \right| < \lambda \right] / \hat{\mu}_M, \hat{\sigma}_M \right\} \geq \beta \qquad \text{(eq V.5)}$$

The estimation of the expected proportion is given by the β-expectation tolerance intervals [33]:

$$E_{\hat{\mu}_M,\hat{\sigma}_M} \left\{ P_{x_i} \left[\hat{\mu}_M - k\hat{\sigma}_M < x_i < \hat{\mu}_M + k\hat{\sigma}_M \middle| \hat{\mu}_M, \hat{\sigma}_M \right] \right\} = \beta \qquad \text{(eq V.6)}$$

where k is chosen such that the proportion of future results expected to fall into the interval limits equals β.

If the β-expectation tolerance intervals obtained this way are totally included within the tolerance intervals [-5%, 5%], then the expected proportion of future results that will be included within the same acceptance limits is equal to or greater than β.

These β-expectation tolerance intervals must be calculated at each concentration level to be validated. Thus, accuracy profiles are constructed connecting the lower tolerance limits together and the upper tolerance limits together (Figure V.1).

As one can see, the tolerance intervals at concentration level C_1 and C_4 are outside the acceptance limits. The limits of quantification (lower limit of quantification (LLQ) and upper limit of quantification (ULQ)) are therefore at the intersection of the interpolated β-expectation tolerance intervals (dashed blue line) and the acceptance limits.

Analysts may now expect that inside the defined range of concentration a β proportion (e.g. 95%) of future results will fall within the acceptance limits (e.g. ± 5% for determination of active ingredients in pharmaceutical specialties).

Thus, when implementing the method for routine analysis, samples must be within this range of concentration.
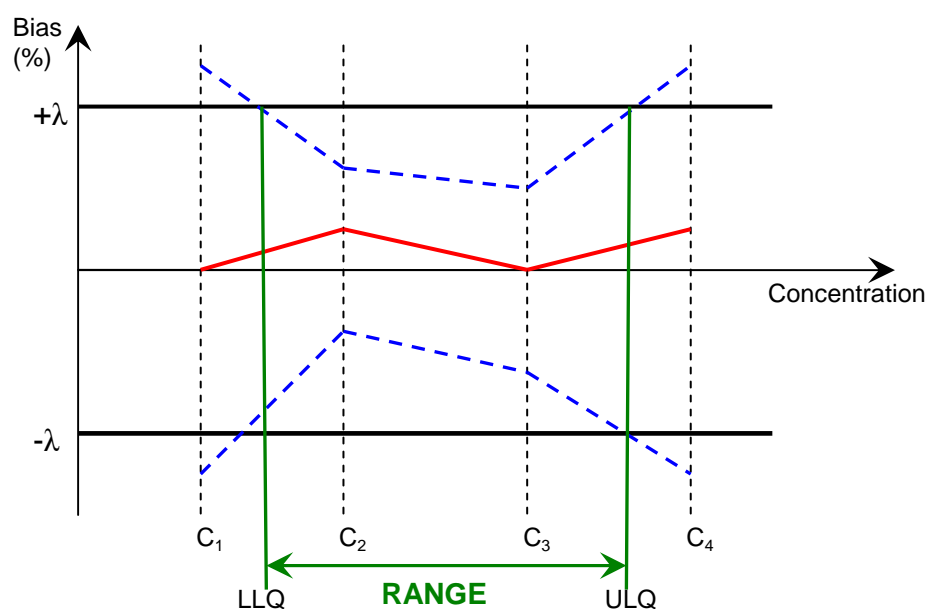
Figure V.1: Accuracy profile constructed with the β-expectation tolerance intervals calculated at the four concentration levels (C_1-C_4). LLQ, lower limit of quantification; ULQ, upper limit of quantification. Dashed blue lines are β-expectation tolerance intervals, bold black lines represent the acceptance limits [-λ, +λ], and bold red line connects the mean measured concentrations at the four concentration levels.

(Reproduced from [23]).

118

2.2.   Method comparison [34-36]:

If the newly developed method's purpose is to replace an old one or is to be used alternatively with another method previously validated, the two methods must be compared. The aim is to know whether the results provided by the two different methods are comparable or even if the new one provides better results. The current analytical method is called the *reference method* while the new one is called the *test method*.

The comparison is performed using hypothesis tests. A first test will compare the mean results of each method by means of a paired t-test.

The null hypothesis H_0 is that the difference between the results of the two methods $\delta = 0$. The alternative hypothesis H_1 is $\delta \neq 0$.

The t-statistic is calculated as:

$$t = \frac{\bar{d}}{\left(s_d / \sqrt{n}\right)}$$
(eq V.7)

with $\bar{d} = \dfrac{\Sigma d_i}{n}$ and $d_i = x_{1,i} - x_{2,i}$; where $x_{1,i}$ is the result obtained with the first method, $x_{2,i}$ is the result obtained with the second method, s_d is the standard deviation of these differences and n is the number of measurements.

t is then compared with a critical value from the Student's t table with n-1 degrees of freedom and the significance level $\dfrac{\alpha}{2}$. If t is smaller than the critical value, then H_0 is accepted and the two methods are said to have comparable results.

The variances of both methods may also be compared by the means of an F-test. The null hypothesis becomes then $H_0 : \sigma_1^2 = \sigma_2^2$ where σ_1^2 is the variance of the first method and σ_2^2 the one of the second method. The alternative hypothesis is $H_1 : \sigma_1^2 \neq \sigma_2^2$.

The F-statistic is calculated as:

$$F = \frac{\sigma_1^2}{\sigma_2^2}$$
(eq V.8)

The numerator is always the highest value. F is compared with a critical value from the Snedecor's F table with n-1 degrees of freedom and the significance level $\dfrac{\alpha}{2}$.

If F is smaller than the critical value, then H_0 is accepted and the two methods are said to have comparable variances.

Besides these two tests, one may also perform an interval hypothesis test. An interval is calculated around the mean difference between the two methods:

$$\left[\left|\overline{x}_1 - \overline{x}_2\right| - \left(s_D \times t_{\alpha;\nu_d}\right) ; \left|\overline{x}_1 + \overline{x}_2\right| + \left(s_D \times t_{\alpha;\nu_d}\right)\right] \qquad \text{(eq V.9)}$$

where $\overline{x}_1$ and $\overline{x}_2$ are the mean results for the first and the second method respectively, s_D is the standard deviation of the differences and $t_{\alpha;\nu_d}$ is the critical value for ν_d degrees of freedom and the significance level α.
These intervals must be within the *a priori* fixed acceptable bias.

Another method of comparison is to realise a plot of the relative difference between the two methods against their mean. Figure V.2 shows the difference plot of ten measurements.
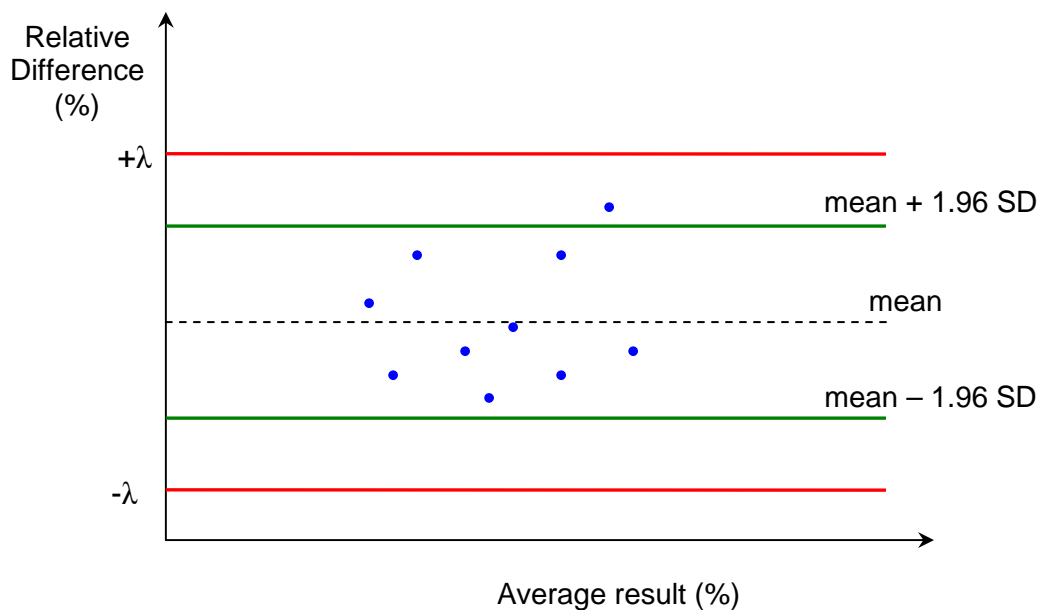
Figure V.2: Difference Plot of ten samples concentration measured by both test and reference methods. Red lines are maximal acceptable relative difference between the two methods [-λ, +λ]; green lines are 95 %agreement limits of the relative differences.

Relative differences are calculated as:

$$Relative\ difference\ (\%) = \left(\frac{x_1 - x_2}{x_2} \right) \times 100 \qquad\qquad \text{(eq V.10)}$$

where x_1 and x_2 are the results obtained with the test method and the reference method respectively.

As they are normally distributed (Gaussian), 95% of the relative differences are comprised between their mean ± 1.96 SD (*agreement limits*).
If the agreement limits are comprised within the maximal acceptable relative differences, the methods can be considered as comparable.

2.3. Chromatographic Fingerprints

The treatment of chromatographic data as fingerprints is widely used in the field of pharmacognosy for quality control of plants [37-42]. Chromatographic fingerprints allow a reliable evaluation of the quality and the identity of plant extracts even if neither the identity nor the quantity of the constituents are known.
In the pharmaceutical field, the impurities of preparations are monitored by means of impurity profiling. These profiles are sometimes used as impurity fingerprints for the characterization of drug substance impurities [43] or the identification of the synthesis pathway used for the production [44].

In the frame of counterfeit drug detection, chromatographic impurity fingerprints is interesting. Indeed, a major hazard of counterfeit products is the presence of toxic impurities in unknown amount. Thus, as it is the case for herbal medicines, the fingerprint approach allows the discrimination of tablets according to their chromatographic profiles without knowing *a priori* the identity nor the quantity of the constituents.
However, to obtain good and reliable results, the pre-processing step is crucial. This step is mainly composed of signal enhancement, warping and mixture analysis.

A chromatogram contains three major components (Figure V.3):

- Noise (highest frequency component)
- Signal (intermediate frequency component)
- Background (lowest frequency component)

The signal enhancement is achieved eliminating the noise and the background components.
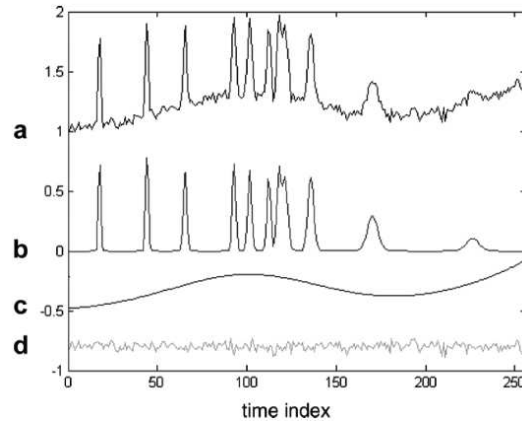
Figure V.3: Components of analytical signal: (a) overall signal; (b) relevant signal; (c) background and (d) noise. (Reproduced from [45])

When performing several chromatographic analyses, a shift in retention times appears. This shift is mainly due to stationary phase degradation, temperature variations and fluctuations in mobile phase composition. Thus, once the ratio signal to noise has been sufficiently enhanced, chromatograms must be aligned (warping step).

During this thesis, we applied a simple peak correction. The peaks of all chromatograms are aligned with respect to the corresponding peaks in the reference chromatogram. Thus, the choice of the reference chromatogram is of great importance for the final results. Daszykowski et al. demonstrated that the best results are obtained when selecting the chromatogram with the highest mean Pearson's correlation coefficient with respect to the remaining chromatograms as reference [46].

Pearson's correlation coefficient, r, is calculated as:

$$r(y_1, y_2) = \frac{\Sigma(y_{1i} - \bar{y}_1)(y_{2i} - \bar{y}_2)}{\sqrt{\Sigma(y_{1i} - \bar{y}_1)^2 \Sigma(y_{2i} - \bar{y}_2)^2}} \qquad \text{(eq V.11)}$$

where $y_{11}, y_{12}, y_{13}, ..., y_{1n}$ and $y_{21}, y_{22}, y_{23}, ..., y_{2n}$ are two sets of n measurements with respective means $\bar{y}_1$ and $\bar{y}_2$.

The correlation coefficient is a dimensionless number between -1 and +1. Values of -1 or +1 indicate a perfect linear negative or positive relationship respectively. If $r = 0$, there exist no linear relationship [36].

Once the reference chromatogram has been selected, the largest peak is identified in all signals and this peak is used as a marker peak for the alignment. Then, the signals are transformed by linear interpolation so that positions of the largest peak in all signals matched the position of the largest peak in the reference signal

During alignment procedure, each signal was split into two parts defined by the apex of the marker peak. Each part was then independently aligned.

Linear interpolation compresses or extends a signal by changing a sampling rate over x-axis of a signal. Keeping in mind the desired number of sampling points of a signal, a new uniform grid of points is constructed over a certain range (with less or more points). Then, the unknown y-values for x-points on a new grid of points are calculated using the following expression:

$$y = y_0 + (x - x_0)\frac{y_1 - y_0}{x_1 - x_0}$$ (eq V.12)

where, y is the predicted y-value at location x on a new grid of points, x_0 and x_1 are x-points of the original axis and define interval containing point x, whereas y_0 and y_1 are their respective y-values.

Once the dataset is correctly pre-processed, multivariate analysis may be performed (see chapter 3).

References:

[1] Shin MH., Hong MK., Kim WS., Lee YJ., Jeoung YC., Identification of a new analogue of sildenafil added illegally to a functional food marketed for penile erectile dysfunction, Food Additives and Contaminants (2003) 20, 793-796

[2] Blok-Tip L.,Zomer B., Bakker F., Hartog K.D., Hamzink M., ten Hove J., Vredenbregt M., de Kaste D., Structure elucidation of sildenafil analogues in herbal products, Food Additives and Contaminants (2004) 21, 737-748

[3] Shin C., Hong M., Kim D., Lim Y., Structure determination of a sildenafil analogue contained in commercial herb drinks, Magnetic Resonance in Chemistry (2004) 42, 1060-1062

[4] Hou P., Zou P., Low M-Y., Chan E., Koh H-L., Structural identification of a new acetildenafil analogue from pre-mixed bulk powder intended as a dietary supplement, Food Additives and Contaminants (2006) 23, 870-875

[5] Lai K-C., Liu Y-C., Tseng M-C., Lin J-H., Isolation and identification of a sildenafil analogue illegally added in dietary supplements, Journal of Food and Drug Analysis (2006) 14, 19-23

[6] Lin M-C. Liu Y-C., Lin J-H., Identification of a sildenafil analogues adulterated in two herbal food supplements, Journal of Food and Drug Analysis (2006) 14, 260-264

[7] Reepmeyer J., Woodruff J., Use of liquid chromatography-mass spectrometry and a chemical cleavage reaction for the structure elucidation of a new sildenafil analogue detected as an adulterant in an herbal dietary supplement, Journal of Pharmaceutical and Biomedical Analysis (2007) 44, 887-893

[8] Lin M-C, Liu Y-C., Lin Y-L., Lin J-H., Isolation and identification of a novel sildenafil analogue adulterated in dietary supplements, Journal of Food and Drug Analysis (2008) 16, 15-20

[9] Zou P., Hou P., Oh S.S-Y., Chong Y.M., Bloodworth B.C., Low M-Y., Koh H-L., Isolation and identification of thiohomosildenafiland thiosildenafil in health supplements, Journal of Pharmaceutical and Biomedical Analysis (2008) 47, 279-284

[10] Venhuis B.J., Zomer G., de Kaste D., Structure elucidation of a novel synthetic thiono analogue of sildenafil detected in an alleged herbal aphrodisiac, Journal of Pharmaceutical and Biomedical Analysis (2008) 46, 814-817

[11] Reepmeyer J., André d'Avignon D., Structure elucidation of thioketone analogues of sildenafil detected as adulterants in herbal aphrodisiacs, Journal of Pharmaceutical and Biomedical Analysis (2009) 49, 145-150

[12] Gratz S., Zeller M., Mincey D., Flurer C., Structural characterization of sulfoaildenafil, an analogue of sildenafil, Journal of Pharmaceutical and Biomedical Analysis (2009) 50,228-231

[13] Venhuis B.J., Zomer G., Hamzink M., Meiring H.D., Aubin Y., de Kaste D., The identification of a nitrosated prodrug of the PDE-5 inhibitor aildenafil in a dietary supplement: a Viagra with a pop, Journal of Pharmaceutical and Biomedical Analysis (2011) 54, 735-741

[14] Venhuis B.J., Zomer G., Vredenbregt M.J., de Kaste D., The identification of (-)-trans-tadalafil and sildenafil in counterfeit Cialis® and the optical purity of tadalafil stereoisomers, Journal of Pharmaceutical and Biomedical Analysis (2010) 51, 723-727

[15] Häberli A., Girard P., Low M-Y., Ge X., Isolation and structure elucidation of an interaction product of aminotadalafil found in an illegal health food product, Journal of Pharmaceutical and Biomedical Analysis (2010) 53, 24-28

[16] Reepmeyer J., Woodruff J., Use of liquid chromatography-mass spectrometry and a hydrolytic technique for the detection and structure elucidation of a novel synthetic vardenafil designer drug added illegally to a "natural" herbal dietary supplement, Journal of Chromatography A (2006) 1125, 67-75

[17] Lai K-C., Liu Y-C., Tseng M-C., Lin Y-L., Lin J-H., Isolation and identification of a vardenafil analogue in a dietary supplement, Journal of Food and Drug Analysis (2007) 15, 220-227

[18] Lam Y-H., Poon W-T., Lai C-K., Chan A Y-W., Mak T W-L., Identification of a novel vardenafil analogue in herbal product, Journal of Pharmaceutical and Biomedical Analysis (2008) 46, 804-807

[19] Lee H-M., Kim C.S., Jang Y.M., Kwon S.W., Lee B-J., Separation and structural elucidation of a novel analogue of vardenafil included as an adulterant in a dietary supplement by liquid chromatography-electrospray ionization mass spectrometry, infrared spectroscopy and nuclear magnetic resonance spectroscopy (2011) 54, 491-496

[20] Hasegawa T., Takahashi K., Saijo M., Ishii T., Nagata T., Kurihara M., Haishima Y., Goda Y., Kawahara N., Isolation and structural elucidation of cyclopentynafil and N-octylnortadalafil found in dietary supplement, Chemical and Pharmaceutical Bulletin (2009) 57, 185-189

[21] Ge X., Low M-Y., Zou P., Lin L., Yin S.O.S., Bloodworth B.C., Koh H-L.? Structural elucidation of a PDE-5 inhibitor detected as an adulterant in a health supplement, Journal of Pharmaceutical and Biomedical Analysis (2008) 48, 1070-1075

[22]ICH, International Conference on Harmonization, Validation of Analytical Procedures : Text and Methodology Q2(R1), 1995. http://www.ich.org

[23] De Beer J.O., Van Poucke C., Ensuring the quality of results from food control laboratories: laboratory accreditation, method validation and measurement uncertainty, *in* De Saeger S. (Ed), Determining mycotoxins and mycotoxigenic fungi in food and feed, Woodhead Publishing, Cambridge, UK, 2011, 194-222

[24]   http://www.aoac.org/dietsupp6/Dietary-Supplement-web-site/HORRAT_SLV.pdf   (last accessed 19/05/2011)

[25] Rozet E., Ceccato A., Hubert C., Ziemons E., Oprean R., Rudaz S., Boulanger B., Hubert Ph., Analysis of recent pharmaceutical regulatory documents on analytical method validation, Journal of Chromatography A (2007), 1158, 111-125

[26] Hubert Ph., Nguyen-Huu J.-J., Boulanger B., Chapuzet E., Chiap P., Cohen N., Compagnon P.-A., Dewé W., Feinberg M., Lallier M., Laurentie M., Mercier N., Muzard G., Nivet C., Valat L., Harmonization of strategies for the validation of quantitative analytical procedures: A SFSTP proposal – part I, Journal of Pharmaceutical and Biomedical Analysis (2004), 36, 579-586

[27] Rozet E., Marini R.D., Ziemons E., Dewé W., Rudaz S., Boulanger B., Hubert Ph., Total error and uncertainty: Friends or Foes?, Trends in Analytical Chemistry (2011), 30, 797-806

[28] Araujo P., Key aspects of analytical method validation and linearity evaluation, Journal of Chromatography B (2009), 877, 2224-2234

[29] Boulanger B., Chiap P., Dewé W., Crommen J., Hubert Ph., An analysis of the SFSTP guide on validation of chromatographic bioanalytical methods: progresses and limitations, Journal of Pharmaceutical and Biomedical Analysis (2003), 32, 753-765

[30] Hubert Ph., Nguyen-Huu J.-J., Boulanger B., Chapuzet E., Chiap P., Cohen N., Compagnon P.-A., Dewé W., Feinberg M., Lallier M., Laurentie M., Mercier N., Muzard G., Nivet C., Valat L., Rozet E., Harmonization of strategies for the validation of quantitative analytical procedures: A SFSTP proposal – part II, Journal of Pharmaceutical and Biomedical Analysis (2007), 45, 70-81

[31] Hubert Ph., Nguyen-Huu J.-J., Boulanger B., Chapuzet E., Cohen N., Compagnon P.-A., Dewé W., Feinberg M., Laurentie M., Mercier N., Muzard G., Valat L., Rozet E., Harmonization of strategies for the validation of quantitative analytical procedures: A SFSTP proposal – part III, Journal of Pharmaceutical and Biomedical Analysis (2007), 45, 82-96

[32] Hubert Ph., Nguyen-Huu J.-J., Boulanger B., Chapuzet E., Cohen N., Compagnon P.-A., Dewé W., Feinberg M., Laurentie M., Mercier N., Muzard G., Valat L., Rozet E., Harmonization of strategies for the validation of quantitative analytical procedures: A SFSTP proposal – part IV. Examples of applicaion, Journal of Pharmaceutical and Biomedical Analysis (2008), 48, 760-771

[33] Mee R.W., β-content tolerance limits for balanced one-way ANOVA random model, Technometrics (1984), 26, 251-254

[34] Bland J. M., Altman D.G., Statistical methods for assessing agreement between two methods of clinical measurement, The Lancet (1986), 8, 307-310

[35] Kuttatharmakul S., Massart D.L., Smeyers-Verbeke J., Comparison of alternative measurement methods, Analytica Chimica Acta, 391, 203-225

[36] Massart D.L., Vandeginste B.G.M., Buydens L.M.C., De Jong S., Lewi P.J., Smeyers-Verbeke J.: Handbook of Chemometrics and Qualimetrics-Part A, Elsevier Science, Amsterdam, 1997

[37] Xu C.-J., Liang Y.-Z., Chau F.-T., Vander Heyden Y., Pretreatments of chromatographic fingerprints for quality control of herbal medicines, Journal of Chromatography A (2006) 1134, 253-259

[38] Yan S.-K., Xin W.-F., Luo G.-A., Wang Y.-M., Cheng Y.-Y, An approach to develop two-dimensional fingerprint for the quality control of *Qingkailing* injection by high-performance liquid chromatography with diode array detection, Journal of Chromatography A (2005) 1090, 90-97

[39] Han C., Shen Y., Chen J., Lee F.S., Wang X., HPLC fingerprinting and LC-TOF-MS analysis of the extract of *Pseudostellaria heterophylla* (Miq.) Pax root, Journal of Chromatography B (2008) 862, 125-131

[40] Hu P., Liang Q.-L., Luo G.-A., Zhao Z.-Z., Jiang Z.-H., Multi-component HPLC fingerprinting of *Radix Salviae Miltiorrhizae* and its LC-MS-MS identification, Chemical & pharmaceutical bulletin (2005) 53, 677-683

[41] Ni Y., Lai Y., Brandes S., Kokot S., Multi-wavelength HPLC fingerprint from complex substances: An exploratory chemometrics study of the Cassia seed example, Analaytica Chimica Acta (2009) 647, 149-158

[42] Xiaohui F., Yi W., Yiyu C., LC/MS fingerprinting of Shenmai injection: a novel approach to quality control of herbal medicines, Journal of Pharmaceutical and Biomedical Analysis (2006) 40, 591-597

[43] Nicolas E., Scholz T., Active drug substance impurity profiling part II. LC/MS/MS fingerprinting, Journal of Pharmaceutical and Biomedical Analysis (1998) 16, 825-836

[44] Dumarey M., van Nederkassel A.M., Stanimirova I., Daszykowski M., Bensaid F., Lees M., Martin G.J., Desmurs J.R., Smeyers-Verbeke J., Vander Heyden Y., Recognizing paracetamol formulations with the same synthesis pathway based on their trace-enriched chromatographic impurity profiles, Analytica Chimica Acta (2009) 655, 43-51

[45] Daszykowski M., Walczak B., Use and abuse of chemometrics in chromatography, Trends in Analytical Chemistry (2006) 25, 1081-1096

[46] Daszykowski M., Walczak B., Target selection for alignment of chromatographic signals obtained using monochannel detectors, Journal of Chromatography A (2007) 1176, 1-11

3. <u>Results</u>

3.1. *Development and validation of a UHPLC-UV method for the detection and quantification of erectile dysfunction drugs and some of their analogues found in counterfeit medicines.*

As a control laboratory, the drug analysis laboratory of the IPH analyses frequently illegal preparations for the FAMHP. Some of them are illegal preparations containing sildenafil, tadalafil or some of their analogues.

Therefore, an analytical method was developed to identify and quantify the active compounds. The analogues of the registered API's were chosen according to their availability and their structural differences. The diastereoisomer of tadalafil, (-)-trans-tadalafil, was produced in the laboratory starting from tadalafil as no standard was commercially available. Therefore, it was not quantified but its separation from the other peaks is important since it is frequently present in illegal preparations as an impurity.

The method has been validated using spiked herbal matrix placebo as validation samples. This is justified by the fact that the method could be applied to a great variety of matrixes (among them, vegetal matrixes are the most complex) and that analogues are essentially found in vegetal alimentary complements. The validation acceptance limits were set at +/- 5% as for pharmaceutical specialities.

Once developed and validated, the method has been compared to the reference method published in Pharmeuropa [1] to ensure that both methods gave comparable results.

Chromatographic conditions, validation and comparison results are presented in the article:

Sacré P-Y, Deconinck E, Chiap P, Crommen J, Mansion F, Rozet E, Courselle P, De Beer J, Development and validation of a UHPLC-UV method for the detection and quantification of erectile dysfunction drugs and some of their analogues found in counterfeit medicines, Journal of Chromatography A (2011) 1218, 6439-6447

References:

[1] European Directorate for the Quality of Medicines, Draft monography of Sildenafil citrate, Pharmeuropa 23 (2011), 381–383.

Development and validation of a UHPLC-UV method for the detection and quantification of erectile dysfunction drugs and some of their analogues found in counterfeit medicines.

Pierre-Yves Sacré[a,b], Eric Deconinck[a], Patrice Chiap[c], Jacques Crommen[b], François Mansion[b], Eric Rozet[d], Patricia Courselle[a], Jacques O. De Beer[a,*]

[a] *Laboratory of Drug Analysis, Scientific Institute of Public Health, Brussels, Belgium*
[b] *Department of Analytical Pharmaceutical Chemistry, Institute of Pharmacy, University of Liège, Liège, Belgium.*
[c] *Advanced Technology Corporation (A.T.C.), University Hospital of Liège, Liège, Belgium*
[d] *Department of Analytical Chemistry, Institute of Pharmacy, University of Liège, Liège, Belgium.*

Abstract

Pharmaceutical counterfeiting is a permanently growing problem. Control laboratories are constantly analysing counterfeit medicines. In industrialised countries, one of the main counterfeited class of medicines are erectile dysfunction drugs. This paper describes the development and validation of a fast method to detect and quantify the three authorised phosphodiesterase type 5 inhibitors and five analogues. The method is based on the use of a sub-2 microns polar-embedded column with a gradient using acetonitrile as organic modifier and 10 mM ammonium formate buffer (pH 3.5) as aqueous component of the mobile phase. The separation was achieved in less than 4.5 min. The method has also been compared to the registered HPLC method for the assay of Viagra® which was considered as the reference method.

The method is also compatible with on-line coupling mass spectrometry and will significantly reduce analysis times and solvent consumption.

Keywords:

Phosphodiesterase type 5 inhibitors; UHPLC; method validation, analogues, counterfeit drugs, accuracy profiles.

1. <u>**Introduction**</u>

The number of cases of pharmaceutical counterfeiting is constantly growing since the first cases were detected in the early 90's [1]. In industrialised countries, one of the most counterfeited classes of medicines is the phosphodiesterase type 5 inhibitors (PDE5-i) [2]. Among them only three drugs are approved and marketed: sildenafil citrate (Pfizer), tadalafil (Eli Lilly) and vardenafil hydrochloride (Bayer). These drugs are used in erectile dysfunction disorders (Viagra®, Cialis ® and Levitra®). Sildenafil citrate is also used in pulmonary arterial hypertension (Revatio®).

Due to the taboo associated with erectile dysfunction, PDE5-inhibitors are widely sold over the internet as both counterfeited medicines and illegal adulterants in herbal dietary supplements. In the latter the biggest diversity of analogues was found [2-4]. For this study, three analogues of sildenafil (acetildenafil, hydroxyacetildenafil and dimethylsildenafil), one of vardenafil (pseudovardenafil), one of tadalafil (aminotadalafil) and the bioactive diastereoisomer of tadalafil (trans-tadalafil) have been chosen. Their chemical structures are shown in Figure 1. These compounds are representative of what is commonly found in illegal preparations.

All of these analogues have already been found in illegal preparations. These preparations have been analysed using different analytical systems (LC-UV, LC-MS, IR, NMR, X-ray diffraction, etc.) [5-28]. The presented validated method allows a fast separation and quantification of the three authorised PDE5-i and five of their analogues. This method may constitute a good basis for the analysis of illegal erectile dysfunction medicines by official control laboratories.

The present paper describes a method enabling the separation and quantification of nine PDE5 inhibitors in a single run: sildenafil, tadalafil, vardenafil and some of their analogues and impurities (trans-tadalafil [16]). A full validation using spiked placebo validation samples has been performed using the "total error" approach [31-38]. The robustness of the method has also been investigated. The precision and accuracy for the quantification of sildenafil citrate in Viagra® tablets has been compared to the HPLC method from the Viagra® registration dossier set as reference method. The method described here can be used as routine method for the analysis of PDE5-inhibitors and can be coupled in principle to a mass spectrometer for identity confirmation or structure elucidation.

The proposed method allows a faster and more environmental friendly high throughput analysis of both illegal and legal preparations containing PDE5-inhibitors.
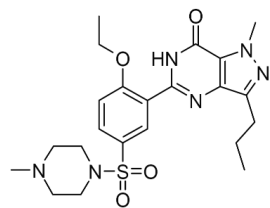
sildenafil
(present as citrate salt in Viagra®)
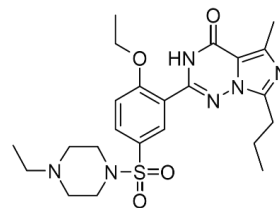
vardenafil
(present as hydrochloride salt in Levitra®)
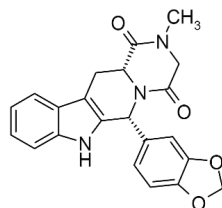
tadalafil (Cialis®)
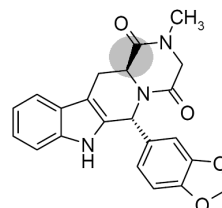
(-)-trans-Tadalafil
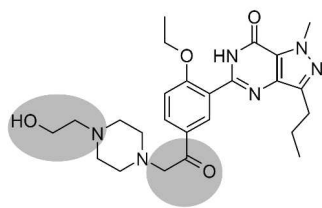
hydroxyacetildenafil (hydroxyhongdenafil)
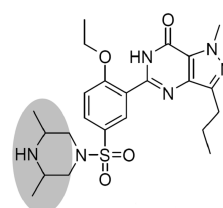
dimethylsildenafil
(aildenafil, methisosildenafil)
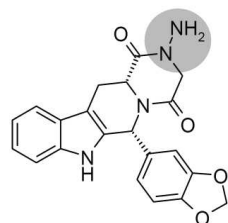
aminotadalafil
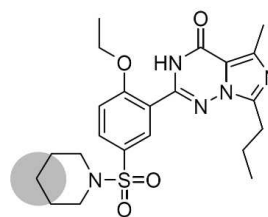
pseudovardenafil (piperidenafil)
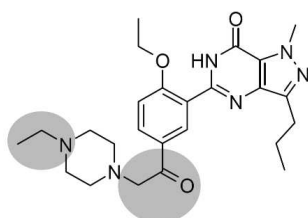
acetildenafil (hongdenafil)

Figure 1: Chemical structures of the studied compounds. The structural differences with the registered APIs are indicated in grey. (Reproduced from [2]).

131

2. **Material and methods**

2.1. Standards

The reference standards of sildenafil citrate (batch 904958), tadalafil (batch RS0480) and vardenafil dihydrochloride trihydrate (batch BXR3835 R-1013-02B) were kindly provided by Pfizer SA/NV (Belgium), Eli Lilly SA/NV (Benelux) and Bayer SA/NV (Belgium), respectively. Reference standards of hydroxyacetildenafil (batches 1068-005A2 and 1068-013A2), acetildenafil (batch 1046-011A2), dimethylsildenafil (batch 1035-122A1), aminotadalafil (batch 1034-001A1) and pseudovardenafil (batch 1070-002A2) were purchased from TLC Pharmachem (Ontario, Canada).

2.2. Samples

Pfizer SA/NV (Belgium) kindly provided one batch of each different dosage of Viagra® (25 mg, 50 mg, 100 mg). Two other batches of each dosage were purchased in a local pharmacy in Belgium.

2.3. Reagents

HPLC-grade acetonitrile was purchased from Biosolve (Valkenswaard, The Netherlands), formic acid and sodium hydroxide were obtained from VWR International (Leuven, Belgium) and ammonia solution 25 % was purchased from Merck (Darmstadt, Germany). Trifluoroacetic acid was purchased from Sigma Aldrich (Saint-Louis, USA). The water used was produced by a milliQ-Gradient A10 system (Millipore, Billerica, USA). The herbal matrix used to realize the validation samples comes from a placebo dietary supplement received for PDE5 inhibitors screening.

2.4. Sample preparation

2.4.1. Preparation of standards

According to their absorbance, the substances were divided into two groups. Group 1 contains hydroxyacetildenafil, acetildenafil and tadalafil. Stock solutions of each compound of group 1 were prepared in double, diluting 10.0 mg of pure substance (basic form) with 50.0 ml of a mixture of H_2O/ACN (50:50, v/v) (final concentration of 0.2 mg mL^{-1} of the basic form) The second group contains vardenafil, sildenafil, dimethylsildenafil, aminotadalafil and

pseudovardenafil. Stock solutions of each compound of group 2 were prepared in double diluting 30.0 mg of pure substance (basic form) with 50.0 ml of a mixture of H_2O/ACN (50:50, v/v) (final concentration of 0.6 mg mL^{-1}of the basic form).

Calibration standards were then prepared by diluting the stock solutions to obtain the concentrations indicated in Table 1. All solutions were prepared in a mixture of H_2O/ACN (50:50, v/v).

Table 1: Concentrations of the calibration standards and the validation samples. These concentrations are based on the basic form of each compound.

concentration levels	calibration standards group 1	calibration standards group 2	validation samples group 1	validation samples group 2
1	3 µg/ml	9 µg/ml	6 µg/ml	18 µg/ml
2	10 µg/ml	30 µg/ml	12 µg/ml	36 µg/ml
3	12 µg/ml	36 µg/ml	24 µg/ml	72 µg/ml
4	14 µg/ml	42 µg/ml		
5	32 µg/ml	96 µg/ml		

2.4.2. Preparation of spiked placebo validation samples

The samples stock solutions were prepared the same way as the reference standards with the addition of 200 mg herbal matrix to the pure substances. These solutions were magnetically stirred for 30 minutes, sonicated for 10 minutes and diluted to obtain the three concentration levels presented in Table 1. These levels were chosen with a ratio 0.5/1/2 to cover a large concentration range and to take into account the differences in concentration of the approved medicines. These final solutions were filtered with 0.2 µm PTFE filters before injection.

2.4.3. Preparation of samples for the comparison of methods

Five tablets of each dosage form of different batches of Viagra$^{®}$ samples were pulverised. An amount of the pulverised tablets of 25 mg, 50 mg and 100 mg was accurately weighed and diluted in a mixture of H_2O/ACN (50:50, v/v) to obtain the concentration levels 1, 2 and 3 respectively. Concentrations of sildenafil at the levels 1, 2 and 3 were 16 µg mL^{-1}, 36 µg mL^{-1} and 72 µg mL^{-1}, respectively. Three different samples were weighed daily for each concentration level and were analysed three times per day for seven consecutive days (see section 3.3.).

2.5. Equipment and chromatographic conditions

The HPLC experiments were performed on an Alliance 2690 HPLC system (Waters, Milford, USA) coupled to a 996 PDA detector (Waters). Data acquisition and treatment were performed with the Empower2 software (Waters).

The method optimisation and validation were performed on an Acquity UPLC^{TM} system (Waters). This system is composed of a binary solvent manager, a sample manager and a PDA detector. Data acquisition and treatment were also performed with the Empower2 software (Waters).

The initial method was developed in HPLC with a XTerra^{TM} RP18 (150 mm x 4.6 mm, 5 µm particle size) column (Waters). The optimisation and validation of the UHPLC gradient were performed on an Acquity^{TM} BEH Shield RP18 (100 mm x 2.1 mm, 1.7 µm particle size) column. Mobile phase A consisted of a 10 mM ammonium formate buffer (pH 3.5) and mobile phase B was acetonitrile. The gradient conditions are presented in Tables 2 and 3. After each injection, the systems were reconditioned for 10 min for HPLC and 4 min for UHPLC (Ultra High Pressure Liquid Chromatography).

The quantitative results of the developed UHPLC method were compared to the results obtained with the reference method used in our lab for the assay of the Viagra$^{®}$ samples. For confidentiality reasons, the method is not described in this paper. The statistical comparison was performed using the method described by Kuttatharmakul et al. [29].

Table 2: HPLC and initial UHPLC gradient conditions. For more details see text section 2.5.

HPLC conditions					Initial UHPLC conditions			
Time (min)	Flow rate (ml/min)	% A	% B		Time (min)	Flow rate (ml/min)	% A	% B
0	1.0	70	30		0	0.55	70	30
5.0	1.0	65	35		2.2	0.55	65	35
8.0	1.0	55	45		2.7	0.55	55	45
9.0	1.0	20	80		2.9	0.55	20	80
11.0	1.0	20	80		3.5	0.55	20	80
12.0	1.0	70	30		4.0	0.55	70	30

injection volume:	20µl			injection volume:	2.8µl	
Column temperature:	30°C			Column temperature:	40°C	

Table 3: Final UHPLC gradient conditions. For more details see text section 2.5.

Time (min)	Flow rate (ml/min)	% A	% B
0	0.55	75	25
2.5	0.55	65	35
3.5	0.55	55	45
3.8	0.55	30	70
4.5	0.55	30	70
5.0	0.55	75	25

injection volume: 1.5µl

Column temperature: 40°C

2.6. Method transfer

Figure 2 illustrates a chromatogram obtained by applying the initial HPLC gradient conditions presented in Table 2. These HPLC conditions were then adapted to obtain a UHPLC method by using the Waters Acquity UPLC^TM column calculator 1.0. This software optimizes the UHPLC parameters based on the HPLC conditions (for HPLC parameters see section 2.5) and column dimensions. The deduced conditions are presented in Table 2. The sub-2 micron polar-embedded stationary phase was chosen as the closest to the chemistry of the XTerra^TM RP18 material column. These initial gradient conditions were modified to obtain a greater resolution between the peaks corresponding to vardenafil and acetildenafil which led to a more robust method. The final conditions are illustrated in Table 3. Figure 3 shows the corresponding chromatogram.
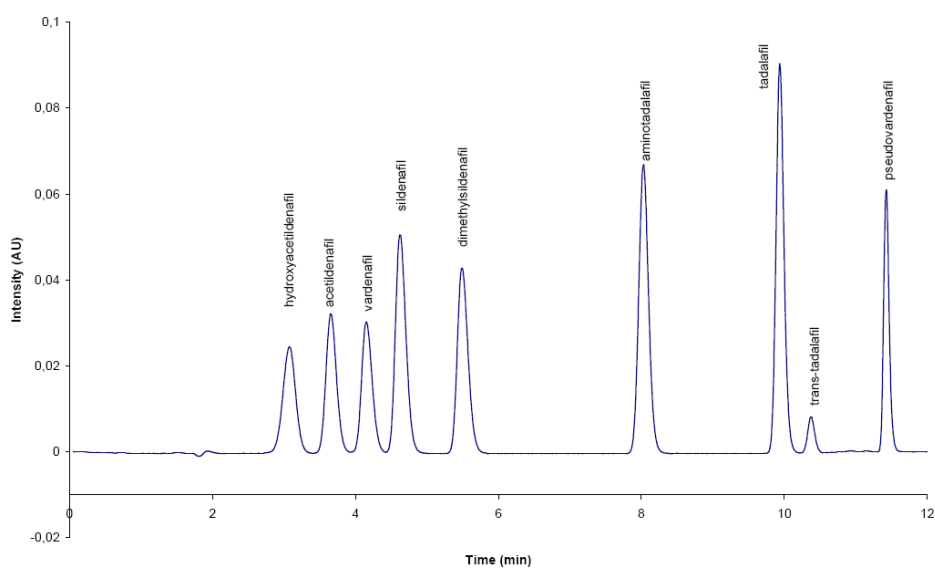
Figure 2: Typical chromatogram obtained by applying the gradient conditions of the HPLC method.
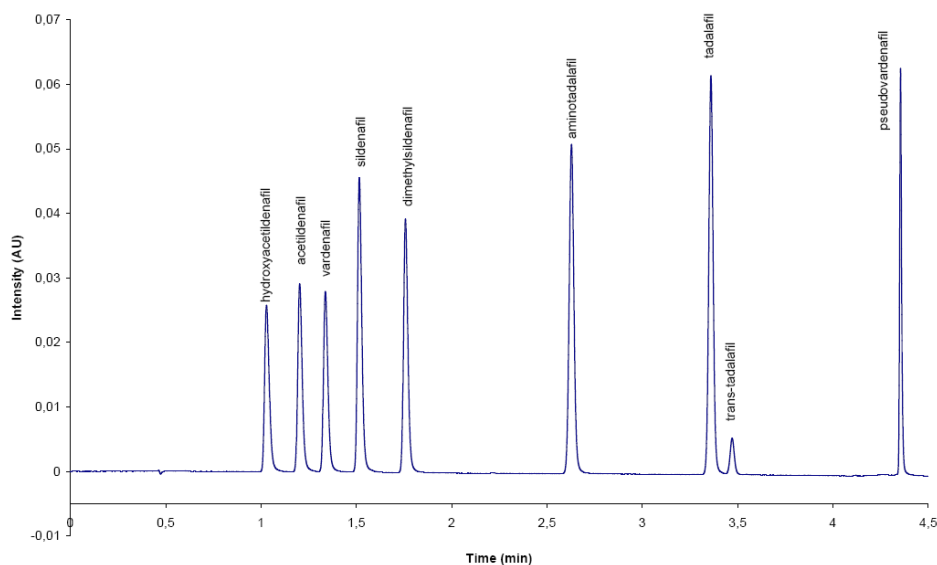
Figure 3: Typical chromatogram obtained by applying the final gradient conditions for the UHPLC method.

2.7.   System suitability testing

System suitability testing was performed on the validation standard with the medium concentration. The acceptance criteria were a relative standard deviation (RSD) values for areas and retention times of less than 1.0 % for 8 replicate injections.

2.8.   Method validation

This method has been validated using the "total error" approach in accordance with the validation requirements in the ISO-17025 norm and the guidelines of the French Society of Pharmaceutical Sciences and Techniques (SFSTP) [30-38].

The "total error" approach adds the systematic error (bias or trueness) and the random error (precision or standard deviation) to know the difference between the observed result and the true value. Thus, the total error estimation of an analytical method shows the biggest errors that may be encountered while using it.

The goal of the validation of an analytical method is to guarantee that a chosen proportion (set at 95 % during this study) of future samples will fall between the acceptance limits fixed *a priori* (for pharmaceutical specialties, [-5 %;5 %]). This proportion is evaluated by the β-expectation tolerance intervals (well described in [33]) at each concentration level studied. If the β-expectation tolerance intervals are comprised within the acceptance limits then the expected proportion of results will be included within these limits.

136

The results obtained during the validation process are plotted with their β-expectation tolerance intervals and the acceptance limits, allowing a simple and fast evaluation of the present and future accuracy of the method.

2.9. Robustness

Robustness was performed on a standard solution prepared by mixing 25.0 ml of the validation standard solution of groups 1 and 2 at the medium concentration.

The diastereoisomer of tadalafil, trans-tadalafil, was prepared for the robustness testing. Sodium hydroxide was added to a solution of tadalafil in a mixture of H_2O/ACN (50:50 v/v). After mixing for 30 min, the solution was neutralized with trifluoroacetic acid. An aliquot of 3.0 ml of this solution was added to the 50.0 ml standard solution used for the robustness test.

2.10. Statistics

The statistics and computations were performed using Microsoft® Office Excel 2003.

The choice of the calibration model and the validation of the Excel results were performed with the E-noval™ software V3.0 (Arlenda, Liège, Belgium).

3. Results and discussion:

3.1. Method Development

3.1.1. Initial conditions selection

The separation method has been developed in HPLC with UV detection in order to be applicable by a large amount of control laboratories. Acetonitrile was chosen as organic modifier as it causes less back pressure and better baseline stability than methanol. A 0.1 % formic acid aqueous solution (pH 2.8) was used as aqueous component of the mobile phase to be compatible with on-line mass spectrometry.

Initial HPLC conditions were a linear gradient starting from 5 % acetonitrile to 100 % in 27 min. The gradient time was calculated using the following equation considering 150 x 4.6 mm column dimensions:

$$\bar{k} \cong \frac{F \times t_G}{\Delta\phi \times V_m \times S} \tag{1}$$

where $\overline{k}$ is the mean retention factor (here set at 4), t_G is the gradient time (min), F is the flow rate (ml min^{-1}), $\Delta\phi$ is the difference between the final and initial percents of organic modifier divided by 100, V_m is the column dead volume (ml) and S is a constant (equal to 4 for small molecules).

The presented gradient conditions were used on different stationary phases (results not shown). The best results were obtained with a C_{18} polar embedded stationary phase such as an XTerra™ RP18.

During the optimization process, no satisfactory conditions were found with the 0.1 % formic acid solution (pH 2.8) as aqueous phase. The problem comes from the fact that vardenafil co-eluted with hydroxyacetildenafil before the start of the gradient. Indeed, at pH 2.8, the three basic nitrogens of vardenafil are ionised decreasing the retention of the molecule in reversed phase conditions. It was then decided to set the pH at 3.5 to deprotonate partially vardenafil (pKa values of 8.8, 6.7 and 3.4). This pH value was obtained using a 10mM ammonium formate buffer. The change of pH resulted in a higher retention of vardenafil. It was then possible to slightly adjust the gradient conditions to obtain the desired separation. These final gradient conditions are presented in Table 2.

3.1.2. Method transfer

The HPLC conditions were transferred to UHPLC as described in section 2.6. The calculated initial UHPLC gradient conditions were slightly modified to obtain a better separation. Especially for the two critical pairs: acetildenafil/vardenafil and tadalafil/trans-tadalafil. The final UHPLC conditions (shown in Table 3) were then validated.

3.2. Method Validation

3.2.1. Selectivity

The method selectivity was assessed by the constancy of the retention times and the UV spectrum of each component determined separately during the validation process.

3.2.2. Response Function

Several response functions were tested. They are the unweighted linear regression, the linear regression after mathematic transformations (log, square root), the weighted linear

regression (1/X, 1/X²) and the weighted quadratic regression (1/X, 1/X²). The unweighted linear regression model was chosen since it gives comparable results with the more complicated calibration models tested.

3.2.3. Linearity

The linearity of the relationship between the measured and theoretical concentrations was investigated over the concentration range described in Table 1. The measured concentrations were back-calculated using the selected calibration model. Validation results for tadalafil were both computed with an in-house Excel template and the E-noval software. The results obtained with Excel were comparable with those obtained with E-noval. The linearity of the results is expressed by the coefficient of determination (r^2). For the eight compounds the relationship was linear as the r^2 values were all > 0.99 and the equation was close to $y = x$.

3.2.4. Trueness, precision, accuracy and uncertainty assessment

A statistical approach based on the "total error" profiles was applied to validate the method.
All validation samples were analysed in triplicate for four consecutive days.
The concentrations were back-calculated using the calibration lines described in 2.4.1. These concentrations were used to determine the relative bias, the repeatability, the intermediate precision and the β-expectation tolerance intervals at the 95 % probability level. The results are shown in Table 4.
The RSD values of repeatability and intermediate precision were inferior to 1 % and 1.37 %, respectively. These values are said acceptable since their maximal Horwitz ratio is inferior to 0.5 [39] (0.251 for sildenafil in Viagra®, 0.249 for tadalafil in Cialis® and 0.393 for vardenafil in Levitra®).

As the method will also be used for the analysis of registered medicines, the acceptance limits were set at ±5 %. As shown in Figure 4, the β-expectation tolerance intervals of each substance are within the acceptance limits with a probability of 95 % except for the medium concentration level of acetildenafil and the highest concentration level of pseudovardenafil. However, the tolerance limits remain close to 5 %.

Table 4: Trueness, precision, accuracy and uncertainty

	concentration level	hydroxy acetildenafil	acetildenafil	vardenafil	sildenafil	dimethyl sildenafil	amino tadalafil	tadalafil	pseudo vardenafil
trueness									
relative bias (%)	1	0.30	1.02	0.33	0.68	1.38	0.97	0.29	1.31
	2	-0.31	0.59	0.28	0.38	0.62	0.58	0.37	1.21
	3	-1.48	-0.04	-0.11	-0.10	0.05	0.24	-0.24	0.71
intra-assay precision									
repeatability (RSD%)	1	0.55	0.39	0.66	0.38	0.44	0.48	0.54	0.35
	2	0.49	0.23	0.43	0.27	0.26	0.34	0.34	0.26
	3	0.26	0.17	0.51	0.40	0.45	0.43	0.15	0.46
between-assay precision									
intermediate precision (RSD %)	1	1.37	0.50	1.10	0.38	0.52	0.78	0.64	0.80
	2	1.24	0.24	0.55	0.47	0.31	0.51	0.41	0.51
	3	1.00	0.31	0.82	0.66	0.64	0.79	0.77	0.76
accuracy									
β-expectation tolerance limits (%)	1	[-3.85;4.45]	[-0.27;2.30]	[-3.01;3.68]	[-0.22;1.58]	[0.08;2.67]	[-1.25;3.19]	[-1.22;1.79]	[-1.52;4.14]
	2	[-4.03;3.42]	[0.04;1.14]	[-1.11;1.68]	[-1.06;1.82]	[-0.14;1.39]	[-0.85;2.02]	[-0.60;1.33]	[-0.36;2.78]
	3	[-4.47;1.52]	[-0.98;0.91]	[-2.39;2.18]	[-1.94;1.74]	[-1.64;1.74]	[-2.17;2.65]	[-2.95;2.48]	[-1.62;3.04]
uncertainty									
relative expanded uncertainty (%)	1	2.99	1.09	2.41	0.81	1.12	1.73	1.35	1.78
	2	2.67	0.50	1.18	1.04	0.66	1.12	0.87	1.13
	3	2.16	0.68	1.78	1.43	1.38	1.74	1.71	1.68
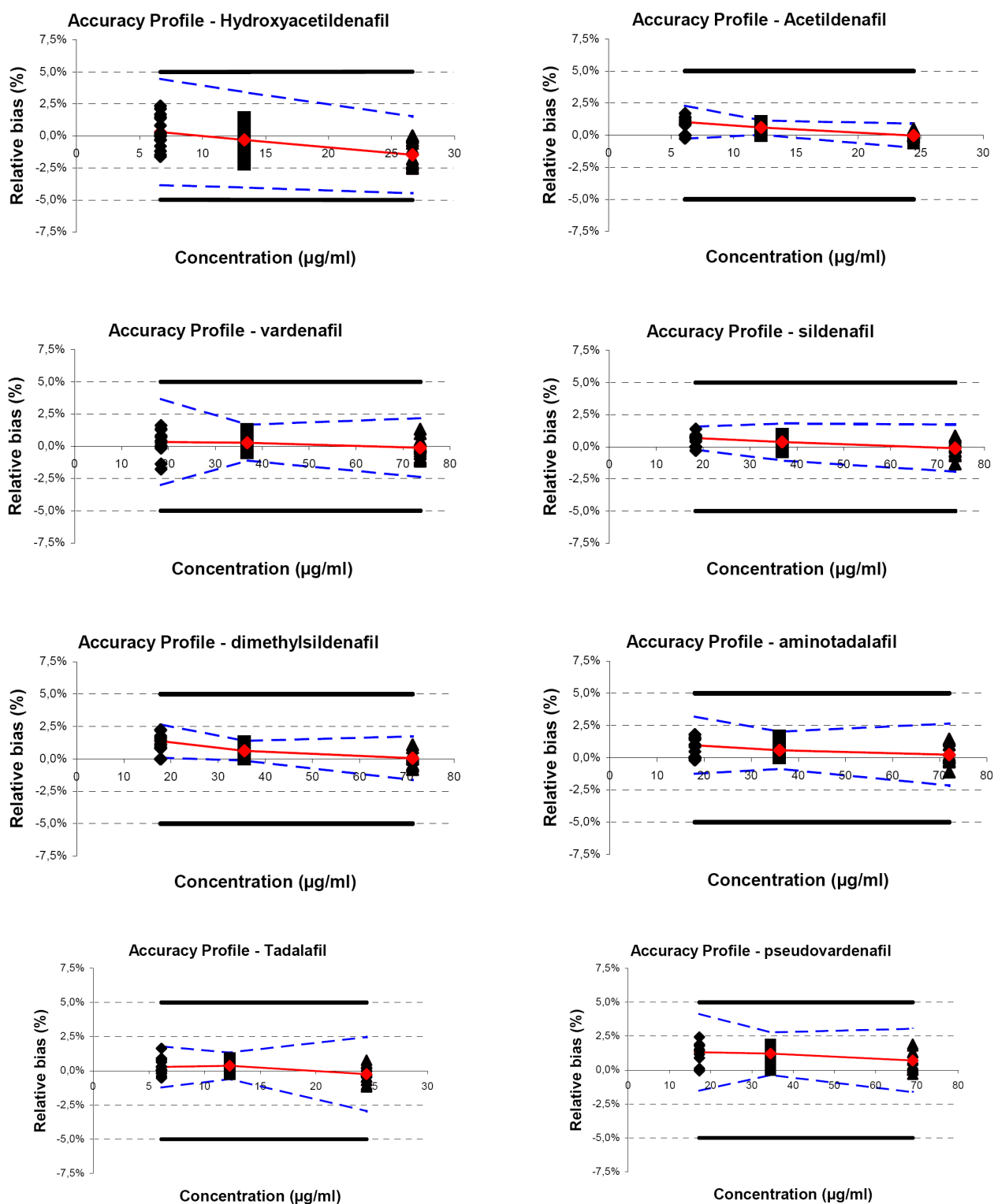
Figure 4: Accuracy profiles of the studied compounds. The plain line is the relative bias, the dashed lines are the β-expectation tolerance limits (β=95%) and the bold plain lines are the acceptance limits set at 5%. The dots represent the relative back-calculated concentrations of the validation samples, plotted with regards to their target concentration.

The uncertainty of measurement [35] characterises the dispersion of the values that could reasonably be attributed to the analyte. The expanded uncertainty represents the interval around the results where the unknown true value can be observed at a confidence level of 95 %. Relative expanded uncertainties (%) are obtained by dividing the corresponding expanded uncertainty by the corresponding concentration. The values are presented in Table 4 and are all below 3 %.

3.2.5. Robustness

Robustness is the evaluation of the constancy of the results when variables inherent to the method of analysis are varied deliberately.

The test was performed by a three-factor three-level full factorial design [40]. The factors were the flow rate of the mobile phase, the column temperature and the pH of the ammonium formate buffer. The response was the resolution between tadalafil and trans-tadalafil (critical pair). The values were chosen to cover typical errors that could occur. Table 5 shows the experimental design. Each experiment was performed in triplicate and the mean value was used for computations.

The effect of each factor was calculated for its signification at 5 % level using an ANOVA analysis. The regression is meaningful since the value of R^2 is 99.96 %. From the ANOVA table, it can be seen that only the pH and the flow rate have a significant effect on the resolution (p-values < 0.0001). However this effect is still very small since the resolution varies between 2.64 and 2.79.

The method can be considered as robust since only a very small change in resolution occurs.

Table 5: 3-factors 3-levels full factorial design performed for robustness evaluation.

pH	temperature (°C)	flow (ml/min)	Resolution tadalafil/trans-tadalafil
3.4	39	0.50	2.74
3.4	39	0.55	2.73
3.4	39	0.60	2.68
3.4	40	0.50	2.75
3.4	40	0.55	2.71
3.4	40	0.60	2.66
3.4	41	0.50	2.75
3.4	41	0.55	2.72
3.4	41	0.60	2.68
3.5	39	0.50	2.75
3.5	39	0.55	2.69
3.5	39	0.60	2.64
3.5	40	0.50	2.73
3.5	40	0.55	2.70
3.5	40	0.60	2.65
3.5	41	0.50	2.73
3.5	41	0.55	2.71
3.5	41	0.60	2.67
3.6	39	0.50	2.77
3.6	39	0.55	2.76
3.6	39	0.60	2.70
3.6	40	0.50	2.78
3.6	40	0.55	2.76
3.6	40	0.60	2.71
3.6	41	0.50	2.79
3.6	41	0.55	2.76
3.6	41	0.60	2.69

3.3. Method comparison

The method was compared with a validated method considered as reference method.

The samples were prepared as described in section 2.4.3. and analysed three times per day for seven consecutive days by applying UHPLC and HPLC methods. The minimum of days required and the comparison were performed according to the method described by Kuttatharmmakul et al. [29]. Results are shown in Table 6.

The variances of both methods were compared using a two-sided F-test at a significance level $\alpha = 0.05$ (6 degrees of freedom for both methods). The variances were not shown as statistically different since all F-statistics are below the critical value of 5.82.

Table 6: Results of the comparison tests

	Concentration level 1	Concentration level 2	Concentration level 3
variance of the reference method (σ^2_A)	0.429	0.113	2.825
variance of the new method (σ^2_B)	0.516	0.091	2.624
t-statistics for bias between both methods	0.14	1.22	1.02
interval hypothesis test (%)	[-1.06;1.25]	[-0.35;1.86]	[-0.74;2.75]

The bias between the methods was tested using a paired t-test comparing the grand means of both methods. The differences between the grand means was considered statistically non significant since their value is below the critical value of 2.18 ($\alpha/2 = 0.025$, 12 degrees of freedom for both methods).

The interval hypothesis test described by Hartman et al. [41] was performed to be sure of not accepting a new method with an unacceptable bias. For the interval hypothesis test, a bias of 2 % was said to be acceptable. As can be seen in Table 6, these requirements are fulfilled for the concentration levels 1 and 2. However, the highest concentration level has an unacceptable bias which means that the HPLC method is best suited at that concentration for the assay of sildenafil citrate in Viagra® tablets.

A Bland and Altman plot [42] is shown in Figure 5. This plot represents the relative differences (%) between the HPLC reference method and the new UHPLC method against the average content of API (%) for the three concentration levels. As one can see, 95 % of the relative differences are comprised between [-2,61 %; 1,18%]. Those results are comprised between the maximum acceptable relative differences between the two methods set at ±5 %. It is finally concluded that the two methods gave comparable results.
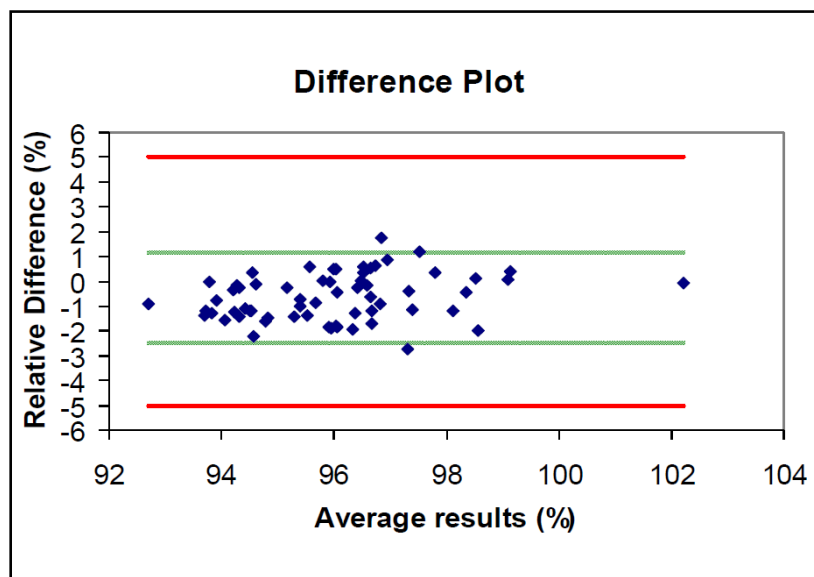
Figure 5: Bland and Altman plot of the relative differences (%) of the results obtained by the HPLC reference method and the new UHPLC method against the average content of API (%) for the three concentration levels results of the two methods. *Dashed lines*: 95% agreement limits of the relative differences; *Continuous lines*: maximum acceptable relative difference between the two methods set at ±5%; *Dots*: relative differences.

4. Conclusion

This paper describes for the first time a fully validated method which enables the detection and the quantification of authorised phosphodiesterase type 5 inhibitors and some of their analogues in less than 4.5 minutes. This rapidity associated to a low flow rate permits the analysis of a large number of samples with a reduced cost and associated solvent consumption.

The main problem with counterfeit medicines is that their chemical composition is unknown. This is why they represent a real danger for public health. The method permits the detection of all PDE5 inhibitors even other new structurally related substances as it covers a wide range of polarity. The elucidation of structures and the confirmation of identity may be performed by UHPLC-MS systems since the mobile phase is compatible.

The method has already been applied to real samples and showed no interference with common other substances present as yohimbine (retention time of 0.77 min) and caffeine (retention time of 0.57 min).

An important point in counterfeit medicines detection is the cost of the UHPLC system and its applicability in developing countries. However, this is not really a problem since PDE5 inhibitors are mainly sold in rich and industrialised countries.

References

[1] Deisingh A., Pharmaceutical counterfeiting, Analyst (2005) 130, 271-279

[2] Venhuis B.J., Barends D.M., Zwaagstra M.E., de Kaste D., Recent developments in counterfeit and imitations of Viagra®, Cialis® and Levitra®, RIVM Report 370030001/2007, Bilthoven, 2007

[3] Lee H.M., Kim C.S., Jang Y.M., Kwon S.W., Lee B.J., Separation and structural elucidation of a novel analogue of vardenafil included as an adulterant in a dietary supplement by liquid chromatography-electrospray ionization mass spectrometry, infrared spectroscopy and nuclear magnetic resonance spectroscopy, Journal of Pharmaceutical and Biomedical Analysis, (2011) 54, 491-496

[4] Singh S., Prasad B., Savaliya A., Shah R., Gohil V., Kaur A., Strategies for characterizing sildenafil, vardenafil, tadalafil and their analogues in herbal dietary supplements, and detecting counterfeit products containing these drugs, Trends in Analytical Chemistry 28 (2009) 13-28

[5] Gratz S., Zeller M., Mincey D., Flurer C., Structural Characterization of Sulfoaildenafil, an analog of sildenafil, Journal of Pharmaceutical and Biomedical Analysis (2009) 50, 228-231

[6] Reepmeyer J., d'Avignon D.A., Structure elucidation of thioketone analogues of sildenafil detected as adulterants in herbal aphrodisiacs, Journal of Pharmaceutical and Biomedical Analysis (2009) 49, 145-150

[7] Lin M.C., Liu Y.C., Lin J.H., Identification of a sildenafil analogue adulterated in two herbal food supplements, Journal of Food and Drug Analysis (2006) 14, 260-264

[8] Lai K.C., Liu Y.C., Tseng M.C., Lin J.H., Isolation and identification of a sildenafil analogue illegally added in dietary supplements, Journal of Food and Drug Analysis (2006) 14, 19-23

[9] Hou P., Zou P., Low M.Y., Chan E., Koh H.L., Structural identification of a new acetildenafil analogue from pre-mixed bulk powder intended as a dietary supplement, Food Additives and Contaminants: Part A (2006) 23, 870-875

[10] Shin C., Hong M., Kim D., Lim Y., Structure determination of a sildenafil analogue contained in commercial herb drinks, Magnetic Resonance in Chemistry (2004) 42, 1060-1062

[11] Blok-Tip L., Zomer B., Bakker F., Hartog K.D., Hamzink M., ten Hove J., Vredenbregt M., de Kaste D., Structure elucidation of sildenafil analogues in herbal products, Food Additives and Contaminants: Part A (2004) 21, 737-748

[12] Nagaraju V., Sreenath D., Tirumala Rao J., Nageswara Rao R., Separation and determination of synthetic impurities of sildenafil (Viagra) by reversed-phase high-performance liquid chromatography, Analytical Sciences (2003) 19, 1007-1011

[13] Dinseh N.D., Vishukumar B.K., Nagaraja P., Made Gowda N.M., Rangappa K.S., Stability indicating RP-LC determination of sildenafil citrate (Viagra) in pure form and in pharmaceutical samples, Journal of Pharmaceutical and Biomedical Analysis (2002) 29, 743-748

[14] Daragmeh N., Al-Omari M., Badwan A.A., Jaber A.M.Y., Determinaton of sildenafil citrate and related substances in the commercial products and tablet dosage form using HPLC, Journal of Pharmaceutical and Biomedical Analysis (2001) 25, 483-492

[15] Häberli A., Girard P., Low M.Y., Gei X., Isolation and structure elucidation of an interaction product of aminotadalafil found in an illegal health food product, Journal of Pharmaceutical and Biomedical Analysis (2010) 53, 24-28

[16] Venhuis B.J., Zomer G., Vredenbregt M.J., de Kaste D., The identification of (–)-trans-tadalafil, tadalafil, and sildenafil in counterfeit Cialis® and the optical purity of tadalafil stereoisomers, Journal of Pharmaceutical and Biomedical Analysis (2010) 51, 723-727

[17] Aboul-Enein H.Y., Ali I., Determination of tadalafil in pharmaceutical preparation by HPLC using monolithic silica column, Talanta (2005) 65, 276-280

[18] Reepmeyer J.C., Woodruff J.T., Use of liquid chromatography–mass spectrometry and a hydrolytic technique for the detection and structure elucidation of a novel synthetic vardenafil designer drug added illegally to a "natural" herbal dietary supplement, Journal of Chromatography A (2006) 1125, 67-75

[19] De Orsi D., Pellegrini M., Marchei E., Nebuloni P., Gallinella B., Scaravelli G., Martufi A., Gagliardi L., Pichini S., High performance liquid chromatography-diode array and electrospray-mass spectrometry analysis of vardenafil, sildenafil, tadalafil, testosterone and local anesthetics in cosmetic creams sold on the Internet web sites, Journal of Pharmaceutical and Biomedical Analysis (2009) 50, 362-369

[20] Gryniewicz C.M., Reepmeyer J.C., Kauffman J.F., Buhse L.F., Detection of undeclared erectile dysfunction drugs and analogues in dietary supplements by ion mobility spectrometry, Journal of Pharmaceutical and Biomedical Analysis (2009) 49, 601-606

[21] Savalyia A.A., Shah R.P., Prasad B., Singh S., Screening of Indian aphrodisiac ayurvedic/herbal healthcare products for adulteration with sildenafil, tadalafil and/or vardenafil using LC/PDA and extracted ion LC–MS/TOF, Journal of Pharmaceutical and Biomedical Analysis (2010) 52, 406-409

[22] Choi D.M., Park S., Yoon T.H., Jeong H.K., Pyo J.S., Park J., Kim D., Kwon S.W., Determination of Analogs of Sildenafil and Vardenafil in Foods by Column Liquid Chromatography with a Photodiode Array Detector, Mass Spectrometry, and Nuclear Magnetic Resonance Spectrometry, Journal of AOAC International (2008) 91, 580-588

[23] Park H.J., Jeong H.K., Chang M.I., Im M.H., Jeong J.Y., Choi D.M., Park K., Hong M.K., Youm J., Han S.B., Kim D.J., Park J.H., Kwon S.W., Structure determination of new

analogues of vardenafil and sildenafil in dietary supplements, Food Additives and Contaminants: Part A (2007) 24, 122-129

[24] Gratz S.R., Gamble B.M., Flurer R.A., Accurate mass measurement using Fourier transform ion cyclotron resonance mass spectrometry for structure elucidation of designer drug analogs of tadalafil, vardenafil and sildenafil in herbal and pharmaceutical matrices Rapid Communication in Mass Spectrometry (2006) 20, 2317-2327

[25] Zou P., Oh S.S.-Y., Hou P., Low M.-Y., Koh H.-L., Simultaneous determination of synthetic phosphodiesterase-5 inhibitors found in a dietary supplement and pre-mixed bulk powders for dietary supplements using high-performance liquid chromatography with diode array detection and liquid chromatography–electrospray ionization tandem mass spectrometry, Journal of Chromatography A (2006) 1104,113-122

[26] Zhu X., Xiao S., Chen B., Zhang F., Yao S., Wan Z., Yang D., Han H., Simultaneous determination of sildenafil, vardenafil and tadalafil as forbidden components in natural dietary supplements for male sexual potency by high-performance liquid chromatography–electrospray ionization mass spectrometry, Journal of Chromatography A (2005) 1066, 89

[27] Fleshner N., Harvey M., Adomat H., Wood C., Eberding A., Hersey K., Guns E., Evidence for contamination of herbal erectile dysfunction products with phosphodiesterase type 5 inhibitors, Journal of Urology (2005) 174, 636-641

[28] Gratz S.R., Flurer C.L., Wolnik K.A., Analysis of undeclared synthetic phosphodiesterase-5 inhibitors in dietary supplements and herbal matrices by LC–ESI–MS and LC–UV Journal of Pharmaceutical and Biomedical Analysis (2004) 36, 525-533

[29] Kuttatharmmakul S., Massart D.L., Smeyers-Verbeke J., Comparison of alternative measurement methods, Analytica Chimica Acta (1999) 391, 203-225

[30] ISO/IEC 17025, General requirements for the competence of testing and calibration laboratories, ISO, Geneva, 2005

[31] Hubert Ph., Nguyen-Huu J.-J., Boulanger B., Chapuzet E., Chiap P., Cohen N., Compagnon P.-A., Dewé W., Feinberg M., Lallier M., Laurentie M., Mercier N., Muzard G., Nivet C., Valat L., Harmonization of strategies for the validation of quantitative analytical procedures: A SFSTP proposal – part I, Journal of Pharmaceutical and Biomedical Analysis (2004), 36, 579-586

[32] Hubert Ph., Nguyen-Huu J.-J., Boulanger B., Chapuzet E., Chiap P., Cohen N., Compagnon P.-A., Dewé W., Feinberg M., Lallier M., Laurentie M., Mercier N., Muzard G., Nivet C., Valat L., Rozet E., Harmonization of strategies for the validation of quantitative analytical procedures: A SFSTP proposal – part II, Journal of Pharmaceutical and Biomedical Analysis (2007), 45, 70-81

[33] Hubert Ph., Nguyen-Huu J.-J., Boulanger B., Chapuzet E., Cohen N., Compagnon P.-A., Dewé W., Feinberg M., Laurentie M., Mercier N., Muzard G., Valat L., Rozet E.,

Harmonization of strategies for the validation of quantitative analytical procedures: A SFSTP proposal – part III, Journal of Pharmaceutical and Biomedical Analysis (2007), 45, 82-96

[34] Hubert Ph., Nguyen-Huu J.-J., Boulanger B., Chapuzet E., Cohen N., Compagnon P.-A., Dewé W., Feinberg M., Laurentie M., Mercier N., Muzard G., Valat L., Rozet E., Harmonization of strategies for the validation of quantitative analytical procedures: A SFSTP proposal – part IV. Examples of applicaion, Journal of Pharmaceutical and Biomedical Analysis (2008), 48, 760-771

[35] Feinberg M., Boulanger B., Dewé W., Hubert Ph, New advances in chemical data quality: method validation abd measurement uncertainty, Analytical and Bioanalytical Chemistry (2004) 380, 502-514

[36] Feinberg M., Validation of analytical methods based on accuracy profiles, Journal of Chromatography A (2007) 1158, 174-183

[37] Rozet E., Ceccato A., Hubert C., Ziemons E., Oprean R., Rudaz S., Boulanger B., Hubert Ph., Analysis of recent pharmaceutical regulatory documents on analytical method validation, Journal of Chromatography A (2007) 1158, 111-125

[38] Araujo P., Key aspects of analytical method validation and linearity evaluation, Journal of Chromatography B (2009) 877, 2224-2234

[39] Horwitz W., Albert R., The Horwitz ratio (HorRat): A useful index of method performance with respect to precision, Journal of AOAC International (2006) 89, 1095-1109

[40] Massart D.L., Vandeginste B.G.M., Buydens L.M.C., De Jong S., Lewi P.J., Smeyers-Verbeke J., Handbook of Chemometrics and Qualimetrics: Part A, Elsevier Science, Amsterdam, 1997

[41] Hartmann C., Smeyers-Verbeke J., Penninckx W., Vanderheyden Y., Vankeerberghen P., Massart D.L., Reappraisal of Hypothesis Testing for Method Validation: Detection of Systematic Error by Comparing the Means of Two Methods or of Two Laboratories, Analytical Chemistry (1995) 67, 4491-4499

[42] Bland J.M., Altman D.G., Statistical methods for assessing agreement between two methods of clinical measurement, The Lancet (1986) 307-310

3.2. *Impurity fingerprints for the identification of counterfeit medicines - a feasibility study*

One of the major problems with counterfeit medicines is their unknown chemical composition. Indeed, most of them are manufactured in non good manufacturing practices (GMP) environments by uncontrolled or street laboratories. In addition, the conservation conditions are generally very bad. All these conditions imply that impurities may be present in variable amounts in counterfeit drugs.

Based on these assumptions, discrimination between illegal and genuine drugs based on their impurity profiles should be possible. An easy way to achieve this goal is to use chromatographic impurity profiles as fingerprints and treating them like spectroscopic data. The major advantages of this approach are the general overview of the chemical composition of the drug with a possibility of identification of the active compounds or impurities and the simultaneous quantification of the active compounds.

It has been decided to perform the experiments on a classical HPLC-DAD system which is present in almost every control laboratory. The chromatographic conditions are the one described in Pharmeuropa (or slightly modified) and are dedicated to the detection of specific impurities related to the considered API.

The predictive properties of the approach were evaluated. This has been performed to check whether it could be implemented in a control laboratory for the analysis of suspect samples.

More details and the results can be found in the following publication:

Sacré P-Y, Deconinck E, Daszykowski M, Courselle P, Vancauwenberghe R, Chiap P, Crommen J, De Beer J, Impurity fingerprints for the identification of counterfeit medicines - a feasibility study, Analytica Chimica Acta (2011) 701, 224-231

Impurity fingerprints for the identification of counterfeit medicines - a feasibility study

Pierre-Yves Sacré[a,d], Eric Deconinck[a], Michal Daszykowski[b], Patricia Courselle[a], Roy Vancauwenberghe[e], Patrice Chiap[c], Jacques Crommen[d], Jacques O. De Beer[a,*]

[a] *Laboratory of Drug Analysis, Scientific Institute of Public Health, Brussels, Belgium*

[b] *Department of Analytical Chemistry, Institute of Chemistry, The University of Silesia, Katowice, Poland*

[c] *Advanced Technology Corporation (A.T.C.), University Hospital of Liège, Liège, Belgium*

[d] *Department of Analytical Pharmaceutical Chemistry, Institute of Pharmacy, University of Liège, Liège, Belgium*

[e] *Federal Agency for Medicines and Health Products, Brussels, Belgium*

Abstract

Most of the counterfeit medicines are manufactured in non good manufacturing practices (GMP) conditions by uncontrolled or street laboratories. Their chemical composition and purity of raw materials may, therefore, change in the course of time. The public health problem of counterfeit drugs is mostly due to this qualitative and quantitative variability in their formulation and impurity profiles.

In this study, impurity profiles were treated like fingerprints representing the quality of the samples. A total of 73 samples of counterfeit and imitations of Viagra® and 44 samples of counterfeit and imitations of Cialis® were analysed on a HPLC-UV system. A clear distinction has been obtained between genuine and illegal tablets by the mean of a discriminant partial least squares analysis of the log transformed chromatograms. Following exploratory analysis of the data, two classification algorithms were applied and compared. In our study, the k-nearest neighbour classifier offered the best performance in terms of correct classification rate obtained with cross-validation and during external validation. For Viagra®, both cross-validation and external validation sets returned a 100% correct classification rate. For Cialis® 92.3% and 100% correct classification rates were obtained from cross-validation and external validation, respectively.

Keywords:

Impurities, Fingerprints, Classification, Counterfeit, Phosphodiesterase type 5 inhibitors

1. Introduction

The problem of pharmaceutical counterfeiting has widely grown since 1990 when it has been first detected. In industrialized countries, drug counterfeiting accounts for less than 1% of the market value, but in developing countries in Africa, Asia and Latin America, it represents a much higher percentage of the medicines on sale mostly due to the lack of regulatory systems and effective market control. The World Health Organization (WHO) defines a counterfeit medicine as "one which is deliberately and fraudulently mislabelled with respect to identity and/or source" [1, 2]. This definition underlines the fact that the source and the manufacturing conditions of the counterfeit drugs are unknown. Most of them are manufactured in non good manufacturing practices (GMP) environment by uncontrolled or street laboratories [3]. Thus, their chemical composition and purity of raw materials may change in the course of time and they may not meet the European Pharmacopoeia requirements. The risks for public health of counterfeit drugs are mostly due to this variability. The impurities in drug products may have different origins [4], for instance:

- starting materials,
- by-products and residual solvents from the API synthesis,
- degradants formed during the process and long-term storage, and
- contaminants from packaging components and other drug products manufactured in the same facility.

The impurities can also be formed as a result of heat, light and oxidants. They can be catalysed by trace metal impurities, change in the pH of the formulation, interaction with packaging components [5], excipients and other active ingredients in the case of combination products.

Several studies have reported the use of spectroscopic fingerprints provided by nuclear magnetic resonance (NMR) [6-8], near infrared spectroscopy (NIR) [9-11] and Fourier transform infrared spectroscopy (FT-IR) [12, 13] in the field of quality control and/or discrimination of food origin. The main drawback of these techniques is their complexity of interpretation. This is why, more and more, chromatographic techniques are used to provide fingerprints. The use of HPLC-UV by Dumarey et al. allowed the synthesis pathway of four acetaminophen formulations to be distinguished [14]. The HPLC-DAD fingerprints have also been used in the field of quality control [15-17], but to obtain the maximum information from the samples, the use of a coupled mass spectrometer is necessary.

LC-MS has been used for impurity profiling [18, 19] and is widely spread for the control of herbal medicines [20-23]. Although less used, the fingerprinting by GC-MS has also gained attention [24-26].

In this study, 73 counterfeit and imitations of Viagra®, 10 genuine Viagra®, 44 counterfeit and imitations of Cialis® and 5 genuine Cialis® were analysed. The aim of this study was to discriminate illegal samples from genuine ones based on their impurity profiles and to build a predictive classification model. For this purpose, k-nearest neighbour (k-NN) and soft independent modelling by class analogy (SIMCA) were applied and compared.

2. **Experimental**

2.1. Samples

The counterfeit and imitation tablets were donated by the Federal Agency for Medicines and Health Products in Belgium (AFMPS/FAGG). They all come from postal packs ordered by individuals through internet sites. All samples were delivered in blisters or in closed jars with or without packaging. All samples, once received, were stored at ambient temperature and protected from light.

Pfizer SA/NV (Belgium) kindly provided one batch of each different dosage of Viagra® (25mg, 50mg, 100mg). Two other batches of each dosage were purchased in a local pharmacy in Belgium.

Eli Lilly SA/NV (Benelux) kindly provided one batch of commercial packaging of Cialis® (10mg and 20mg). Two other batches of Cialis® 20mg were purchased in a local pharmacy in Belgium.

All references were delivered in closed blisters with packaging and were stored protected from light at ambient temperature.

2.2. Instrumental

Impurity profile analyses were performed on an Alliance 2690 HPLC system (Waters, Milford, USA) coupled to a 2487 dual λ absorbance detector (Waters). Data acquisition and treatment were performed with the Empower2 software (Waters).

For the Viagra-like samples, the HPLC method is the one published in Pharmeuropa (draft monography for the European Pharmacopoeia) [27]. Chromatography was performed at 30°C on a Symmetry C_{18} 150 mm x 4.6 mm with a 5µm particle size (Waters). The mobile phase was a mixture of 17 volumes of acetonitrile, 25 volumes of methanol and 58 volumes of a 0.7 % (v/v) solution of triethylamine adjusted to pH 3.0 ± 0.1 with orthophosphoric acid. The flow rate was set at 1 mL min^{-1} and the injection volume was 20 µl of a solution of 500 µg mL^{-1} of sildenafil. The samples were diluted in the mobile phase and the detection was performed at 290 nm ($λ_{max}$ for sildenafil).

For the Cialis-like samples, the method has been slightly adapted from the Pharmeuropa method [28]. Chromatography was performed at 30°C on a Zorbax C_8 150 mm x 4.6 mm with a 3,5µm particle size (Agilent Technologies, Santa Clara, USA). The mobile phase was a mixture of 35 volumes of acetonitrile and 65 volumes of a 0.1 % (v/v) aqueous solution of trifluoroacetic acid. The flow rate was set at 1 mL min^{-1} and the injection volume was 20 µl of a solution of 400 µg mL^{-1} of tadalafil. The samples were diluted in the mobile phase and the detection was performed at 285 nm (λ_{max} for tadalafil).

2.3. Data analysis

All data treatments were done using Matlab (The Matworks, Natick, MA, USA, version 7.9.0). The SIMCA analysis was performed using the PLS_toolbox for Matlab (Eigenvector Research, Inc., Wenatchee, WA, USA, version 6.0.1).

2.4. Chemometric methods

2.4.1. Data pre-processing

Pre-processing of chromatographic fingerprints is a crucial step that can strongly affect results of further analysis and interpretation. Usually, pre-processing of chromatographic fingerprints requires improvement of the signal-to-noise ratio (noise reduction, baseline elimination), normalization (e.g., to remove differences in sample volumes) and peak alignment [29]. In our study, noise reduction and baseline correction were unnecessary because all signals have a relatively good signal-to-noise ratio. A detailed analysis of consecutive signals revealed a systematic offset. Therefore, from all elements of the signals at a given retention time their minimal value was subtracted.

In our study only a simple peak correction was needed to obtain a satisfactory overall alignment of all signals. The major steps of the alignment procedure followed by us can be summarized as follows. Firstly, the target signal was selected as the one that resembles the largest mean correlation between all chromatograms [30]. Then, in all signals the largest peak was identified (using the threshold approach) and this peak served as a marker peak for the alignment. Afterwards, all signals were transformed using the linear interpolation so that positions of the largest peak in all signals matched the position of the largest peak in the target signal. During alignment procedure, each signal was split into two parts defined by the apex of the marker peak and then independently warped using linear interpolation towards the corresponding section in the target signal.

The linear interpolation is a procedure of compressing or extending a signal by changing a sampling rate over x-axis of a signal. Bearing in mind the desired number of sampling points of a signal, a new uniform grid of points is constructed over a certain range (with less or more points). Then, the unknown y-values for x-points on a new grid of points are calculated using the following expression:

$$y = y_0 + (x - x_0)\frac{y_1 - y_0}{x_1 - x_0} \tag{1}$$

where, y is the predicted y-value at location x on a new grid of points, x_0 and x_1 are x-points of the original axis and define interval containing point x, whereas y_0 and y_1 are their respective y-values.

2.4.2. Principal component analysis

Principal component analysis (PCA) is an exploratory technique. It allows original variables, **X**, to be represented by a limited number of orthogonal latent variables, called principal components (PCs). They are constructed as linear combinations of original variables and explain the largest part of the data variability [31]. The importance of the original variables in the construction of a given principal component is indicated by the magnitude of its absolute loading value. The projections of the objects onto the space of principal components are called the scores of the objects. The selected pairs of scores are summarizing a large part of the data variance. They can be further used to examine and interpret similarities among samples. More details about the PCA method can be found in [32].

2.4.3. Discriminant partial least squares

Discriminant partial least squares (D-PLS) is a supervised method, aiming to discriminate among known groups of samples. This goal is achieved using a few latent variables, called the PLS-factors being linear combinations of the original variables, **X**. They are constructed in such way that the covariance between the data variable and the response variable, **y**, which represents to which group a sample belongs, is maximal. This is why the PLS-factors capture better differences among known groups of samples than PCA latent factors. Especially when groups of samples are not distributed along the directions of the largest data variability. In this study, a binary response variable was used to code two groups of samples. Zeros in the response variable represent illegal samples and ones genuine samples. This

differentiation between two groups of samples was possible since the genuinity of the reference samples is certified [32].

2.4.4. Selection of a test set for external validation of models

In order to perform an external validation of the classification models, the aligned chromatographic fingerprints were split into a training and test set applying the Kennard and Stone algorithm [33]. The Kennard and Stone algorithm allows the selection of samples in the dataset in such way that their distribution in the data space is as uniform as possible. The uniform selection of samples guarantees that the main sources of data variability will be incorporated during the construction of a model. The model will thus be general enough when used for prediction purposes.

2.4.5. K-nearest neighbour

The k-nearest neighbour method [34], k-NN, is a classification technique where neighbourhoods of training set objects are used for the construction of classification rules. During the classification procedure, the Euclidian distances between an unknown object and each of the objects of the training set are computed. For a dataset with n samples, n distances are calculated. Then, for a new object its k closest neighbours from the training set are examined. The unknown object is classified into the group to which the majority of the k neighbouring objects of the training samples belong.

2.4.6. Soft Independent Modelling by Class Analogy (SIMCA)

SIMCA [34] is a classification technique that models each group of samples separately using a few principal components obtained from PCA. The optimal number of principal components, required to describe the training class, is evaluated using a cross-validation procedure. To construct classification rules, two critical values are considered obtained for the Euclidian distances towards the SIMCA model (the so-called orthogonal distances) and the Mahalanobis distances computed in the space of scores. The two critical values define a limited space around the samples of the training set in the model space with respect to their orthogonal distance and Mahalanobis distance. The position of a new object in the studied space is computed using the scores and loadings of the constructed PCA model. If the object is located within the defined limited space of orthogonal and Mahalanobis distances for the training class then it is said to belong to this class. Otherwise, the object is considered as an outlier, i.e. not belonging to this group. Confidence limits were set at 95%. Since SIMCA

belongs to the so-called soft classification methods, it is possible that a new sample can be assigned to one or more existing groups or to any. This is a direct consequence of building disjoint classification models for each group of samples.

3. **Results and Discussion**

3.1. **Measurements**

Each sample has been analysed in triplicate. Figure 1 shows typical impurity profiles of both legal and illegal tablets. The chromatograms were aligned using linear interpolation with respect to the highest peak. Figure 2 shows a signal of the chromatograms before and after alignment. After alignment, replicate chromatograms obtained for a given sample were averaged.

a.

b.

c.

d.
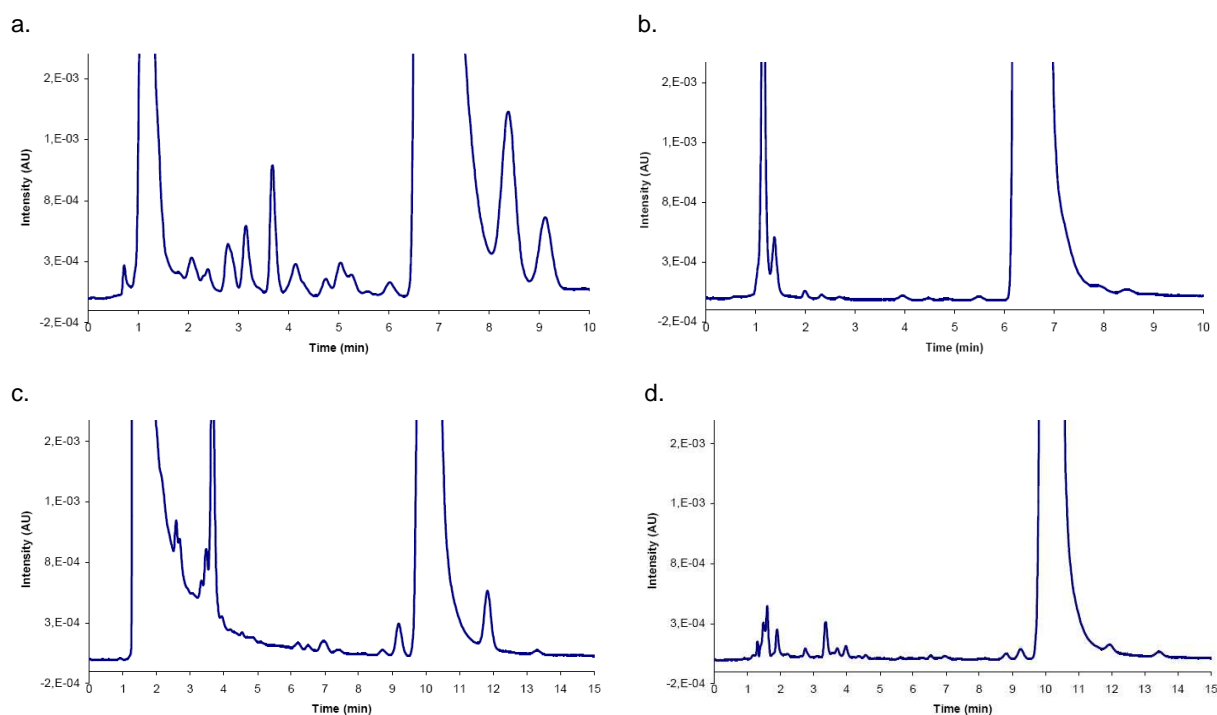
Figure 1:

    a.   Impurity profile of a counterfeit tablet of Viagra[®]

    b.   Impurity profile of a genuine tablet of Viagra[®]

    c.   Impurity profile of a coloured imitation tablet of Cialis[®]

    d.   Impurity profile of a genuine tablet of Cialis[®].

3.2. **Exploratory analysis on raw data**

An exploratory analysis of raw chromatographic fingerprints using both PCA and D-PLS did not reveal a clear discrimination between genuine and illegal samples. This is mainly due to

the fact that too much importance was given to noise and inevitable baseline shifts. In order to reduce the importance of these differences, a common logarithmic transformation of the dataset was performed.

a.

b.

c.

d.
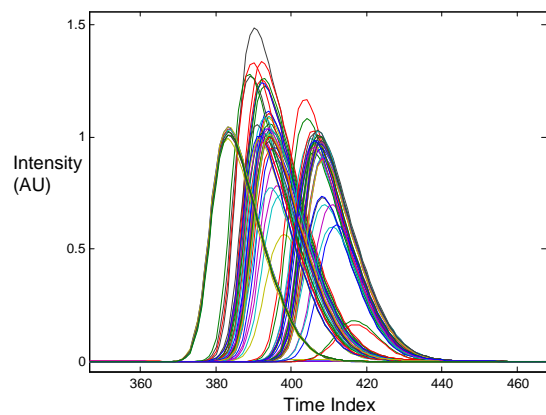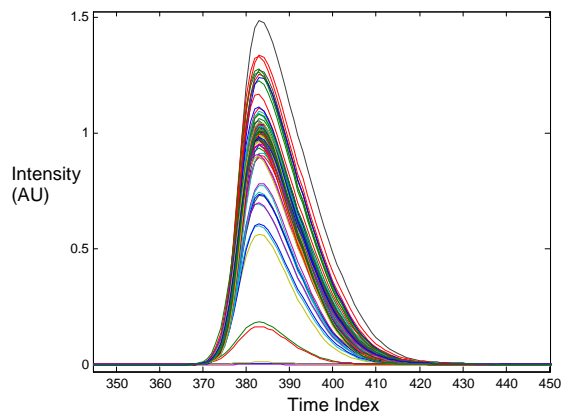
Figure 2:

    a.   Superposition of the non aligned peak of sildenafil

    b.   Superposition of the aligned peak of sildenafil;

    c.   Superposition of the non aligned peak of tadalafil

    d.   Superposition of the aligned peak of tadalafil.

3.3. Viagra®

3.3.1. Exploratory analysis

3.3.1.1. PCA analysis

The log transformed data, containing fingerprints of Viagra® samples, have been compressed using PCA into a few principal components to reveal possible differ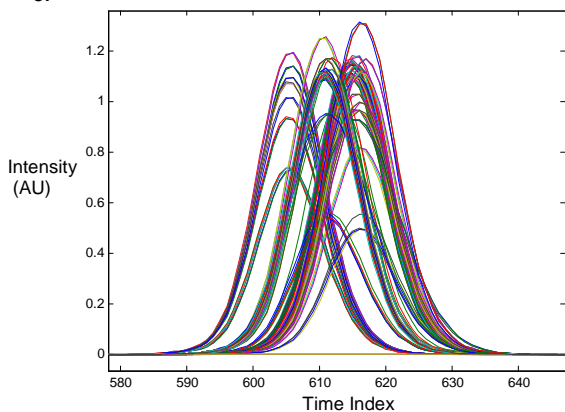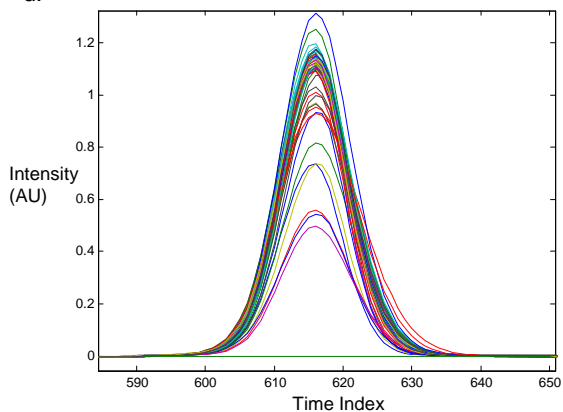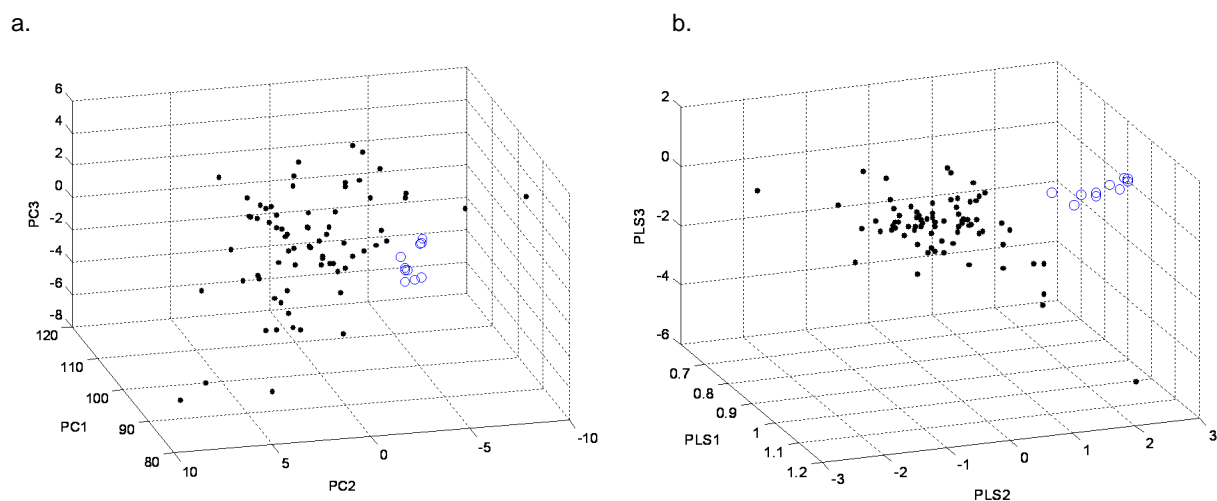ences between genuine and illegal samples. Unfortunately, the discrimination obtained is too weak to be acceptable (Figure 3a). Therefore, the supervised D-PLS approach was applied to enhance this discrimination.

a.   b.

Figure 3:
a.   PCA 3 dimensional plot of the log transformed Viagra® dataset. Black points are the illegal samples and blue circles are the genuine ones;
b.   PLS 3 dimensional plot of the log transformed Viagra® dataset. Black points are the illegal samples and blue circles are the genuine ones.

3.3.1.2. D-PLS analysis

Figure 3b gives an indication that there exists a good discrimination between genuine and illegal samples.
The illegal samples are spread widely and no clustering tendency among them was observed.
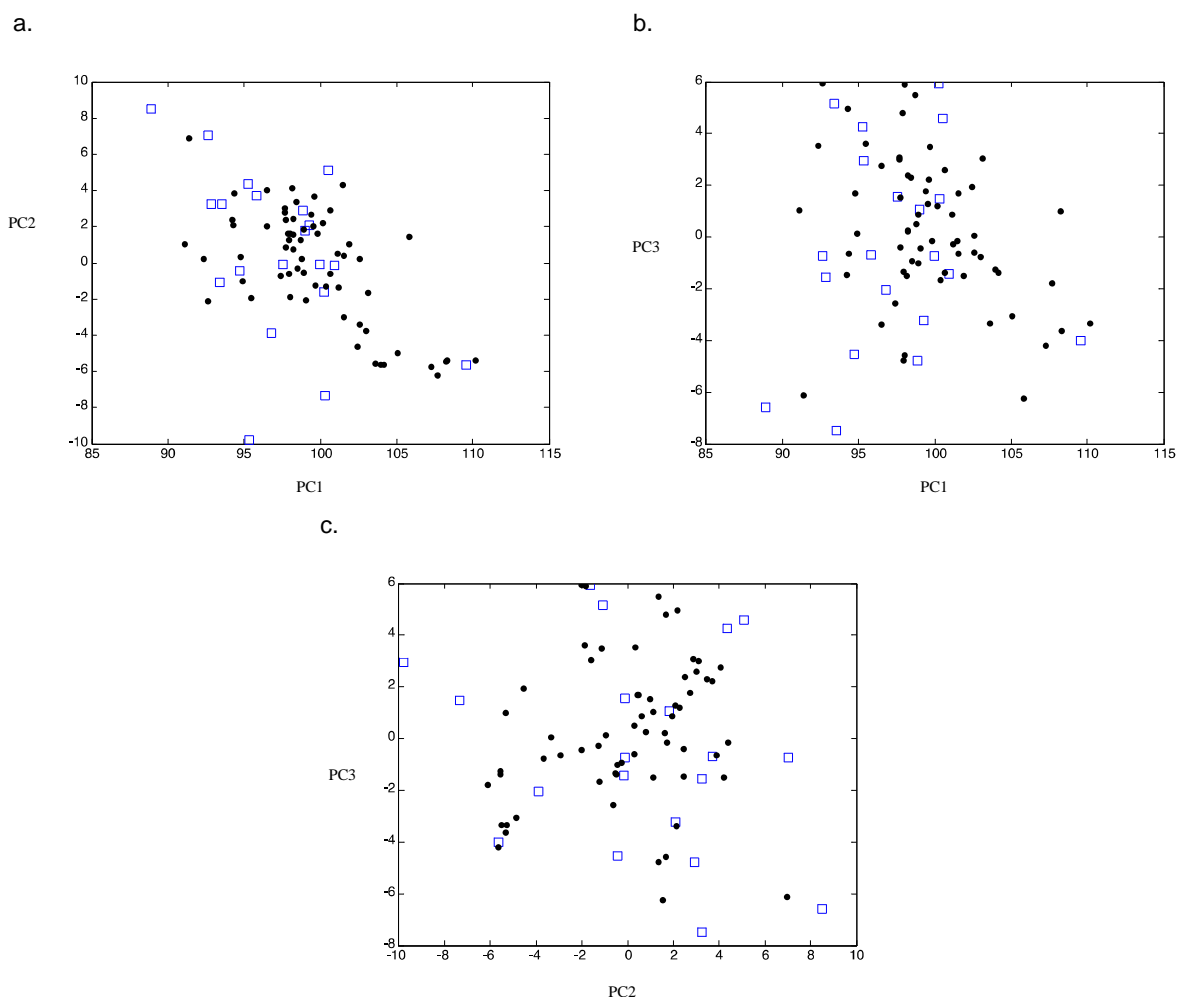
3.3.1.3. Classification

The possibility to predict whether a sample is genuine or not has been tested using two different classification algorithms: k-NN and SIMCA. Before construction of classification

models, the log transformed fingerprints were divided into a training set and a test set using the Kennard and Stone algorithm. For each classification model, its prediction abilities were examined by means of internal (using leave-one-out cross-validation) and external validation.

For classification purposes, training and test sets were constructed such that the training set contained 55 illegal samples and eight genuine samples, and the test set 20 samples including two genuine samples. Figure 4 provides a confirmation of the relatively homogenous distribution of the test set among the samples of the training set.

For the studied data, the k-NN classifier allows 100% of correct classification to be reached evaluated using leave-one-out cross-validation and external validation. The closest neighbours were equal to 3.

a.

b.

c.

Figure 4: a. PC1-PC2; b. PC1-PC3 and c. PC2-PC3 plot of the training set (black points) and the test set (blue squares) determined by the Kennard and Stone algorithm applied on the Viagra® dataset.

When the SIMCA classification has been applied, both legal and illegal groups of samples were described by one principal component. With the SIMCA model tested using cross-validation and external validation set 100% correct classification rates were achieved.

The comparison of the two classification methods indicates that k-NN is the best suited method for this dataset because of the satisfactory results obtained and its simplicity (Table 1).

Table 1: Results obtained applying classification algorithms.

Viagra-like samples		TP	FP	TN	FN	% CCR
k-NN						
	Training set	8	0	55	0	100
	Test set	2	0	18	0	100
SIMCA						
	Training set	8	0	55	0	100
	Test set	2	0	18	0	100
Cialis-like samples		TP	FP	TN	FN	% CCR
k-NN						
	Training set	3	3	33	0	92,3
	Test set	2	0	8	0	100
SIMCA conditions 1						
	Training set	3	5	31	0	87,2
	Test set	2	0	8	0	100
SIMCA conditions 2						
	Training set	3	3	33	0	92,3
	Test set	2	1	7	0	90

TP, true positives (genuine correctly classified); FP, false positives (illegal classified as genuine); TN, true negatives (illegal correctly classified); FN, false negatives (genuine classified as illegal); CCR, correct classification rate.
See text for SIMCA conditions 1 and 2.

3.4. *Cialis*®

3.4.1. *Exploratory analysis*

3.4.1.1. *PCA analysis*

For the Cialis® set of samples, the exploratory analysis did not highlight evident differences between genuine and imitation samples. In general, the genuine samples were scattered among professional imitation samples. The characteristics of the professional imitations are that they contain the correct API within 90-110% of the declared value and that they do not have the same appearance as genuine tablets.

They can be considered as good quality samples in comparison with the other illegal samples. It is therefore comprehensible that the difference between the professional imitations chromatograms and the genuine ones are not directly related to main data variability and thus the first principal components did not reveal a good discrimination between the two groups of samples. For this reason again, D-PLS was applied.

3.4.1.2. *D-PLS analysis*

As can be seen in Fig. 5, discrimination between genuine and illegal samples was achieved. The discrimination is mainly captured by PLS factor 2 and 3. Although the illegal samples seem quite close to each other, some differences may be observed. A group of four samples can be distinguished from the other ones (samples in a circle). These samples represent non-coated tablets, and their cores have intensive orange colour. Chromatographic fingerprints of these tablets reveal an intensive absorbance of the UV light at signal's beginning. In Fig. 5, one can observe that one sample, indicated with an arrow, is relatively far away from remaining illegal samples. This phenomenon can be explained by the fact that this sample contains only traces of both sildenafil and tadalafil.

In Fig. 5c, a separation line is drawn that splits the illegal samples in two groups, denoted as A and B. Group A (above the discrimination line) may be considered as a group containing samples of bad quality and/or recognized as dangerous. Indeed, 13 samples out of 17 contain, besides tadalafil, sildenafil in amounts as high as 7mg per tablet. Among these samples were all the counterfeited Cialis® tablets. On the other hand, group B (below the separation line) contains imitations samples of reasonable good quality. These tablets contain only tadalafil (except two of them, in which traces of sildenafil were identified) within the 90-110% range of the declared value. It can be concluded that samples from group A are more hazardous than samples from group B because their chemical composition seems

whimsical. This lack of confidence in the chemical composition of the medicines increases the hazard of their intake.

a.

b.

c.
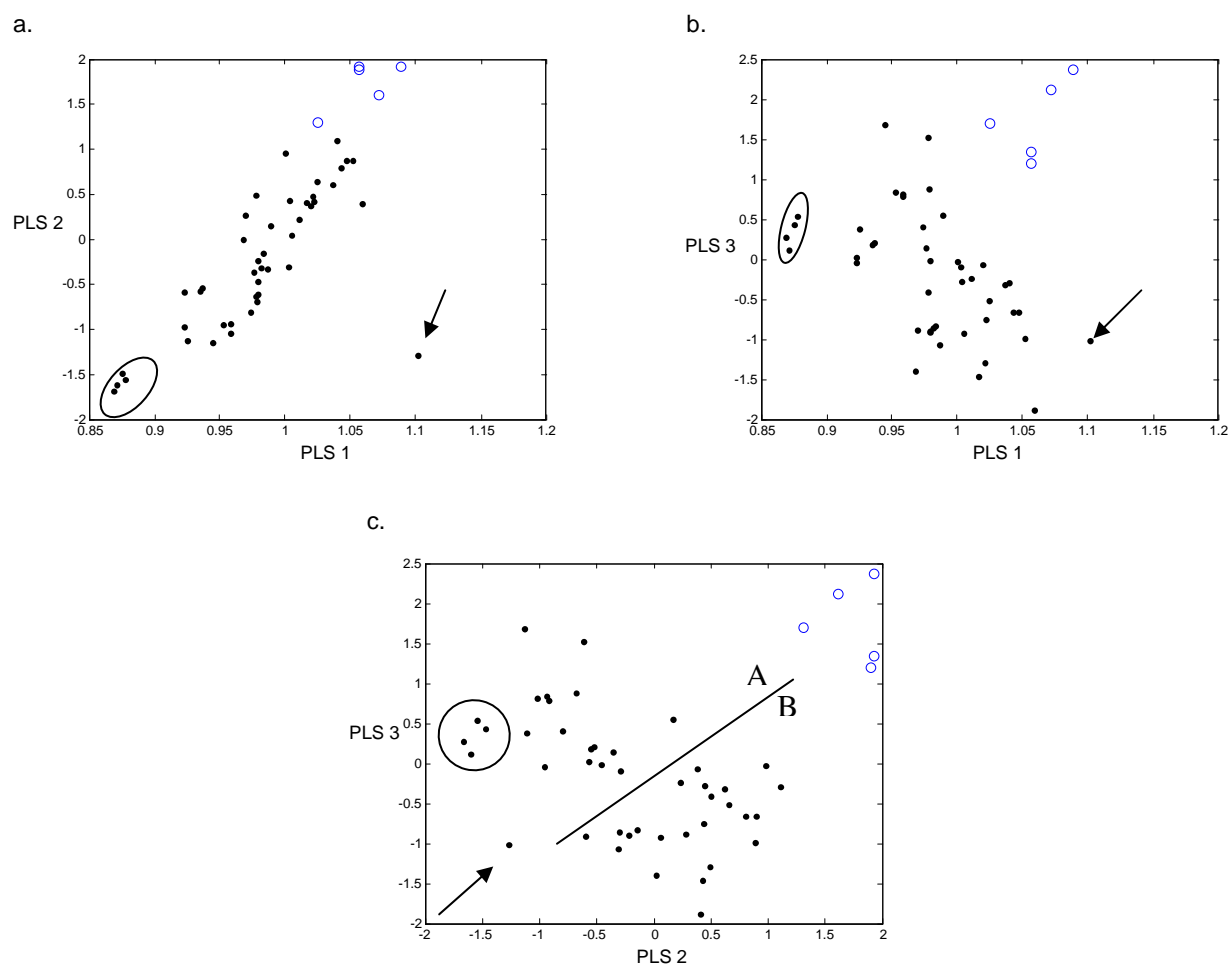
Figure 5:
   a.   PLS1-PLS2 plot of the log transformed Cialis[®] dataset. Black points are the illegal samples and blue circles are the genuine ones. For explanations about the arrow and the circle see text section 2.3.2.
   b.   PLS1-PLS3 plot of the log transformed Cialis[®] dataset. Black points are the illegal samples and blue circles are the genuine ones. For explanations about the arrow and the circle see text section 2.3.2.
   c.   PLS2-PLS3 plot of the log transformed Cialis[®] dataset. Black points are the illegal samples and blue circles are the genuine ones. All samples above the line (except genuine ones and the ones that are surrounded) form the Group A. The samples under the line form the Group B. For explanations about the arrow and the circle see text section 2.3.2.

3.4.1.3.   *Classification*

By analogy with the Viagra[®] samples, k-NN and SIMCA were applied on the Cialis[®] dataset. To construct and validate the classification models, the data was split into a training set containing 36 illegal samples and three genuine samples and a test set of ten samples including two genuine samples. The training and test set were determined using the Kennard and Stone algorithm. Figure 6 shows a quite homogenous distribution of the test set samples among the samples of the training set.

The k-nearest neighbour classifier allows to obtain 92.3% correct classification rate (3 illegal samples misclassified, and all genuine samples were correctly classified) evaluated using leave-one-out cross-validation. All samples from the independent test set were classified appropriately. The closest neighbours were equal to 3.

a.

b.

c.
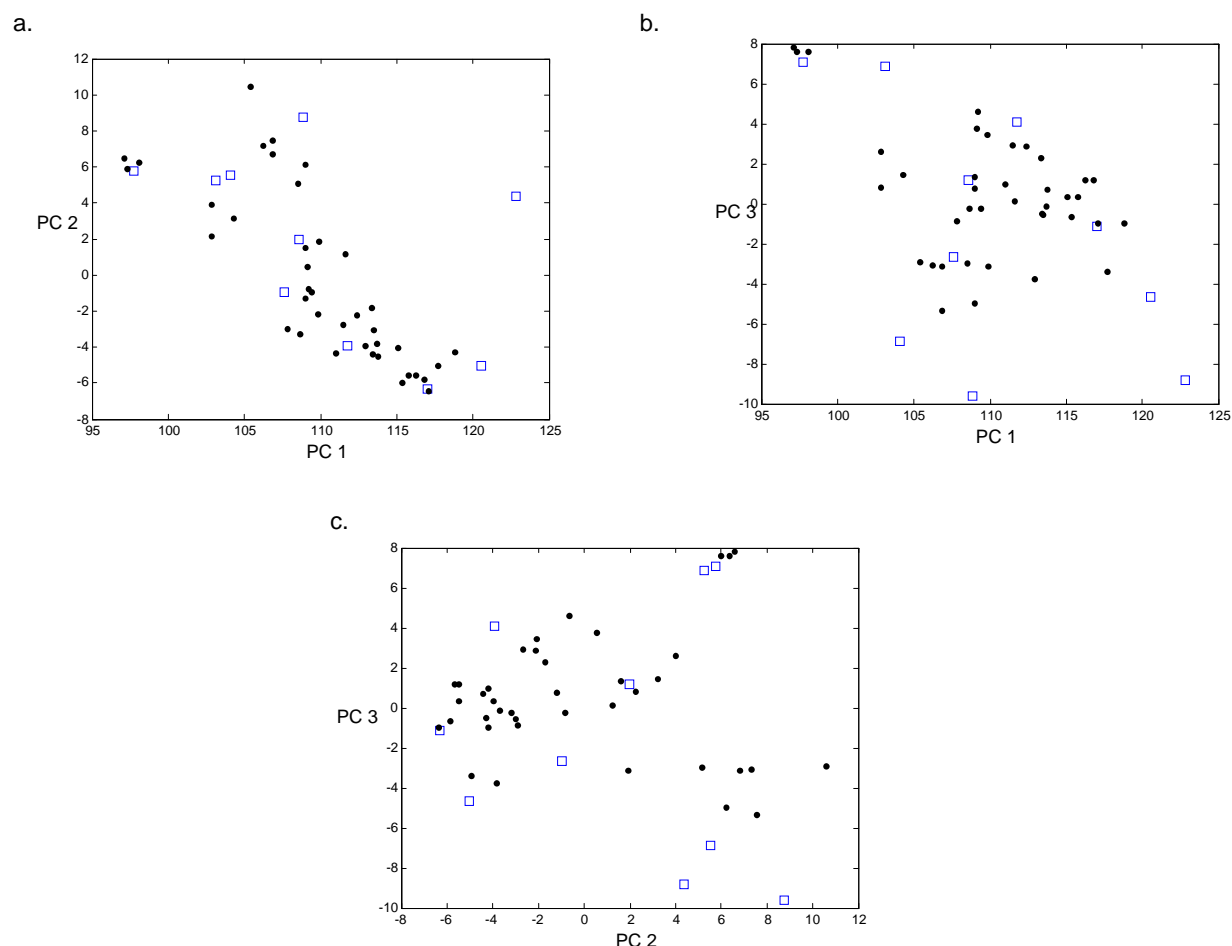
Figure 6:
   a. PC1-PC2 plot of the training set (black points) and the test set (blue squares) determined by the Kennard and Stone algorithm applied on the Cialis[®] dataset.
   b. PC1-PC3 plot of the training set (black points) and the test set (blue squares) determined by the Kennard and Stone algorithm applied on the Cialis[®] dataset.
   c. PC2-PC3 plot of the training set (black points) and the test set (blue squares) determined by the Kennard and Stone algorithm applied on the Cialis[®] dataset.

In addition to k-NN classification, the SIMCA classification was also evaluated. One principal component was found to be sufficient to build the model for the genuine samples. To describe the illegal samples, models containing 2 and 3 PCs were tested. When using 2 PCs (conditions 1) to model the illegal samples, a correct classification rate of 87.2% was achieved (5 illegal samples were misclassified, and all genuine samples were correctly classified) during cross-validation. External validation resulted in a 100% correct classification rate. When 3 PCs (conditions 2) were used to model the illegal samples, cross

validation returned 92.3% correct classification rate (3 illegal samples misclassified, all genuine samples correctly classified) and external validation misclassified 1 sample out of ten, though all genuine samples were classified as genuine.

The comparison of the two classification approaches favours k-NN since it allows obtaining a slightly better classification results compared to SIMCA (Table 1). It can be finally concluded that k-NN is the best suited method since it provides satisfactory classification results and is simple to implement.

4. <u>Conclusion</u>

As the manufacturing processes of counterfeit drugs are not controlled properly or made by not scrupulous people, their chemical composition is not known. This problem ranges from using wrong excipients to instable or improper quantity of active pharmaceutical ingredient. Even when the correct amount of API is present at the correct dosage, impurities may be detected at too high concentrations. These impurities come from starting materials of questionable quality, cross-contamination, improper manufacturing processes and/or conservation conditions. The presence of various compounds in various amounts represents a real thread for the public health.

In this study, it has been investigated whether differences in impurity profiles could be used to detect counterfeit tablets. Impurity profiles of 77 counterfeit and imitations of Viagra[®], 10 genuine Viagra[®], 44 counterfeit and imitations of Cialis[®] and 5 genuine Cialis[®] were obtained by applying classical reversed phase methods on a common HPLC-UV system.

After the log transformation of chromatographic fingerprints and using the discriminant PLS approach for exploratory analysis, a clear discrimination between legal and illegal samples was achieved.

Two classification algorithms (k-NN and SIMCA) were applied and compared in terms of the correct classification rates obtained during leave-one-out cross-validation and for external validation samples. From the obtained results, it is concluded that the k-NN algorithm is the best suited since it provides 100% correct classification rate for both cross-validation and external validation for the Viagra[®] dataset and 92.3% (all genuine samples correctly classified) and 100% correct classification rate during respectively cross-validation and external validation for the Cialis[®] dataset.

To the best of our knowledge, this is the first time that chromatographic fingerprints are used to distinguish counterfeit medicines according to their impurities content. The obtained results show that this would be interesting to develop a routine method to obtain impurity profiles that could be used to detect counterfeit tablets by a control laboratory. This might be

found as a useful approach especially in developing countries with basic analytical equipment.

However, further investigations should be done to see whether the obtained results may be applicable to other kind of medicines.

References

[1] Deisingh A., Pharmaceutical counterfeiting, Analyst (2005) 130, 271-279

[2] WHO, Fact sheet n° 275 Medicines: counterfeit medicines, January 2010. http://www.who.int/mediacentre/factsheets/fs275/en/index.html

[3] EAASM, The counterfeiting superhighway report, Surrey, 2008

[4] Kovaleski J., Kraut B., Mattiuz A., Giangiulio M., Brobst G., Cagno W., Kulkarni P., Rauch T., Impurities in generic pharmaceutical development, Advanced Drug Delivery Reviews (2007) 59, 56-63

[5] Häberli A., Girard P., Low M.Y., Ge X., Isolation and structure elucidation of an interaction product of aminotadalafil found in an illegal health food product, Journal of Pharmaceutical and Biomedical Analysis (2010) 53, 24-28

[6] Bigler P., Brenneisen R., Improved impurity fingerprinting of heparin by high resolution ^{1}H NMR spectroscopy, Journal of Pharmaceutical and Biomedical Analysis (2009) 49, 1060-1064

[7] Alonso-Salces R.M., Héberger K., Holland M.V., Moreno-Rojas J.M., Mariani C., Bellan G., Reniero F., Guillou C., Multivariate analysis of NMR fingerprint of the unsaponifiable fraction of virgin olive oils for authentication purposes, Food Chemistry (2010) 118, 956-965

[8] Silvestre V., Maroga Mboula V., Jouitteau C., Akoka S., Robins R. J., Remaud G. S., Isotopic ^{13}C NMR spectrometry to assess counterfeiting of active pharmaceutical ingredients: Site-specific ^{13}C content of aspirin and paracetamol, Journal of Pharmaceutical and Biomedical Analysis (2009) 50, 336-341

[9] Roggo Y., Roeseler C., Ulmschneider M., Near infrared spectroscopy for qualitative comparison of pharmaceutical batches, Journal of Pharmaceutical and Biomedical Analysis (2004) 36, 777-786

[10] Vredenbregt M.J., Blok-Tip L., Hoogerbrugge R., Barends D.M., de Kaste D., Screening suspected counterfeit Viagra® and imitations of Viagra® with near-infrared spectroscopy, Journal of Pharmaceutical and Biomedical Analysis (2006) 40, 840-849

[11] Scafi S. H. F., Pasquini C., Identification of counterfeit drugs using near-infrared spectroscopy, Analyst (2001) 126, 2218-2224

[12] Zhu H., Wang Y., Liang H., Chen Q., Zhao P., Tao J., Identification of *Portulaca oleracea* L. from different sources using GC–MS and FT-IR spectroscopy, Talanta 81 (2010) 129-135

[13] Yap K. Y.-L., Chan S. Y., Lim C. S., Infrared-based protocol for the identification and categorization of ginseng and its products Food Research International (2007) 40, 643-652

[14] Dumarey M., van Nederkassel A.M., Stanimirova I., Daszykowski M., Bensaid F., Lees M., Martin G.J., Desmurs J.R., Smeyers-Verbeke J., Vander Heyden Y., Recognizing

paracetamol formulations with the same synthesis pathway based on their trace-enriched chromatographic impurity profiles, Analytica Chimica Acta (2009) 655, 43-51

[15] van Nederkassel A.M., Xu C.J., Lancelin P., Sarraf M., MacKenzie D.A., Walton N.J., Bensaid F., Lees M., Martin G.J., Desmurs J.R., Massart D.L., Smeyers-Verbeke J., Vander Heyden Y., Chemometric treatment of vanillin fingerprint chromatograms effect of different signal alignments on principal component analysis plots, Journal of Chromatography A (2006) 1120, 291-298

[16] Ni Y., Lai Y., Brandes S., Kokot S., Multi-wavelength HPLC fingerprints from complex substances: An exploratory chemometrics study of the *Cassia seed* example, Analytica Chimica Acta (2009) 647, 149-158

[17] Lian H., Wei Y., Chromatographic fingerprints of industrial toluic acids established for their quality control, Talanta (2007) 71, 264-269

[18] Nicolas E. C., Scholz T. H., Active drug substance impurity profiling Part II. LC:MS:MS fingerprinting, Journal of Pharmaceutical and Biomedical Analysis (1998) 16, 825-836

[19] Carrier D., Eckers C., Arnoult T., Thurston T., Major H., Finding key impurities in different manufacturing routes of a drug substance using liquid chromatography/mass spectrometry followed by principal components analysis, Rapid Communications in Mass Spectrometry (2007) 21, 3946-3948

[20] Jiang Y., David B., Tu P., Barbin Y., Recent analytical approaches in quality control of traditional Chinese medicines - A review, Analytica Chimica Acta (2010) 657, 9-18

[21] Xiaohui F., Yi W., Yiyu C., LC/MS fingerprinting of *Shenmai injection*: A novel approach to quality control of herbal medicines, Journal of Pharmaceutical and Biomedical Analysis (2006) 40, 591-597

[22] Hu P., Liang Q.L., Luo G.A., Zhao Z.Z., Jiang Z.H., Multi-component HPLC Fingerprinting of Radix *Salviae Miltiorrhizae* and Its LC-MS-MS Identification, Chemical and Pharmaceutical Bulletin (2005) 53, 677-683

[23] Han C., Shen Y., Chen J., Lee F. S.-C., Wang X., HPLC fingerprinting and LC–TOF-MS analysis of the extract of *Pseudostellaria heterophylla* (Miq.) Pax root, Journal of Chromatography B (2008) 862, 125-131

[24] Lee J. S., Chung H. S., Kuwayama K., Inoue H., Lee M. Y., Park J. H., Determination of impurities in illicit methamphetamine seized in Korea and Japan, Analytica Chimica Acta (2008) 619, 20-25

[25] Xu C.-J., Liang Y.-Z., Chau F.-T., Vander Heyden Y., Pretreatments of chromatographic fingerprints for quality control of herbal medicines, Journal of Chromatography A (2006) 1134, 253-259

[26] Daszykowski M., Sajewicz M., Rzepa J., Hajnos M., Staszek D., Wojtal L., Kowalska T., Waksmundzka-Hajnos M., Walczak B., Comparative analysis of the chromatographic fingerprints of twenty different sage (*Salvia* L.) species, Acta Chromatogr. (2009) 4, 513-530

[27] European Directorate for the Quality of Medicines, draft monography of sildenafil citrate, Pharmeuropa (2011) 23, 381–383.

[28] European Directorate for the Quality of Medicines, draft monography of tadalafil, Pharmeuropa (2010) 22, 328–332.

[29] Daszykowski M., Walczak B., Use and abuse of chemometrics in chromatography, Trends in Analytical Chemistry (2006) 25, 1081-1096

[30] Daszykowski M., Walczak B., Target selection for alignment of chromatographic signals obtained using monochannel detectors, Journal of Chromatography A 1176 (2007) 1-11

[31] Daszykowski M., Walczak B., Massart D.L., Projection methods in chemistry, Chemometrics and Intelligent Laboratory Systems (2003) 6597-112

[32] Massart D.L., Vandeginste B.G.M., Buydens L.M.C., De Jong S., Lewi P.J., Smeyers-verbeke J.: Handbook of Chemometrics and Qualimetrics-Part A, Elsevier Science, Amsterdam, 1997

[33] Kennard R.W., Stone L.A., Computer aided design of experiments, Technometrics (1969) 11, 137-148

[34] Vandeginste B.G.M., Massart D.L., Buydens L.M.C., De Jong S., Lewi P.J., Smeyers-verbeke J.: Handbook of Chemometrics and Qualimetrics-Part B, Elsevier Science, Amsterdam, 1997

4. <u>Discussion</u>

Chromatographic techniques provide data that may be used in several ways.

The previous chapter presents a chromatographic method dedicated to the quantification and identification of three erectile dysfunction drugs and some of their analogues. The quantitative aspect of the method has been validated within the +/- 5% acceptance limits using the total error approach. This method has been implemented as routine method in the Drug Analysis Laboratory of the scientific Institute of Public Health (IPH) for the analysis of illegal preparations containing PDE5-i and analogues.

The other study demonstrates the interest of treating impurity profiles as fingerprints for the detection of illegal medications. The advantages of this method are that it is performed on a classical HPLC-UV system using a simple isocratic reversed-phase separation method. Furthermore this technique allows a fast overview of the chemical composition of the tablet and eventually a simultaneous quantification of the active compound. The obtained validated predictive model allowed predicting whether a new sample was counterfeited.

However, the main drawbacks are that the pre-processing of the data, especially the warping, is critical. Indeed, variations in mobile phase composition, stationary phase degradation etc. may cause peak shifts distorting the results.

Chapter VI. General conclusions and future perspectives

General conclusions and future perspectives

Since the WHO first mentioned it in 1985, the number of reported cases of pharmaceutical counterfeiting has been growing year by year. It is now estimated that counterfeit drugs represent 7% of the global pharmaceutical market.

Counterfeit medicines become more and more sophisticated as well the packaging (i.e. holograms etc.) as the tablet itself. Customs must therefore use more and more sophisticated analytical techniques. Among them a difference must be made between the expensive and complicated ones available in industrialized countries and the less efficient and cheaper ones available in developing countries while these countries are the most affected by the counterfeiting problem.

During this thesis, we developed and tested analytical methods to detect illegal pharmaceutical preparations sold as erectile dysfunction remedies. As counterfeit erectile dysfunction drugs are mainly a problem of industrialized countries, we developed methods using apparatus available in typical control laboratories of these countries. These techniques are divided in two main groups: spectroscopic techniques and chromatographic techniques.

Investigated spectroscopic techniques included the infrared-based techniques: FT-IR, NIR, and Raman spectroscopy.

In a first study, we compared each of these three techniques and their combinations in function of their ability to discriminate illegal preparations from genuine ones and to make clusters among illegal preparations. The clusters were made by visual examination of the PLS factors space. This could have been useful for a further forensic investigation intending to track the sources of these illegal preparations. However, the samples we obtained came only from postal packages and their real origin (or manufacturing site) is therefore unknown. This let us disarmed to choose which clusters are the most meaningful. We evaluated therefore the clusterisation in function of the visual appearance of the tablets, their packaging and their chemical composition (nature and amount of API). It was found that the association of FT-IR (1800-400 cm^{-1}) and NIR (7000-4000 cm^{-1}) was the more interesting for the analysis of Viagra$^{®}$-like samples. On the other hand, the association of NIR (7000-4000 cm^{-1}) and Raman (1190-1400 cm^{-1}) provided the best results for the analysis of Cialis$^{®}$-like samples.

A second study completed these results obtained by visual examination of the data. During this study, a classification and prediction algorithm, CART, was applied on the spectroscopic data. The goal of this study was to evaluate whether it was possible to predict if a new sample was genuine and if not, its RIVM class. For the Viagra$^{®}$ data set, two models were selected: one based on the FT-IR data and one on the NIR data. The two models gave comparable results: all genuine samples were correctly classified and two illegal samples on

twelve were misclassified during external validation. The association of NIR and FT-IR did not improve the results. For Cialis®-like samples, the best model was obtained combining NIR and Raman data. In this case, all samples were correctly classified during external validation. These results are comparable to the one obtained during the first study but they give a plus since they are objective and they allow the prediction of the RIVM class of a new unknown sample. This is very useful to quickly and easily evaluate the potential risk of a sample.

Another study evaluated Raman microspectroscopy. The pharmaceutical applications of this technique are mainly the evaluation of a pharmaceutical formulation based on the distribution of the active compound in the tablet. Therefore, we wanted to know whether it was possible to discriminate between genuine and illegal Viagra® samples based on the difference of distribution of sildenafil in the core of the tablets. Unfortunately, the results showed no discrimination when focusing on sildenafil distribution. However, Raman microspectroscopy gave a good discrimination while using the whole spectrum (200-1800 cm^{-1}) or the peaks attributed to lactose (1200-1290 cm^{-1}). Moreover, using the k-nearest neighbour algorithm to build a predictive model on the 200-1800 cm^{-1} range, it was possible to classify 100% of samples as genuine or illegal during internal and external validation.

The chromatographic part of the present thesis started with the development of a UHPLC-UV method for the analysis of PDE5-i and some of their analogues. This method allows the identification (based on the UV spectra and the retention times) and the quantification of the three authorised PDE5-i and five of their analogues commonly found as adulterants of herbal supplements. This method was validated whithin the +/- 5% acceptance limits by the total error approach. It has also been demonstrated that this new method gave comparable results to the draft reference method published in Pharmeuropa. If needed, it is possible to use a mass spectrometer as detector since the mobile phase is MS compatible. This method has been implemented as routine method at IPH for the analysis of illegal preparations containing PDE5-i and analogues.

The last study investigated the ability of chromatographic fingerprints to detect counterfeit Viagra® and Cialis®. Impurity profiles were recorded for each speciality using the chromatographic conditions described in a monograph proposal in Pharmeuropa (or slightly different). These conditions are especially dedicated to the analysis of impurities of the considered speciality. The chromatograms were obtained on the same HPLC-DAD system with the same mobile phase. However, a shift in retention times was observed and the chromatograms needed an alignment prior any multivariate analysis. For each speciality, chromatograms were aligned in function of the major (largest) peak. Once aligned, the chromatograms underwent logarithmic transformation in order to reduce the influence of

174

remaining slight differences and baseline perturbations. After pre-treatment, PLS was applied on each dataset. The score plots showed a good separation of genuine samples from illegal ones. Predictive algorithms were then applied and predictive models were built. For the Viagra-like samples, both k-NN and SIMCA provided similar good results. For the Cialis-like samples, however, the best results were obtained using the k-NN algorithm. The predictive properties of the built model were validated using an external test set. The results showed that impurity fingerprints can be an interesting approach for the detection of counterfeit drugs.

To conclude, a generic approach to detect counterfeit drugs containing PDE5-i using the tested and developed methods during this thesis is proposed (see Figure VI.1).

When a new sample arrives in the laboratory for analysis, the visual inspection is the first analysis performed. If the samples do not look like genuine drug or if it is a dietary supplement, the only analysis to perform is a qualitative and quantitative analysis using UHPLC-UV and/or LC-MS method. Indeed, no fingerprinting method is necessary since it is evident that it is not a genuine drug. Using the obtained information, it should be possible to classify the sample following the RIVM classification.
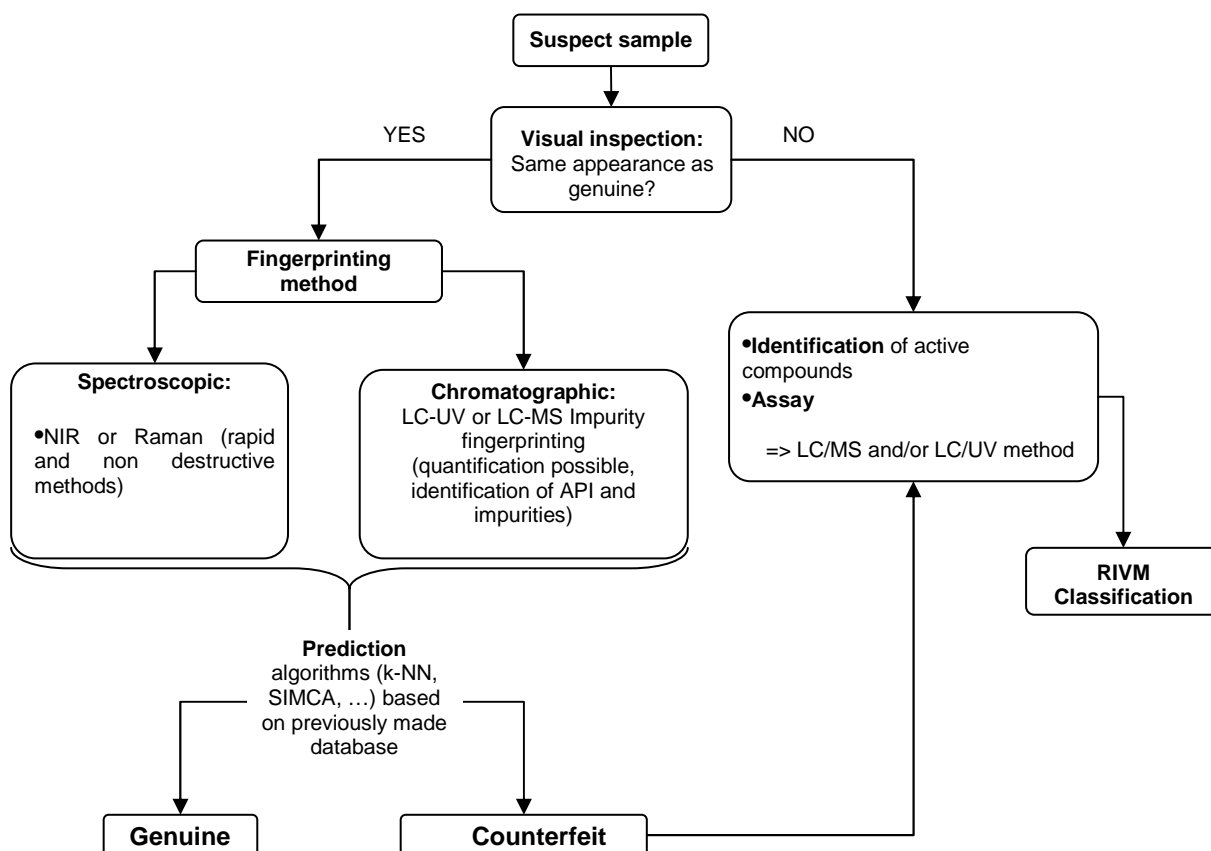
Figure VI.1: General strategy for the detection and classification (RIVM) of samples suspected to contain PDE5-i using methods described in this thesis.

If the new sample has the same appearance as genuine Viagra® or Cialis®, a fingerprinting method is the first recommended analysis. Prior to any fingerprinting analysis, the control laboratory must have developed and validated a predictive model based on the fingerprints of a sufficient number of genuine and illegal samples. Thereafter, each new measured sample will be added to the database and the predictive model rebuilt and revalidated. As time goes by, the model will be more and more accurate as its database grows.

Two kinds of fingerprinting approaches are available: spectroscopic and/or chromatographic fingerprinting.

Spectroscopic fingerprinting is quick, non destructive and reproducible. However, not every laboratory has a NIR or a Raman spectrometer and the equipment is quite expensive.

On the other hand, chromatographic fingerprinting allows chemical analysis of the tablets and the identification of potential toxic impurities while simultaneously quantifying the active ingredient(s). Another advantage is that these fingerprints are obtained on classical HPLC-UV systems present in every control laboratory. However, the main drawbacks are the fact that it is a time consuming method and that a lot of parameters may change (mobile phase composition, different analytical columns, ageing of stationary phase, different HPLC system, etc.). All these parameters introduce changes in chromatograms, complicating data alignment and pre-treatment. In conclusion, we recommend the use of spectroscopic fingerprinting methods. If the tablet has been declared counterfeit, it undergoes quantitative and qualitative analysis with the UHPLC-UV and/or LC-MS method and is classified following the RIVM classification.

As stated above, it is possible to differentiate genuine from illegal samples using their impurity fingerprints. In the future, it would be interesting to identify these impurities. It would allow laboratories to assess more accurately the toxicological risks associated with these drugs and it would perhaps allow the identification of common sources of starting materials or synthesis pathway.

The combination of the different information about the chemical composition (excipients, API, impurities) with the spectroscopic data may allow the distinction between different producers or production sites. This may constitute a first step in tracking counterfeiters. However, without any knowledge about where and how illegal medicines were manufactured, it is impossible to elaborate a predictive model to identify the source of the drugs.

Therefore, if no information is available, control laboratories should focus on fast and reliable estimation of the risks associated with the intake of illegal drugs.

A new challenge is the arrival of authorised generics of Viagra® since the patent expires this year. These new genuine drugs will have to be discriminated from illegal imitations and

counterfeit sildenafil drugs. The analytical methods described in this work should therefore be tested again and re-validated with this new kind of drugs.

Finally, the presented approach could be applied to other types of counterfeit drugs. To do so, they should be specifically adapted to the type of studied medicines.

<u>Appendix</u>

Publications:

1. **Comparison and combination of spectroscopic techniques for the detection of counterfeit medicines**
   Sacré P-Y, Deconinck E, De Beer T, Courselle P, Vancauwenberghe R, Chiap P, Crommen J, De Beer J, Journal of Pharmaceutical and Biomedical Analysis (2010), 53, 445-453

2. **A fast Ultra High Pressure Liquid Chromatographic method for qualification and quantification of pharmaceutical combination preparation of NSAID and antihistaminics**
   Deconinck E, Sacré P-Y, Baudewyns S, Courselle P, De Beer J, Journal of Pharmaceutical and Biomedical Analysis (2011), 56, 200-209

3. **Development and validation of a UHPLC-UV method for the detection and quantification of erectile dysfunction drugs and some of their analogues found in counterfeit medicines**
   Sacré P-Y, Deconinck E, Chiap P, Crommen J, Mansion F, Rozet E, Courselle P, De Beer J, Journal of Chromatography A (2011), 1218, 6439-6447

4. **Detection of counterfeit Viagra® by Raman Microspectroscopy imaging and multivariate analysis**
   Sacré P-Y, Deconinck E, Saerens L, De Beer T, Courselle P, Vancauwenberghe R, Chiap P, Crommen J, De Beer J, Journal of Pharmaceutical and Biomedical Analysis (2011), 56, 454-461

5. **Impurity fingerprints for the identification of counterfeit medicines - a feasibility study**
   Sacré P-Y, Deconinck E, Daszykowski M, Courselle P, Vancauwenberghe R, Chiap P, Crommen J, De Beer J, Analytica Chimica Acta (2011), 701, 224-231

6. **Classification trees based on infrared spectroscopic data to discriminate between genuine and counterfeit medicines**
   Deconinck E, Sacré P-Y, Coomans D, De Beer J, Journal of Pharmaceutical and Biomedical Analysis (2012), 57, 68-75

Poster presentations:

1. **Comparison and combination of spectroscopic techniques for the detection of counterfeit medicines**
   Sacré P-Y, Deconinck E, De Beer T, Courselle P, Vancauwenberghe R, Chiap P, Crommen J, De Beer JO, Drug Analysis 2010, 21-24 septembre 2010, Anvers

2. **Detection of counterfeit Viagra® by Raman Microspectroscopy imaging and multivariate analysis**
   Sacré P-Y, Deconinck E, Saerens L, De Beer T, Courselle P, Vancauwenberghe R, Chiap P, Crommen J, De Beer J, EDQM Counterfeit Symposium for OMCLs, 29-31 March 2011, Strasbourg

3. **Development and validation of a UHPLC-UV method for the detection and quantification of erectile dysfunction drugs and some of their analogues found in counterfeit medicines**
   Sacré P-Y, Deconinck E, Chiap P, Crommen J, Mansion F, Rozet E, Courselle P, De Beer J, HPLC 2011, 19-23 juin 2011, Budapest

4. **Impurity fingerprints for the identification of counterfeit medicines - a feasibility study**
   Sacré P-Y, Deconinck E, Daszykowski M, Courselle P, Vancauwenberghe R, Chiap P, Crommen J, De Beer J, HPLC 2011, 19-23 juin 2011, Budapest

5. **Impurity fingerprints for the identification of counterfeit medicines - a feasibility study**
   Sacré P-Y, Deconinck E, Daszykowski M, Courselle P, Vancauwenberghe R, Chiap P, Crommen J, De Beer J, RDPA 2011, 21-24 septembre 2011, Pavie

Oral communications

1. **"Detection of counterfeit medicines based on their physico-chemical analysis"**
   Sacre P-Y, Tuesday seminars, WIV-ISP, 16 Mars 2010

2. **"Detection of counterfeit Viagra® by Raman Microspectroscopy imaging and multivariate analysis"**

   <u>Sacré P-Y</u>, Deconinck E, Saerens L, De Beer T, Courselle P, Vancauwenberghe R, Chiap P, Crommen J, De Beer J, 15ème Forum des Sciences Pharmaceutiques, Spa, 13 mai 2011

3. **"Classification trees based on infrared spectroscopic data to discriminate between genuine and counterfeit medicines"**

   <u>Deconinck E</u>, Sacré P-Y, Coomans D, De Beer J, RDPA 2011, Pavie, 21-24 septembre 2011,